

Synthesis and biological evaluation of new PAC-1 derivatives

Thesis for Masters degree in pharmacy

Mohammedwali Ahmed Hashi



School of pharmacy

Department of Pharmaceutical Chemistry

Section for Medicinal Chemistry

University of Oslo

15th may 2009.

Acknowledgements

This master thesis has been conducted and written at the School of Pharmacy, Department of Pharmaceutical Chemistry University of Oslo. The work was the brainchild of my supervisor associate professor Trond Vidar Hansen and without his tireless effort and encouraging humour this project would not have been possible. He has not only given me an interesting project, but has also seen to its accomplishment with the tremendous amount of chemistry he taught. A great thank to Professor Ragnhild Paulsen for her suggestions and discussion regarding the biological testing.

I would also have to thank two PhD students in Trond Vidar Hansen's research group, Hany Anwar and Øyvind Akselsen for their input and suggestions, together with Iulianne Johansen whose introduction to the lab and help during the whole period is worth recognition. I will always be in debt to Alexandra Gade for proofreading my thesis and giving lots of advice about it.

A great thank goes to the entire group for the time we spent together and the discussion we had. Last but not least I would like to thank my family for their outstanding support throughout my studying time, without you my entire higher education would not have been a reality.

Oslo, May 2009

Mohammedwali A Hashi

Abstract

Cancer is one of the leading causes of death in the world. In developing countries cancer is claiming more lives than HIV & AIDS, tuberculosis and malaria combined. Cancer is generally known to be a disease with uncontrolled multiplication; in other words, cells reproduce in defiance of normal restraints on cell division. It is also known to invade and colonize territories far from the infection area.

As the science of cancer is developing, researchers are seeing light at the end of the tunnel. Cancer is known to be a disease of genetic disorders, though it is much more than that with hallmarks like evading apoptosis. Most of the chemotherapeutic drugs activate apoptosis by using p53 pathway. Unfortunately, in most of the cancer cases p53 is mutated; therefore efforts were made to bypass this mutation since it happens upstream and make molecules that target further downstream in the signal pathway.

It is the aim of this thesis to shed more light on the possibility of targeting not only downstream targets in the apoptosis cascade, but the main executioner which is caspase-3. The idea was to make more potent derivatives of PAC-1, which can lead to cell death and hopefully new leads for cancer drugs. A total of five compounds were synthesized including PAC-1 as a positive control. The compounds were characterised with the help of ^1H NMR, ^{13}C NMR and LC-MS. They were later subjected to biological testing whereby PC-12 cells were treated with the compounds. After 48 hours of incubation the cell viability was measured. It was found that all the compounds had an effect in reducing cell viability.

Abbreviations

ABC	ATP-binding cassette
Apaf-1	Apoptotic protease activating factor
ATM-PK	Ataxia telangiectasia mutated protein
AQZ	Aniloquinazoles
BIR	Baculovirus IAP repeat
CAM	Cell to cell adhesion molecules
CARD	Caspase recruitment domain
CDK	Cyclin dependent kinase
DD	Death domain
DED	Death effector domain
DISC	Death inducing signalling complex
DNA-PK	DNA-dependent protein kinase
dNTPs	Deoxyribonucleoside triphosphate
DTMP	Deoxythymidylate
ECM	Extra cellular matrix
FADD	Fas associated death domain
FDUMP	Fraudulent nucleoside fluorodeoxyuridine
HTS	High throughput screen
IAP	Inhibitors of apoptosis
IGF	Insulin growth factor
Mab	Monoclonal antibodies
NTP	Nucleoside triphosphate
PAC-1	Procaspase activating molecule
PARP-1	Poly-ADP-ribose polymerase
PETCM	α -trichloro methyl-4-pyridin-ethanol
PHAP	Putative HLA-DR associated protein
ProT	Prothymosin- α
pRB	Retinoblastoma proteins
RIP	Receptor interacting protein
SAR	Structural activity relationship
TGF	Transdermal growth factor

Table of contents

Acknowledgements	2
Abstract	3
Abbreviations	4
Contents	5
1. Introduction	8
1.1. The aim of the project	8
1.2. Cancer	9
1.3. Pathophysiology of cancer	10
1.3.1. Self sufficiency in growth signals	10
1.3.2. Insensitivity to growth signals	12
1.3.3. Evading apoptosis	14
1.3.4. Limitless reproductive potential	16
1.3.5. Sustained angiogenesis	17
1.3.6. Tissue invasion and metastasis	20
1.4. Current cancer management	21
1.4.1. Cytotoxic drugs	21
1.4.2. Alkylating agents	21
1.4.3. Antimetabolites	22
1.4.4. Cytotoxic antibiotics	23
1.4.5. Natural products	24
1.4.6. Hormones	25
1.4.7. Monoclonal antibodies	26

1.5. Cell death	27
1.5.1. Necrosis	29
1.5.2. Apoptosis	30
1.5.3. Apoptosis pathways-intrinsic and extrinsic	30
1.5.4. Caspases	32
1.5.5. Procaspase-3 and caspase-3	33
1.5.6. Inhibitors of caspase-3	34
1.5.7. Activators of caspase-3	35
2. Results and discussion	38
2.1.1. Synthesis of intermediates 1-3	38
2.1.2. Synthesis of new PAC-1 derivatives	48
2.1.3. Efforts to synthesize other PAC-1 derivates	60
2.1.4. Biological testing	61
2.1.5. PAC-1 and its derivatives reduce cell viability	66
2.1.6. Discussion	67
3. Conclusion and further studies	69
4. Experimental	70
4.1.1. General synthesis	70
4.1.2. The apparatus	70
4.1.3. Synthesis of intermediates 18, 21 and 23	72
4.1.4. Synthesis of products 16, 25, 26, 27 and 28	75
4.1.5. Methods	79
4.1.6. Measurement of cell viability	79
4.1.7. PC-12 cells	79
4.1.8. Cell viability studies using MTT	80
5. References	81

6. Appendix I ^1H and ^{13}C NMR	85
7. Appendix II. Raw data from first biological testing	93
8. Appendix III. Raw data from second biological testing	94
9. Appendix IV. Raw data from third biological testing	95

1. Introduction

Research on apoptosis has had tremendous increase and interest in the last two decades. With hundreds of thousands articles in the literature, one can experience the pace at which this field is moving. The reason why there is a great deal of interest in this field is simple, excess of apoptosis leads to the following diseases: myocardial infarction, stroke, sepsis, Alzheimers, Parkinson, Huntington disease and rheumatoid arthritis, while a decrease in apoptosis is associated with cancer and viral infection.

The discovery and development of new drugs often involves lead compounds. These are compounds with not only interesting biological activities but also other characteristics like high toxicity and absorption difficulties. Procaspase activating compound (PAC-1) was a compound discovered through high throughput screening (HTS) by Hergenrother *et al.* in late 2006. This compound was reported to be the first to directly cleave procaspase-3 to caspase-3, thereby inducing cell death.

1.1 The aim of the project

- To synthesize a series of analogues with variation on the phenol moiety
- To conduct SAR studies on the compounds
- To test the compounds for biological activity

1.2. Cancer

Cancer is one of the leading causes of death in the world. In 2007, there were an estimated 12 million new cases of cancer and 7.6 million people died of cancer globally. By 2050, the global cancer burden is expected to grow to 27 million new cases and 17.5 million deaths every year. The trend is increasing at an alarming rate in developing countries. Cancer is killing more people in the developing world than HIV & AIDS, malaria and tuberculosis combined¹.

The development of cancer is complex and dependent on many factors. Some of these factors are more important than others, for example genetic constitution of an individual and the environment around the person. Regardless of circumstances, mutation is unavoidable, because it is an inescapable consequence of fundamental limitations on the accuracy of DNA replication. On the other hand environmental factors that play a part in the disease causation can be avoidable or at least postponable². Considering this one third of the cancer in developing countries is preventable, and another one third more is detectable and treatable while there is still hope for survival¹.

Cancer is a disease in which there is uncontrolled multiplication of cells, in other words cells reproduce in defiance of the normal restraints on cell division. Another property which is shown by these cells is invading and colonizing territories far from infection area which are reserved for normal cells^{2 and 3}. The term cancer, malignant neoplasm and malignant tumours are synonymous; they are distinguished from benign tumors by following properties: dedifferentiation, invasion and metastasis (the ability to spread to other parts of the body via blood or lymph). What both benign and malignant tumors share is the characteristic of uncontrolled proliferation³.

1.3. Pathophysiology of cancer

Even if cancer is a disease with great diversity, efforts were made to characterise its pathophysiology so that a number of properties can characterise cancer cell. For a cell to be successful in its cancer acquisition it has to have a whole range of aberrant properties, the following six key properties make cancer cells capable of growth².

1. Self sufficiency in growth signals
2. Insensitivity to antigrowth signals
3. Evading apoptosis
4. Limitless replicative potential
5. Sustained angiogenesis
6. Tissue invasion and metastasis

1.3.1. Self sufficiency in growth signals

Normal cells require mitogenic growth signals before they move from a quiescent state into an active proliferative state^{4 and 5}. These signals are generally external factors like diffusible growth factors, extracellular matrix components and cell to cell adhesion molecules⁵. Cancer cells generate their own growth signals in an autocrine fashion or by over expressing growth signal receptors to become hyper-responsive to normal tissue levels of growth factors. This leads to reduction of their dependency on stimulation from their normal tissue microenvironment^{4 and 6}. The cancer cells can do this by any of the following: alteration of extracellular growth signals, alteration of transcellular transducers of the signals, or alteration of intracellular circuits that translate those signals into action⁴.

Before a cell can replicate or divide several other things have to be taken care of including doubling of cell mass and chromosome segregation⁵. The coordination of cell cycle event is ordered in S, G₂, M and G₁ phases, where S and M phases represent replication and mitosis respectively, while the G phases represent the gaps or time delays to allow the cell growth^{2 and 5}. See figure 1 in page 11 for description.

During the gap phases, the system determines whether the cell cycle either proceeds or comes to halt momentarily or permanently due to DNA damage. These gaps or checkpoints allow time for repair enzymes to correct the lesion. In cancer cells regulatory proteins at the checkpoints are inactivated⁵.

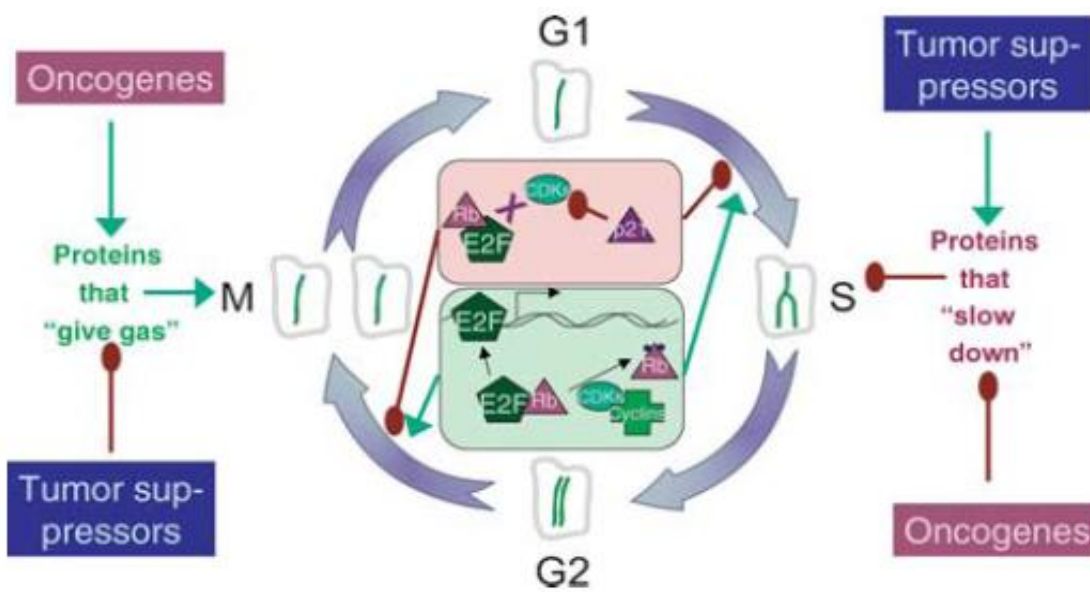


Figure 1. The cell cycle corresponds to the four different phases, each having a distinct function. In G_1 phase the cells are prepared to divide, in the S phase cell division/replication takes place. In G_2 phase chromosomes are doubled and mitosis initiated, whereas in M phase the actual chromosome separation and cell division takes place. This cycle is under strict regulation with RB, CDKs and cyclins being the major players⁹.

1.3.2. Insensitivity to antigrowth signals

Normal cells have antiproliferative signals that maintain tissue homeostasis. These signals are found both as soluble growth inhibitors and immobilized ones in the extracellular matrix. Antigrowth signals work by two ways; either forcing cells out of proliferation into a quiescent state (G_0) from which the cell can re-emerge later when the cell cycle sees it fit, or the cell might be induced to enter post mitotic state. Cancer cells have to find a way of evading both possibilities^{4 and 5}. Most antiproliferative signals use retinoblastoma proteins (pRB) and its relatives like p107 and p13^{4 and 6}.

The following molecular process takes place before a cell is either sent to a quiescent or a post mitotic state is the following. When DNA is damaged, both ataxia-telangiectasia mutated protein kinase (ATM-PK) and DNA dependent protein kinase (DNA-PK) are activated. They will in turn activate the tumour suppressor p53; this will in turn activate p21, which mediates cell cycle arrest through dephosphorylation of the retinoblastoma protein (pRB)⁷. When in a hypophosphorylated state, pRB blocks proliferation by altering the function of E2F transcription factors that control the expression of genes necessary for the progression from G_1 into S phase⁴. In cancer cells, pRB is disrupted resulting in liberation of E2F, which allows cells to proliferate, rendering them insensitive to antigrowth factors that normally operate along the way⁴.

Another molecule that is controlled by pRB is the oncogenic Id. See figure 2 in page 13 for the mechanism. The suppression of this molecule is concentration dependent; meaning when the Id concentration overrides the pRB amount controlling it, tumour cells proliferate⁸. Signalling molecules like $TGF\beta$, for example prevent the phosphorylation that inactivates pRB, meaning $TGF\beta$ blocks the advance through G_1 ^{4 and 5}. The pRB circuit governed by the $TGF\beta$ can be disrupted in several ways by the cancer cells; $TGF\beta$ can lose responsiveness through down regulation of $TGF\beta$ receptors on the cancer cells, while others can display mutant or dysfunctional receptors⁴.

The other way of taking care of DNA damage was to instruct cells to irreversibly enter post mitotic, differentiated states. It is therefore apparent that tumour cells must use various strategies to avoid this terminal differentiation. One such strategy is c-Myc over expression, which leads to Myc-Max complexes that favours growth instead of normal expression of c-Myc, which forms Mad-Max complexes that favours terminal differentiation⁴.

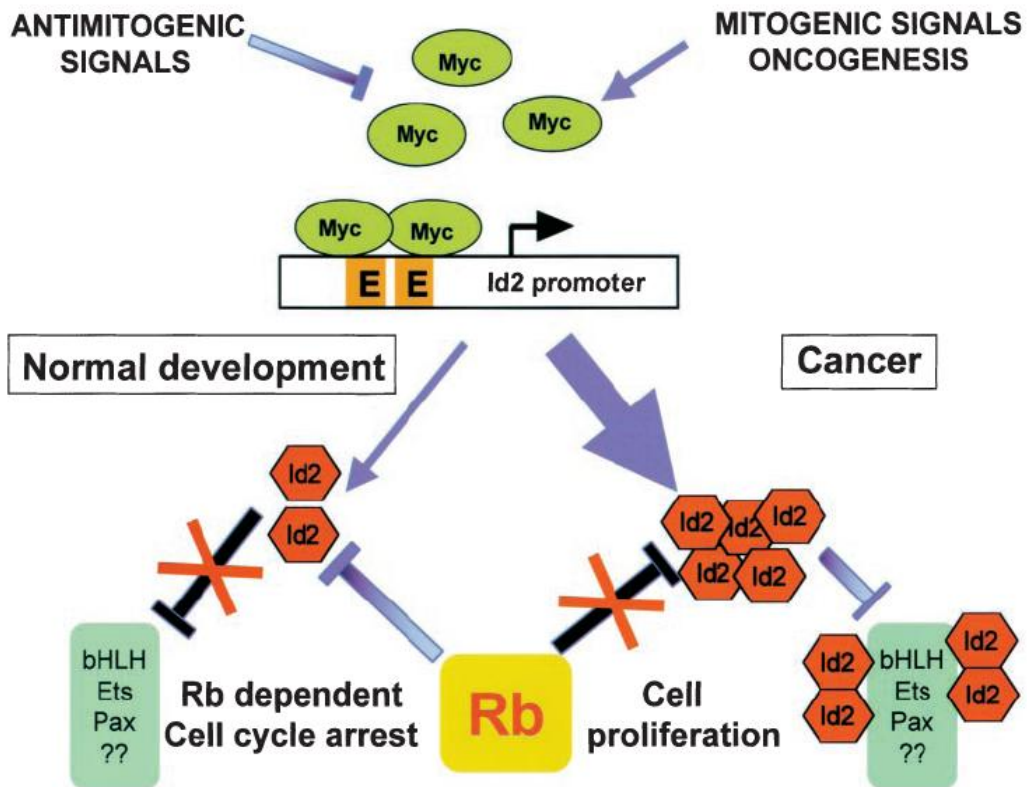


Figure 2. The Myc proteins are targets for both mitogenic and antimitogenic signals. When activated by mitogenic signals, they become powerful oncoproteins. They bind to the E boxes of the Id 2 promoter and activate transcription. The Id 2 increases in concentration so that the pRB, which inhibits it, is defeated. The Id 2 will then be free to inhibit the natural targets that control cell proliferation⁸.

1.3.3. Evading apoptosis

In order to achieve uninterrupted proliferation, cancer cells must not only divide continuously they must also find a way of evading apoptosis, since expansion of tumor cell is determined not only by the rate of cell proliferation but also by the rate of cell attrition⁴. The apoptotic program is present in virtually all cells in a latent form. Once triggered this program unfolds into a controlled series leading to disruption of cellular membranes, breakdown of the cytoplasmic and nuclear skeletons, extrusion of cytosol, degradation of chromosomes and fragmentation of the nucleus. In the end, the waste of such a process is engulfed by nearby cells in a tissue and disappears⁴.

Avoiding or resisting apoptosis is a complex process, which manifest in either of two ways. The first way is through changes in susceptibility to death signals. This effect is mediated by changes in the cells apoptotic machinery represented by proteins from the Bcl-2 family, the p53 tumor suppressor protein, or the CD95 receptor CD95/ligand system. The second way manifests itself as changes in the cells survival system represented by insulin-growth factor IGF/IGFR pair¹⁰.

Resistance to apoptosis occurs when the genes facilitating apoptosis are impaired; an example of such a gene is p53⁴. This gene is involved in cell cycle control, apoptosis and even maintenance of genetic stability. Cells defective of p53 can therefore escape apoptosis and continue dividing when their DNA is damaged. A consequence of defective p53 is that chromosomes get fragmented and incorrectly rejoined creating further rounds of cell division. Such chromosomal mayhem can lead to both loss of tumor suppressor genes and activation of oncogenes².

Apoptosis is an extremely important process; therefore, the final effectors of apoptosis are tightly regulated. The inhibitors of apoptosis protein (IAP) are the only endogenous proteins that regulate initiator and effector caspases^{11 and 12}. Figure 3 in page 15 describes the structural difference between the inhibitors of apoptosis proteins. The human IAPs are seven in number, currently only X-linked inhibitor of apoptosis protein (XIAP) is the suggested to both bind caspases and inhibit apoptosis. The others like cIAP1 and cIAP2 binds caspases but are not direct antagonist¹¹.

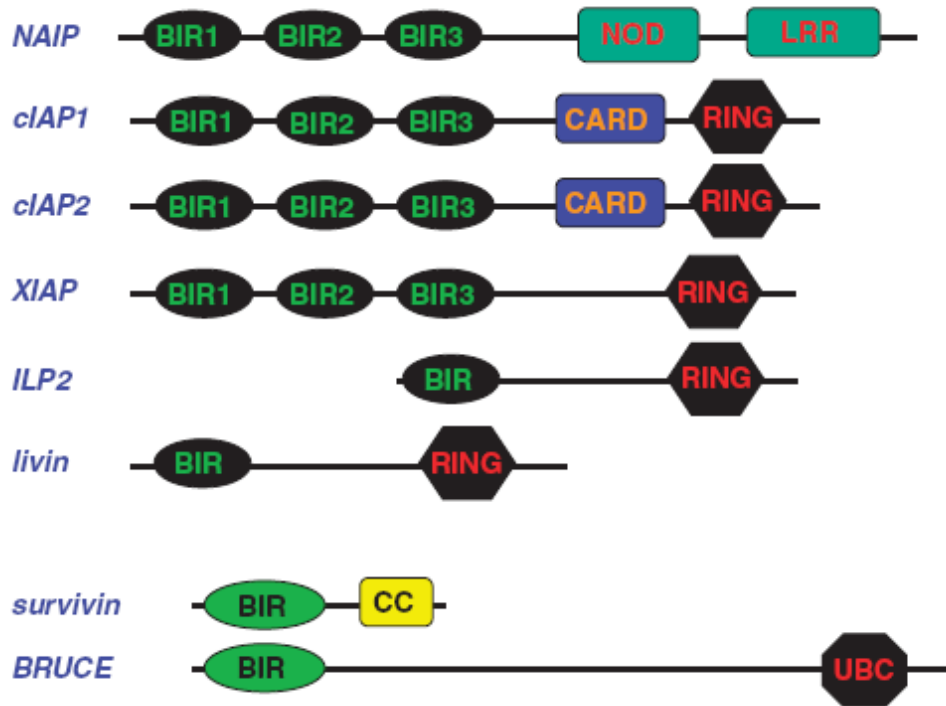


Figure 3. Domain structure of human inhibitors of apoptosis proteins. The presence of at least one baculovirus IAP repeat (BIR) is a defining characteristic of the IAP protein¹¹.

1.3.4. Limitless replicative potential

The three properties named above constitute all cell to cell signalling. Having defects in only cell-to-cell signalling alone does not lead to growth of cancerous tumours. Each cell has its own intrinsic, cell autonomous program that limits their multiplication. Cells have finite replicative potential. Once the cell population has progressed through a certain amount of doubling, they stop growing. This process is called senescence⁴.

This senescence can be circumvented by disabling pRB and p53 tumour suppressor gene, which leads to continued multiplication of the cell until it reaches a state termed crisis. This crisis state is characterised by massive cell death, karyotypic disarray associated with end-to-end fusion of chromosomes and the emergence of 1 in 10⁷ which has acquired the ability to multiply without cell death⁴.

This limitless replication is seen when a cell starts losing its telomeric DNA. See the figure below for illustration. When telomeres are lost the ability to protect the ends of chromosomal DNA is also lost. The unprotected chromosomal end participates in end to end chromosomal fusion leading to the karyotypic disarray associated with the early crisis^{4 and 13}.

This early crisis can be circumvented by the Hayflick limit, but an inactivation of these limits can give advance to early crisis. Continuation of this crisis from an early stage to late stage is hindered by active p53. If the late crisis is reached and no telomere maintenance is evident the cell survives¹³. Telomere dysfunction is evident in all types of cancer. This is possible by either upregulating the expression of telomerase enzyme or by activating ALT, which appears to maintain telomeres through recombination based interchromosomal exchanges of sequence information⁴.

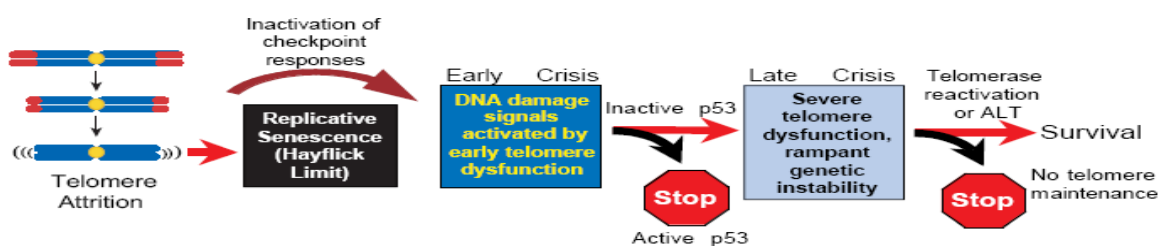


Figure 4. With cell division in the absence of telomerase, the telomere erodes. Such erosion of telomere elicits Hayflick limit preventing the cell from entering an early crisis. Inactivation of Hayflick limit leads to early crisis, which can proceed to late crisis if not averted by active p53. When p53 is bypassed and no telomere maintenance is evident, cell survival is a factum¹³.

1.3.5. Sustained angiogenesis

Mammalian cells are to be located within 100-200µm of blood vessels which is the diffusion limit if they are to be supplied with oxygen and other nutrient necessary for survival. Growth beyond that distance requires recruitment of new blood vessels by vasculogenesis and angiogenesis^{14 and 15}. For an illustration of how blood vessels are formed, see figure 5 in page 18.

Without blood vessels, tumours can neither grow beyond critical size nor metastasize to other organs. In addition, without efficient blood supply delivery of anti cancer drugs to all tumour regions in effective quantities would not be possible¹⁴.

There is a balance between the positive and negative signals, which encourage or block angiogenesis respectively and such a balance is termed as the angiogenic switch^{4, 14 and 15}. The angiogenic switch is off when the effect of pro-angiogenic molecules is balanced by that of anti-angiogenic molecules and on when the balance is tipped in favour of angiogenesis^{14, 15 and 16}. Various signals can trigger this switch, including metabolic stress, mechanical stress, immune/ inflammatory response and genetic mutations¹⁴.

One class of the signal conveyers that initiate angiogenesis is vascular endothelial growth factor (VEGF)¹⁴. Integrins and adhesion molecules mediating cell to matrix or cell to cell association play critical roles also. A class of angiogenesis inhibitors is thrombospondin-1. Integrins contribute to this regulation, whereby quiescent vessels express one class of Integrins while sprouting vessels express another; the signal interference with the latter can lead to inhibiting angiogenesis⁴.

One usually finds a balance between the inducers and inhibitors. This balance can be tipped to favor vascularisation in two ways: either by increasing the concentration of the inducers or decreasing the concentration of the inhibitors¹⁶. One way of increasing inducer concentration is by altering the genetic transcription; this is evidenced by the increased expression of VEGF on tumour cells compared to their normal counterparts. The other way involves downregulation of endogenous angiogenesis inhibitors like thrombospondin⁴.

Oncogenes can influence angiogenesis in the following ways. They can encode secreted proteins that are potent angiogenic factors; others can stimulate the production of angiogenic factors, while sometimes activated oncogenes can indirectly contribute to angiogenesis by stimulating the production and activation of a variety of enzymes that can degrade the matrix and basement membrane which sprouting vessels must transverse¹⁶.

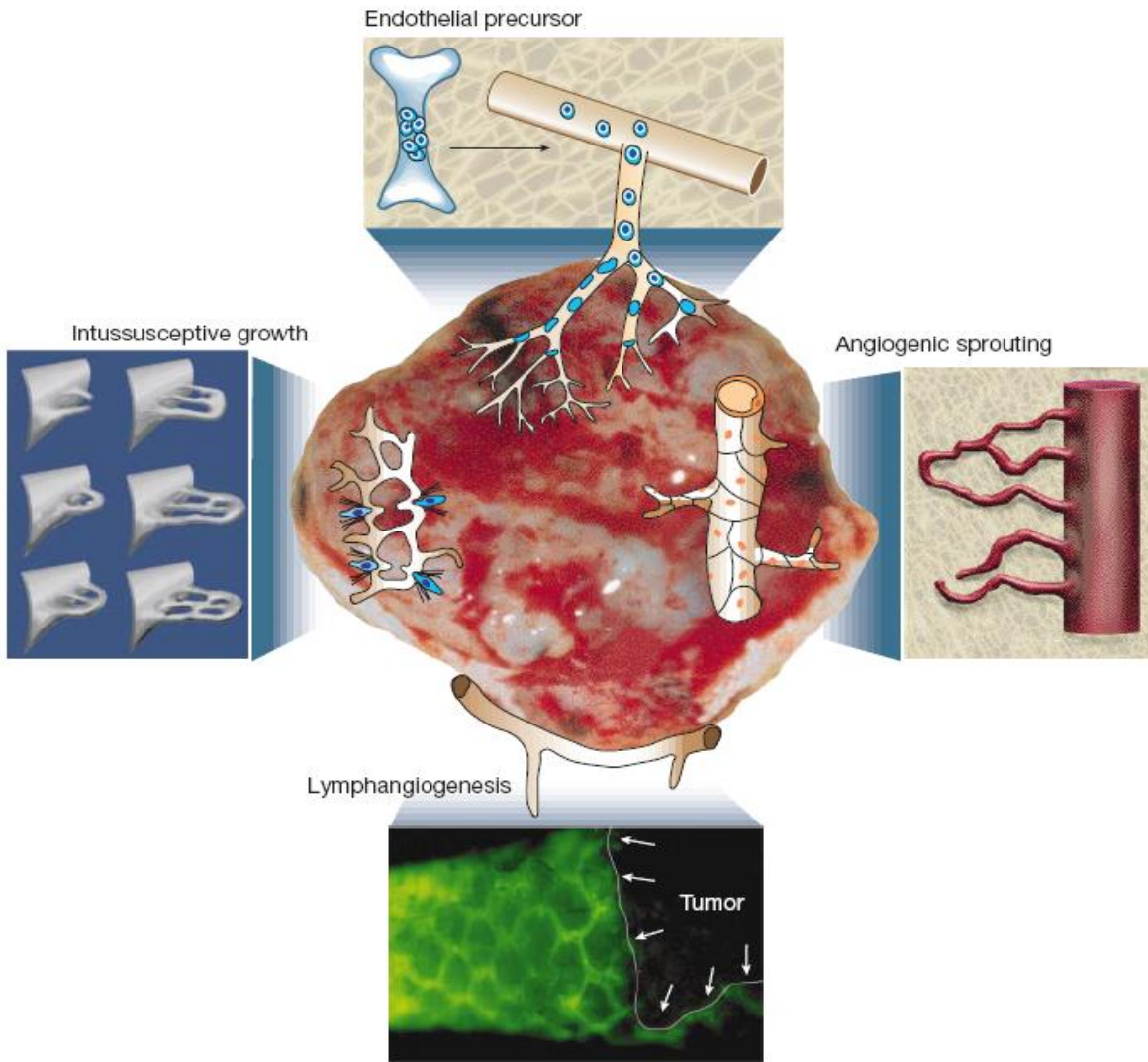


Figure 5. *Mechanisms of tumour angiogenesis. There are three different mechanisms: the first being vascular network expanding by budding of endothelial sprouts, this is termed as angiogenic sprouting. Secondly the tumour vessel can remodel and expand by insertion of interstitial tissue columns into the lumen of pre-existing vessels, this is called intussusceptions. Lastly endothelial cell precursors from the bone marrow flow into the tumour and contribute to the endothelial lining of tumour vessels (vasculogenesis)¹⁴.*

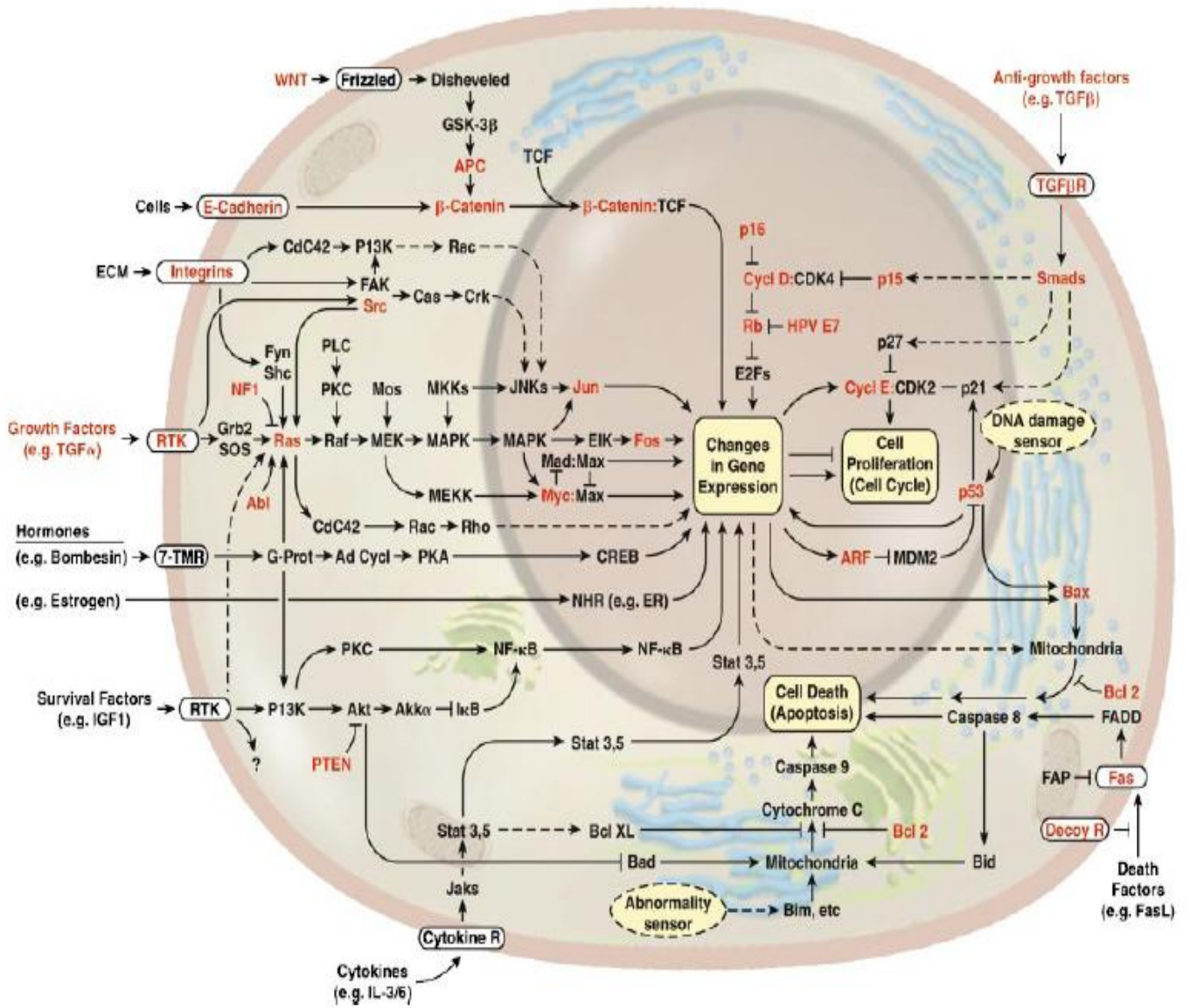


Figure 6. A circuit of the cell with all the involved mediators. Genes known to be functionally altered in cancer are highlighted in red⁴.

1.3.6. Tissue invasion and metastasis

With time most of human cancer cells develop pioneer cells that move out, invade adjacent tissues and travel to sites far from their origin, where they colonise and temporarily get unlimited nutrients and space⁴. The migration to distant sites through the lymphatic system or bloodstream is what makes cancer deadly, as 90 % of cancer death is as a result of metastasis^{4, 17 and 18}.

How successful invasion and metastasis are depends on the other hallmarks of cancer, but what makes them different from the other hallmarks? The answer to this question is that this two properties are complex processes whose genetic and biochemical determinants are not fully understood⁴. What is of no surprise; however is the mechanisms that propel invasive growth and metastasis are also found in embryonic development though to a less aggressive extent in tissue maintenance and repair processes¹⁸.

Cancer cells can preferentially bind to different types of cells like epithelial, fibroblast or even endothelial cells. What makes this possible for cancer cells are cell to cell adhesion molecules (CAM), and they fall into three main families, immunoglobulin, cadherins and the integrins^{4 and 18}. The best way to explain CAM involvement is E cadherin. The function of E cadherin is lost in the majority of epithelial cancer, the mechanism being inactivation of E cadherin⁴.

Forced expression of E cadherin in cultured cancer cells impairs both invasion and metastasis, while interfering with E cadherin enhances both capabilities⁴. This leads to the conclusion that CAMs are not simply superglues organizing cells in static structures, but support and direct the dynamic interchange of information between the two cells by interaction of the cytoplasmatic region and kinases as well as through other growth factor receptors¹⁸.

The integrins also take part of invasion and metastasis. They are essential for progression because when cancer cells invade and move away from the primary site they encounter a different environment that requires adaptation. Part of this adaptation can come from changing some of the integrins that favour extracellular matrix (ECM) to others that preferentially bind the degraded stromal components produced by extracellular proteases^{4 and 18}. In addition they regulate signalling pathway which controls actin and cell movement¹⁸.

1.4. Current cancer management

Anticancer drugs are divided into groups according to their mechanism. The groups are cytotoxic drugs, hormones, immune modulating drugs, cytokines and drugs against growth regulating factors. For a few groups, cancer drugs can lead to curing the disease, but for most types of cancer drug treatment is given only for palliative effect²².

1.4.1. Cytotoxic drugs

As the name implies these are drugs that lead to cell death. Some interfere with DNA synthesis, others with the RNA, others with the proteins and others with enzymes and microtubules. They are ordered into groups depending on their mechanism³.

1.4.2. Alkylating agents

They are defined as compounds capable of replacing a hydrogen atom in another molecule with an alkyl radical¹⁹. Very many different compounds can function as alkylating agents, but only a few of these compounds are useful clinically¹⁹. Structure of the most commonly used alkylating drugs is shown below in figure 7.

They have an alkyl group that forms a covalent bond with the cell substituent, meaning unlike other drugs in medicine their effect is as a result of covalent binding with cell constituents³ and ¹⁹. They form a carbonium ion *i.e.* a carbon atom with only six electrons in the outer shell; such atoms are highly reactive and react instantly with electron donors like amine, hydroxyl or sulfhydryls. Most of the alkylating agents have two such alkylating groups leading to a cross linking that results in defective replication because of the substitution of AT for GC, or it can cause excision of guanine and chain breakage³.

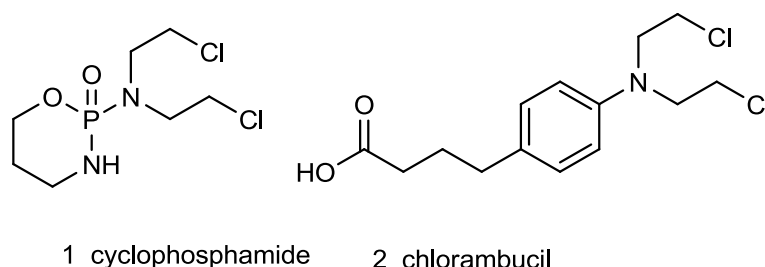


Figure 7. Alkylating agents belonging to nitrogen mustard analogue.

1.4.3. Antimetabolites

Antimetabolites a class of anticancer drugs with resemblance to naturally occurring biological molecules and interfere with essential biochemical processes requiring native metabolites²⁰. They can be divided into folate antagonists, pyrimidine and purine analogues. Methotrexate is an example of folate antagonist; it works by inhibiting dihydrofolate reductase, preventing the generation of tetrahydrofolate from folic acid resulting in interference with thymidylate synthesis and thus synthesis of DNA³. See figure 8 in page 23 for structures.

Both antipurines and antipyrimidines resemble 2'-deoxyadenosine (dA), 2'-deoxyguanosine (dG), 2'-deoxycytosine (dC) and 2'-deoxythymidine (dT) respectively. They therefore interfere with the precursor pools required for DNA synthesis²⁰. The nucleoside triphosphate (NTP) formed with the antipurines and antipyrimidines gets incorporated into the DNA in place of the native dNTPs. Such incorporation alters the structural and biochemical properties of DNA²⁰. These altered properties are responsible for DNA-protein interaction that leads to the interference of the DNA repair and replication²⁰.

Pyrimidine analogues interfere with 2 deoxythymidylate (DTMP), it's converted to fraudulent nucleotide fluorodeoxyuridine (FDUMP), this cannot be converted to DTMP, resulting in the inhibition of DNA synthesis, but not RNA or protein synthesis³. Purine analogues are potent inhibitors of DNA synthesis owing to their direct inhibitory effect on ribonucleotide reductase²¹.

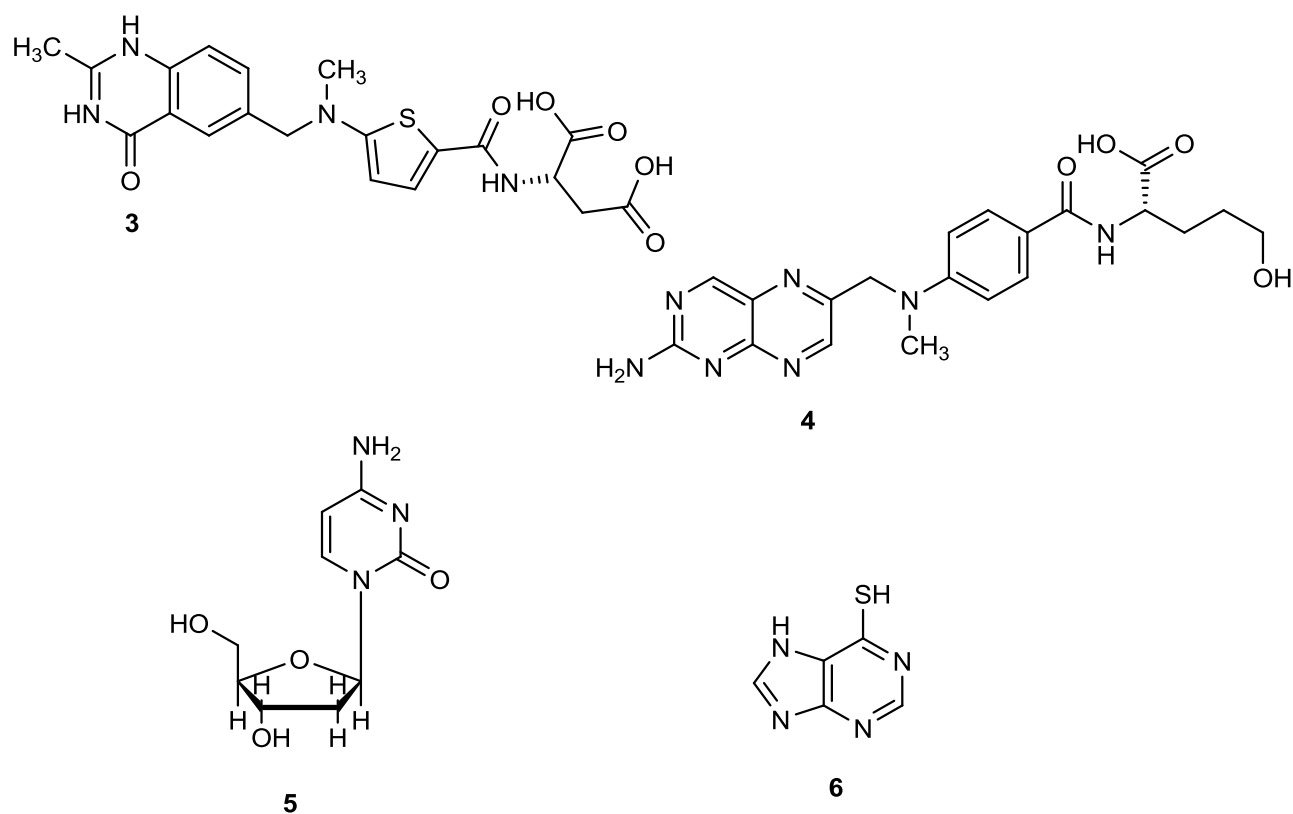


Figure 8. A summary of the most common antimetabolites are presented in the figure. The first two 3 and 4 represent folate antagonist, while the last two represents 5 and 6 are purine and pyrimidine analogues respectively.

1.4.4. Cytotoxic antibiotics

Cytotoxic antibiotics have their main effect by direct interference of DNA function. The main group is the anthracycline derivatives like doxorubicin, epirubicin and daunorubicin. Other antibiotics with cytotoxic activity include mitomycin and streptozocin^{3 and 22}. Mechanisms of action for the anthracycline derivatives include: intercalating DNA, inhibiting topoisomerase II and generating free radicals. The other group of cytotoxic antibiotics are heterogeneous when it comes to both the mechanism and clinical use²². In page 24 structures of some anthracyclines derivatives are presented.

The anthracyclines are the most clinically used cytotoxic antibiotics and the most effective anticancer drugs ever developed²³. However, antibiotic resistance is a major problem with this class of drugs. One of the main reasons for resistance is the over expression of membrane-located efflux pumps of the ATP-

binding cassette family (ABC transporters)²⁴. These are proteins that facilitate transport of the drug out of the cells before reaching their intracellular targets²⁴.

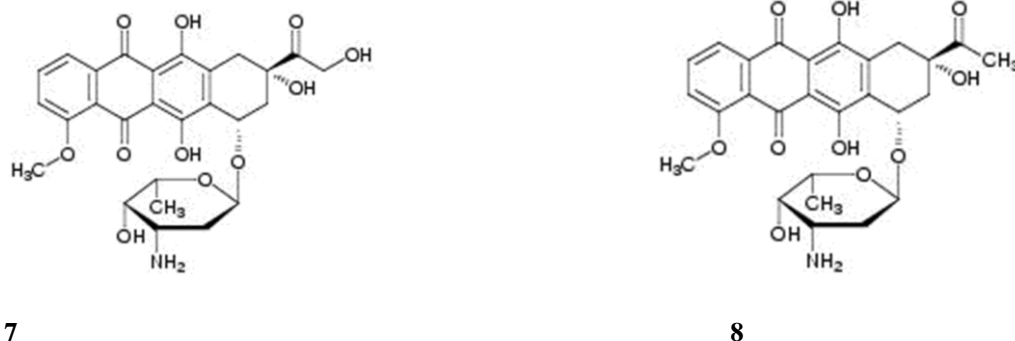


Figure 9. Examples of some cytotoxic antibiotic; doxorubicin and daunorubicin as 7 and 8 are both anthracycline derivatives.

1.4.5. Natural products

The plant derivatives are divided into the following groups: vinka alkaloids, taxanes, etoposide and camptothecins. The vinka alkaloids are vincristine, vinblastine, vinorelbine and vindisine. These are drugs that act by binding to tubulin and inhibit formation of protofilaments and microtubules, which prevents spindle formation in mitosing cells and cause arrest at metaphase^{3, 22 and 25}. The structures of a few examples of plant derivatives are shown in figure 10 in page 25.

The taxanes have different mechanisms of action than the vinca alkaloids which bind to tubulin, they instead bind to microtubules, stabilising them into polymerised state and interfering with the equilibrium between tubulin and microtubules^{3, 22 and 25}. They also bind and inactivate microtubule thereby inhibiting mitosis^{3 and 22}.

Etoposide is derived from mandrake root, its mode of action is not clearly known, but it's believed to act by inhibiting mitochondrial function^{3 and 22}. Etoposide has no affinity for tubulin and doesn't therefore have any effect on the microtubule assembly at clinically relevant levels. Its effect on topoisomerase II is thought to cause an irreversible premitotic block into the late S phase and early G₂ phase²⁵. The camptothecins inhibit topoisomerase I^{3 and 22}. Camptothecins binds to a complex formed by DNA with topoisomerase I, thereby inhibiting protein synthesis and cell division²⁵.

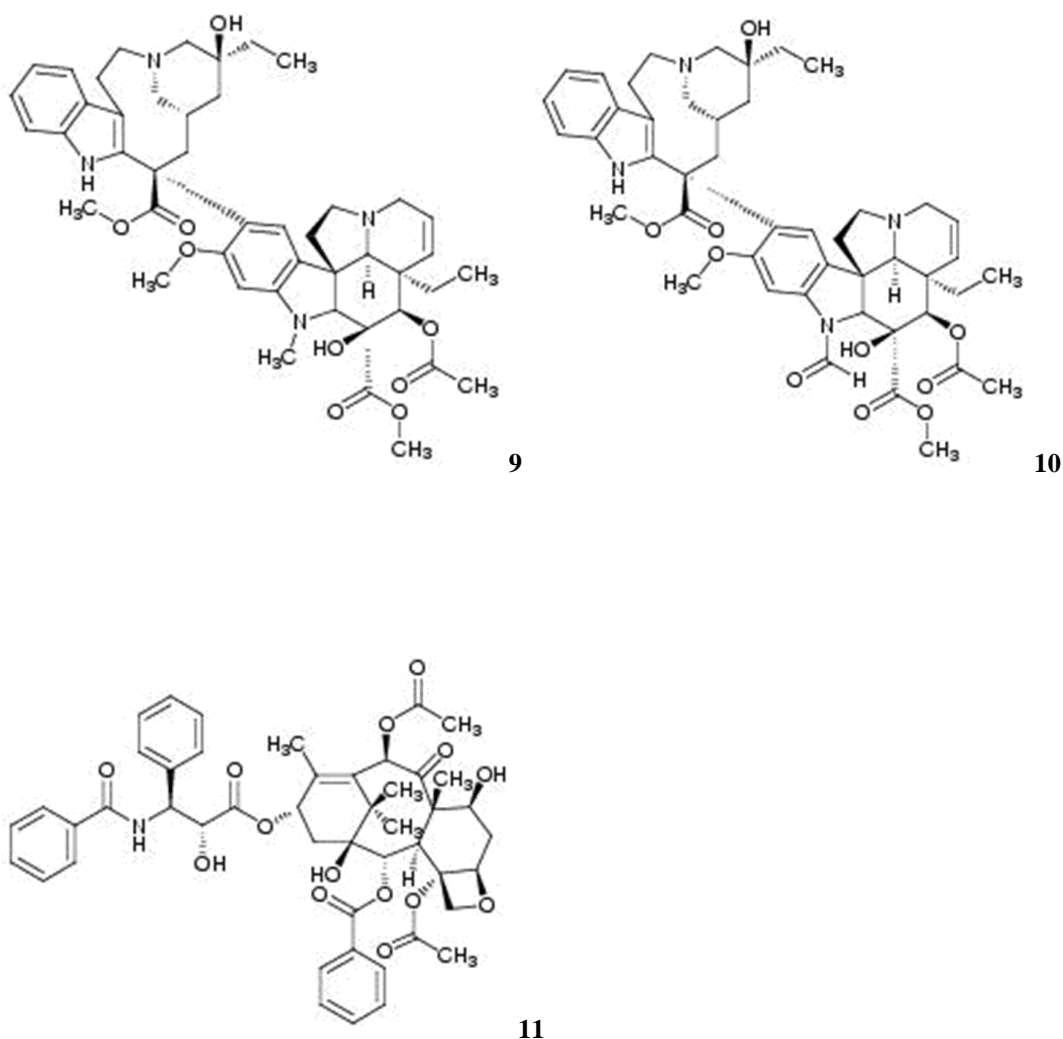


Figure 10. Some natural products used in cancer therapy, **9** is vinblastine, **10** is vinorelbine and **11** is paclitaxel

1.4.6. Hormones

Some tumours can be hormone dependent, use of hormone antagonist or substances that inhibit the synthesis of relevant hormones can be useful drugs for such tumours. As of today the following are hormones that are used as cancer drugs: glucocorticoids for leukaemias, tamoxifen for breast cancer, anti-androgen for prostate cancer and inhibitors of sex hormones synthesis for postmenopausal breast cancer³.

1.4.7. Monoclonal antibodies

Monoclonal antibodies are a new class of drugs; they are also called target therapies. One can distinguish between targeted and non-targeted therapies, the former referring to monoclonal antibodies and the latter to traditional chemotherapy²⁶.

Targeted therapies are designed to selectively inhibit a target that is abnormal and malignant compared to normal cells²⁶. Targeted therapies work on proximal events in signal transduction cascade rather than affecting the downstream outputs of these pathways²⁶. See figure 11 below. This results in drugs with fewer side effects but they are also susceptible to downstream resistance.

They are immunoglobulins that react with a specific molecular target. They can be part mouse, part human or fully human. The following are in the Norwegian market per today with cancer as an indication: alemtuzumab, bevacizumab, Cetuximab, rituximab and trastuzumab^{3 and 22}

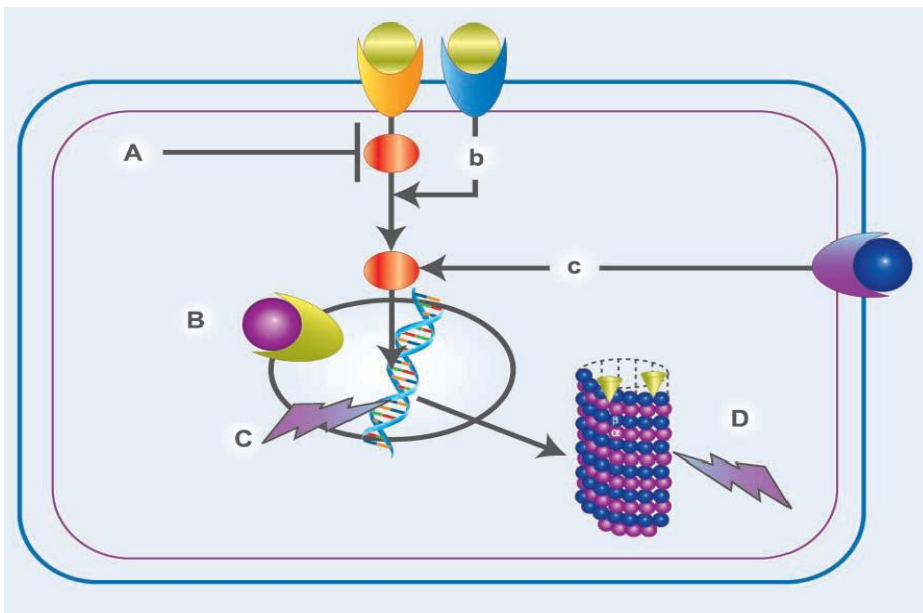


Figure 11. Subcellular localization of targeted and none - targeted therapies. Targeted here means biological or monoclonal antibodies, while none - targeted refers to traditional chemotherapy. Target A refers to targeted therapy; with b and c being pathways which can result in resistance for target A. Target B is less susceptible to this resistance. Target C and D represent none - targeted therapies and are less affected by upstream event²⁶.

1.5. Cell death

Naturally occurring cell death plays a critical role in many normal processes like foetal development and tissue homeostasis³¹. Cell death can be differentiated according to its morphological appearance like apoptosis, necrosis, autophagical etc, according to enzymological criteria like involvement of nucleases, proteases, caspases, calpains, or because of functional aspects (programmed or accidental, pathological or physiological) or because of immunological characteristics like (immunological or non immunological)²⁷.

Cell death is usually discussed as apoptosis and necrosis, where the former means programmed and the latter accidental. Since it is programmed apoptosis avoids eliciting inflammation. Necrosis, on the other hand is passive and accidental which results from environmental disturbances leading to uncontrolled release of inflammatory cellular contents²⁸. Recently, research has proved that necrosis appears to be a well regulated event carried out by a set of controlled signal transduction pathways and execution mechanisms that contribute to both the development and maintenance of homeostasis^{29 and 30}.

Accordingly the nomenclature committee on cell death has proposed in October 2008 unified criteria for the definition of cell death according to its morphology. Apoptosis is thus not defined as programmed cell death but occurs only when the following morphological aspects of cell death are seen: reduction of cellular volume, chromatin condensation, nuclear fragmentation, little or no ultra structural modification of cytoplasmic organelles, plasma membrane blebbing and engulfment by phagocytes.

Autophagic cell death is defined as cell death that occurs in the absence of chromatin condensation, but accompanied by massive autophagic vacuolization of the cytoplasm. Necrotic cell death is characterised by gain in cell volume (oncosis), swelling of organelles, plasma membrane rupture and loss of intracellular contents²⁷. The different type of cell deaths and their end results are shown in figure 12 on page 28.

Cell death whether it comes by apoptosis or necrosis has both physiological and pathological effects. With suppression of cell death one encounters diseases like cancer, atherosclerosis and autoimmune disorders, while increased cell death has a direct link with viral infections like AIDS; neurodegenerative disorders like Alzheimer's disease; autoimmune disorders like multiple sclerosis; haematological disorders like myelodysplastic syndromes and ischemic injuries like myocardial infarction etc^{30 and 31}.

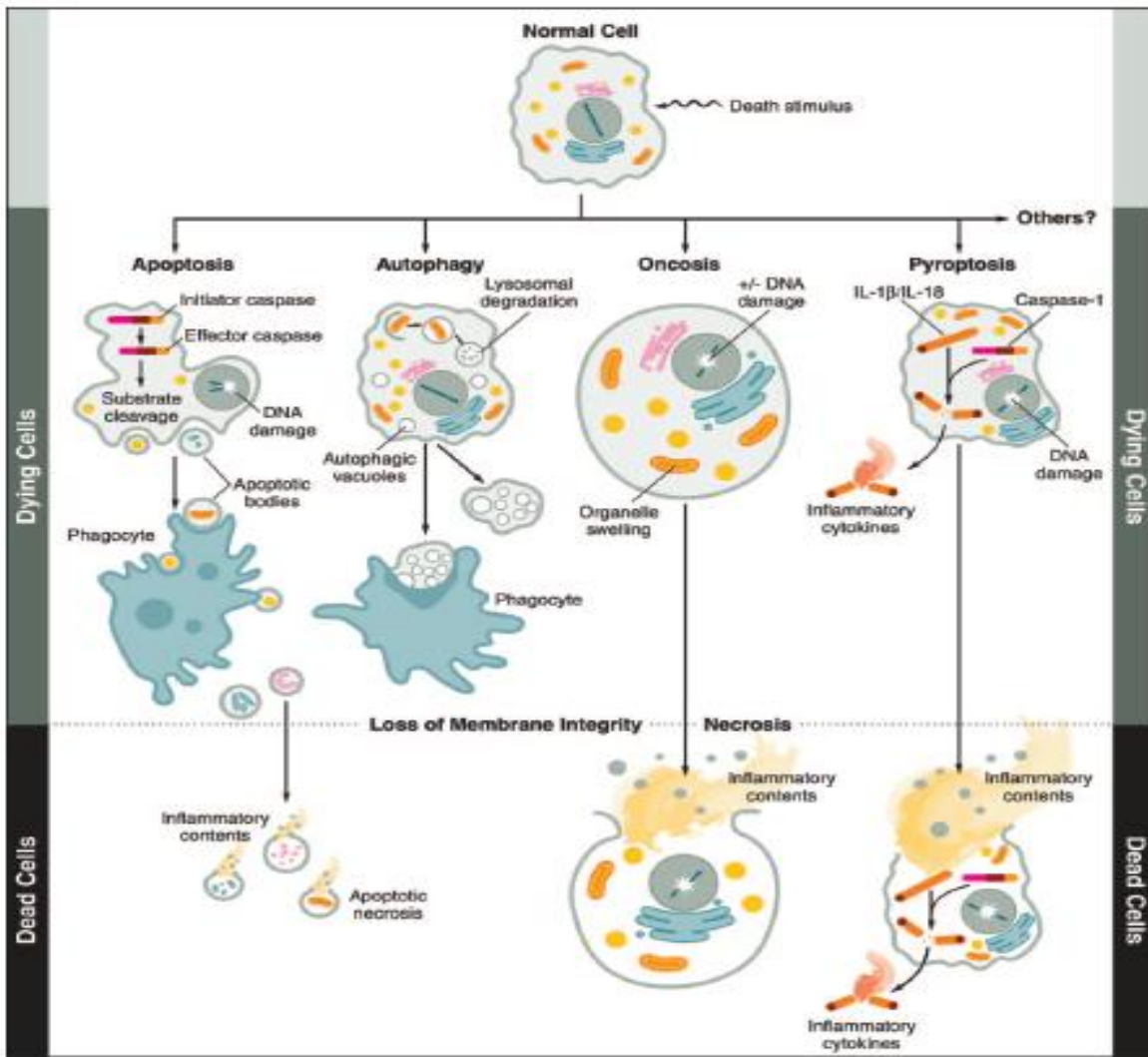


Figure 12. A summary of the type of cell death a normal cell can undergo depending on the type of stimuli with its characteristic features, while the three major types like apoptosis, necrosis and autophagy are known, pyroptosis is mediated by caspase-1 which activates inflammation²⁸.

1.5.1. Necrosis

Until 1971 all types of cell death were termed necrosis. In 1971 Kerr *et.al* observed the first non-pathological cell death and termed it shrinkage necrosis. They later renamed it apoptosis when they saw that it was implicated in the organ`s homeostasis³⁰. Necrosis was, until October 2008, defined as the opposite of apoptosis, or in other words cell death not mediated by apoptosis was termed as necrosis³⁰

Necrotic cell death or necrosis as it is shortly termed is defined as having the following morphological characteristics: gain in cell volume (oncosis), swelling of organelles, plasma membrane rupture and subsequent loss of intracellular contents²⁷. Despite the wide spread belief that necrosis is uncontrolled, accidental, or default cell death, accumulating studies have evidenced that the execution of necrotic cell death may be regulated by a set of well defined signal transduction pathways^{27, 29 and 30}.

It was recently shown that triggering of Fas or tumor necrosis factor that is usually the cornerstone of the apoptosis pathway, can induce necrotic cell death in the presence of caspase inhibitors or absence of Fas-associated death domain (FADD)²⁹. Necrostatins are the first class of inhibitors of *in vitro* necrotic cells; these necrostatins inhibit receptor interacting protein 1 (RIP) 1 kinase activity. Owing to the lack of biomarkers it is difficult to assess the importance of necrotic cell death in pathological conditions²⁹.

Some of the diseases where necrosis is implicated are vascular-occlusive diseases like heart failure, brain damage or limb loss, cancer and neurodegenerative diseases like Alzheimer`s³⁰.

1.5.2. Apoptosis

Apoptosis is a Greek word meaning falling of leaves from a tree in the autumn. The name was first coined by John Kerr in 1972 and refers to the morphological feature of the formation of apoptotic bodies from a cell³². Today apoptosis is known to be a process that is both genetically and biochemically controlled in contrast to necrosis which is known as an accidental and functionally passive process³³. It is a process that is widely known as programmed cell death. Apoptosis or programmed cell death is energy dependent and highly regulated and therefore not easily triggered³³. Apoptosis is required for foetal development and tissue homeostasis³⁴. Dysregulation of apoptosis plays an important role in diseases like neurodegenerative disorders, cancer and autoimmune diseases^{31and 33}.

The morphological properties of apoptosis in contrast it to necrosis include; cell shrinkage, membrane beebbling, partitioning of cytoplasm and nuclear contents into membrane bound apoptotic bodies and specific internucleosomal degradation of cellular DNA, which is the hallmark of this process³³.

Apoptosis can be induced in response to developmental cues or environmental stress (*e.g* viral infection, toxicant exposure). Such an induction can take place when there is a deprivation of survival factors or irreparable internal damage^{33 and 35}. Apoptosis can take place either through the intrinsic or extrinsic pathway and in either pathway the net result is cellular suicide via caspase activation^{31, 33 and 34}.

1.5.3. Apoptosis pathways

The intrinsic pathway is also called mitochondrial pathway by some authors. Participation of mitochondria in apoptosis induction involves the release of caspase activating proteins into the cytosol. Proapoptotic Bcl-2 family members Bax and Bak translocate to the mitochondria. The BH3-only protein Bid activates Bax and Bak to mediate the release of cytochrome c into the cytosol. The release of cytochrome c leads to its binding to the Apoptotic Protease Activating Factor-1 (Apaf-1). Binding of cytochrome c to Apaf-1 triggers the assembly of the apoptosome (Apaf-1and caspase-9) and subsequent activation of the caspase- 3 and cell death. The apoptosome bound procaspase-9 is activated and can then activate an effector caspase like caspase -3, which then cleaves the cellular substrate needed for orchestrating apoptosis^{31, 32, 35 and 36}. An explanatory figure for both the intrinsic the extrinsic pathway, plus the signals involved is shown in figure 13 in page 31.

The extrinsic pathway

The extrinsic pathway is also called the receptor pathway. Cell death in this pathway is initiated by TNF receptor super family, called death receptors (CD95, TRAIL-R1/2 and TNF-R1) after binding of their respective ligand (CD95L, TRAIL, and TNF). The process starts with the recruitment of adaptor proteins like Fas-associated death domain (FADD). This adaptor molecule has death domain (DD) on the one side to bind the receptor and death effector domain (DED) on the other side to bind procaspase-8. Stimulation of the TNF family receptor by their specific ligands results in the formation of death inducing signalling complex (DISC). The DISC comprises adaptor molecules like FADD and procaspase-8. The activation of the initiator procaspase-8 to caspase-8 propagates the apoptosis signal by direct cleavage of downstream effector caspases, like caspase-3. Procaspase-8 can also cleave Bid to truncated Bid which can translocate to the nucleus in order to activate the mitochondria pathway^{31, 32, 35 and 36.}

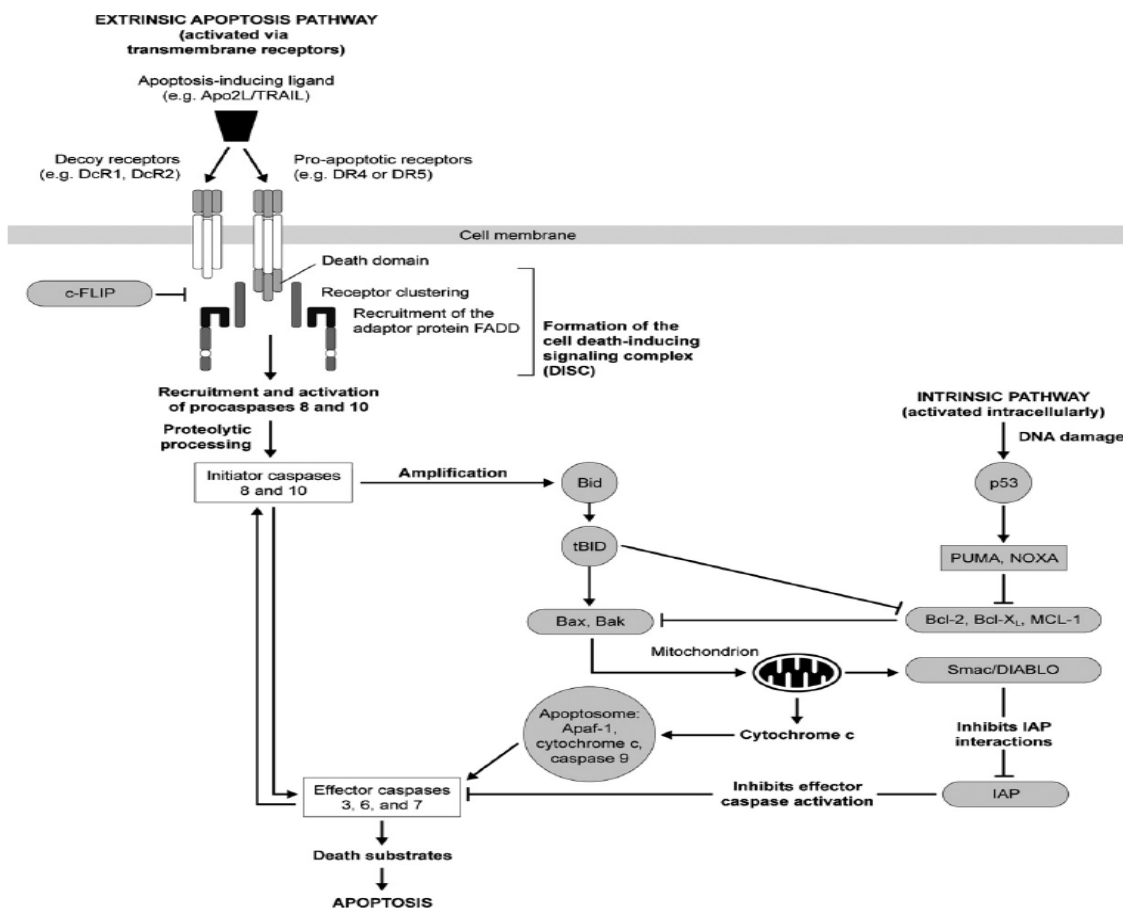


Figure 13. Apoptosis signalling pathways. These are the two important pathways of caspases activation; one involves the intrinsic pathway or mitochondria pathway, while the other one is extrinsic or death receptor pathway. The extrinsic pathway is independent of p53.

1.5.4. Caspases

The name here is the short form for cysteine-containing aspartate-specific proteases. They are intracellular cysteine proteases that have specific substrate recognition and cleave target proteins after their aspartate residue. Caspases are synthesized as inactive zymogens called procaspases in the cytosol. They can be activated either in an autoproteolytic manner or by other caspases in a cascade³⁴.

Caspases can be grouped according to their functionality. We distinguish between initiator and effector caspases. The initiator caspases are characterised by their long prodomain with more than 90 amino acids containing either DED domains, like is the case for caspase-8 and caspase-10, or a caspase recruitment domain (CARD) seen in caspase-2 and caspase-9. The executioner or the effector caspases contain short prodomains and comprise caspase-3, caspase-6 and caspase-7³².

The remaining caspases have their main role in cytokine maturation rather than apoptosis³². The initiator caspases are activated by autoproteolysis following the recruitment of the prodomain into multiprotein-complexes, the effector caspases are activated by the initiator in a cascade pathway³⁴.

Caspases are key effector molecules in apoptosis and therefore targets for pharmacological modulation in various diseases⁴². A high level of caspase activity leads to increased cell death. A number of diseases are as a result of increased levels of caspase; examples being myocardial infarction, stroke, sepsis, Alzheimers, Parkinson, and Huntington disease. Inhibition of caspase activity is predicted to be therapeutically beneficial for these diseases⁴². Inhibition of the caspases that leads to inflammation may help control autoimmune diseases like rheumatoid arthritis. Lastly activation of caspases is an approach that can result in therapeutic treatments for cancer and chronic viral infections⁴².

1.5.5. Procaspace-3 and caspase-3

Procaspace-3 are sometimes also termed immature while caspases are said to be mature. The cleavage of procaspases leads to the formation of two subunits, a large and a small one, which heterodimerize and form the active caspase enzyme³⁵. For all the caspases the active site comprises four loops L1, L2, L3 and L4. While L1 and L3 are well conserved structures, there is a substantial difference in both amino acid composition and length in L2 and L4. The exact position of these loops is what dictates caspase substrate specificity³⁴.

Since caspase-3 is one of the effector caspases it exhibits a very low activity towards self activation. However, such activation can take place by varying the pH³⁷. Other tests have also shown that caspase-3 is more sensitive not only to pH changes but also changes in ion concentration compared to its zymogen³⁸. A change in ionic homeostasis of the cell is one of the events leading to apoptosis.

Under normal conditions cells have intracellular potassium concentration of ca 140 mM; this reduces to less than 50 mM in apoptotic cells. The decrease in intracellular potassium and the associated water movement are contributing factors to the change in cell volume, one of the characteristic observed in apoptosis. Normal potassium concentration is inhibitory to apoptosis, perhaps by acting on and inhibiting apoptotic nuclease. Normal potassium concentration inhibits the cytochrome c-dependent activation of procaspase-3, but not caspase-3. The contribution of intracellular ionic strength, which potassium has shown, is not unique for ion alone, but other monovalent ions give similar effects³⁸.

Caspase-3 is the mediator caspase that is ultimately responsible for the majority of apoptotic effects. In addition to its role in cell death, caspase-3 is also important for survival, this is evidenced by caspase-3 knockout mice that are born at low frequency and die only a few weeks after³⁹.

1.5.6. Inhibitors of caspase-3

In certain pathological conditions like rheumatoid arthritis, liver injury, myocardial infarction and various neurodegenerative disorders, one sees elevated levels of activated caspase-3, which is suspected to be the cause of the excessive cell death⁴⁰. Therefore, the design of caspase inhibitors has become a major research topic for the last 10 years. In these early studies the approach was to make a peptide or a peptide mimicking agents that can inactivate caspase-3. Such research has been hampered by the therapeutic limitation these agents have as a result of poor cell permeability, *in vivo* stability and bioavailability^{36, 40} and 41.

To overcome such limitations one needed non peptide compounds, but these were difficult to identify and optimize. A series of such molecules were recently published. Isatin sulphonamides were the first ones described. They have shown limited selectivity for caspase-3 versus other executioner caspases⁴¹. Recently a series of aniloquinazolines (AQZs) were synthesized. They are structurally distinct from other non-peptide caspase-3 like isatins. The two however share an electrophilic carbonyl that certainly represents the site of nucleophilic attack by the active site cysteine thiolate. The AQZs are however more selective compared to the isatins⁴¹.

A typical peptide that has caspase-3 inhibition needs the following structural characteristics: an electrophilic group, P1 aspartic acid, and P2-P4 peptidomimetic region. The warhead interacts with the cysteine residue. The warhead reversibly binds if it is one of the following; aldehyde, nitrile, or a ketone. If it is a methylketone it binds irreversibly³⁶. The advantage reversible has against irreversible is often debated, but one can generally say that the irreversible warheads are effective in inflammation, while the reversible are effective in apoptosis. In addition the irreversible are usually said to be more specific than the reversible³⁶.

1.5.7. Activators of caspase-3

Caspases are the key effector molecules and are therefore attractive to pharmacological modulations. Activation of caspase-3 is a selective approach that yields treatment for both cancer and chronic viral infections⁴². Most drugs activate apoptosis by using the p53 pathway. Unfortunately in most of the cancer cases p53 is mutated; therefore efforts were made to bypass this upstream mutation and make molecules that target further downstream in the signal pathway⁴³.

An example of such downstream targeting is the inhibitors of antiapoptotic members of Bcl-2 family, Bcl-2 and Bcl-X_L, both of which are over expressed in cancer²⁵. Until recently apoptosome complex was not targeted. In 2003 Sunesis pharmaceuticals reported to have made compounds that promote Apaf-1 oligomerization into a mature apoptosome, resulting in activation of procaspase-9 to caspase-9 which activates caspase-3⁴³. The structures are shown below in figure 14.

These compounds can be divided into two series; the indolone series and the carbamate series. Of the compounds tested, one of the indolone series was the most potent in cells showing strong induction of caspase-3 activation, PARP cleavage, DNA fragmentation and even killing of cells with an IC₅₀ value of ca 4μM⁴³.

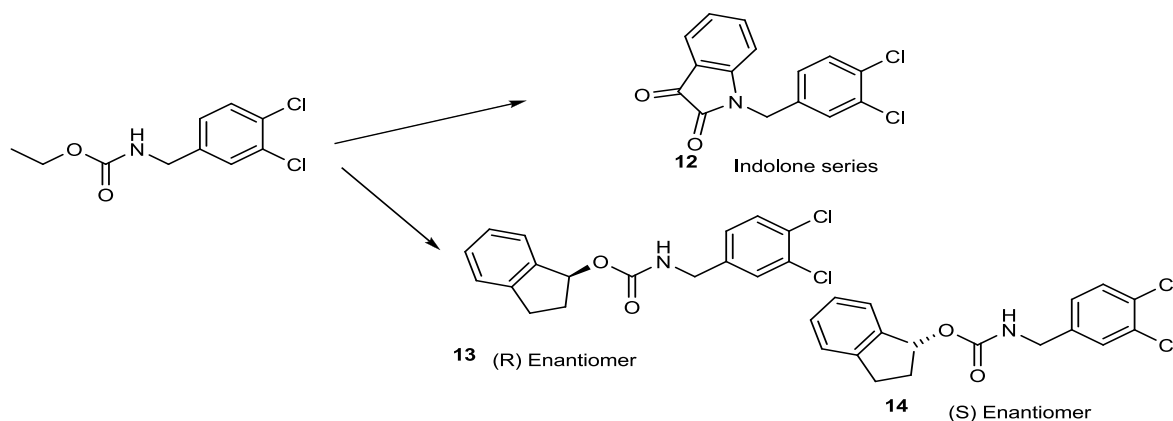
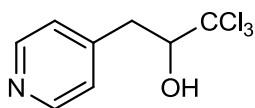


Figure 14. Compounds that affect on oligomerization of the apoptosome⁴³.

α -(trichloromethyl)-4-pyridineethanol (PETCM) is another small molecule that stimulates apoptosome formation and activation of caspase-3, shown in figure 15. This small molecule works by antagonising the effect of prothymosin- α (ProT), an oncoprotein required for cell proliferation, and enhancing the activity of putative HLA-DR associated protein (PHAP), a tumour suppressor protein⁴⁴.



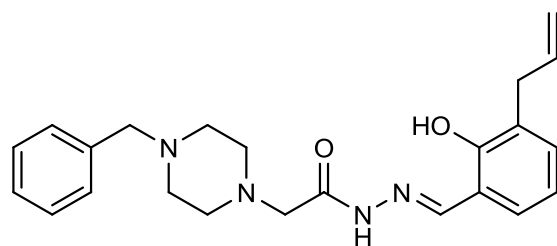
15

α -(trichloromethyl)-4-pyridineethanol (PETCM)

Figure 15. A small molecule that stimulates apoptosome formation and caspase-3 activation⁴⁴.

Efforts were made to target all of the proteins in the apoptotic cascade. Examples include peptides or small molecules binding to p53, peptides or small molecules binding to Bcl-2 family proteins, or even the inhibitors of apoptosis⁴⁵. A uniting factor for all the above targets is that they are in the early or intermediate positions in the apoptotic cascade. Therefore cancers with mutation in the downstream proteins are likely to be resistant to such attack. To make therapeutically viable molecules one needs to target proapoptotic proteins far downstream. Additionally if cancerous cells have higher concentrations of such proapoptotic protein, then this strategy would probably materialise clinically⁴⁵.

Procaspase activating compound (PAC-1) is a small molecule that directly activates procaspase-3 to caspase-3. The structure is shown in figure 16 in page 37. PAC-1 leads to chromatin condensation, cleavage of caspase substrate poly-ADP-ribose polymerase 1 (PARP-1), mitochondrial membrane depolarization and blebbing of cells⁴⁵. Procaspase-3 is a zymogen and part of the caspase group that is activated by the cascade. In order for it to resist autocatalytic activation and proteolysis by caspase-9, it has a tripartite acid safety catch⁴⁵. This safety catch is sensitive to pH; upon cellular acidification the safety catch is thought to allow access to the site of proteolysis⁴⁵. The piperazine nitrogen's of PAC-1 are believed to be positively charged at physiological pH and may directly interact with the tripartite acid safety catch, thereby inducing the auto activation of procaspase-3⁴⁵.



16 PAC-1

Figure 16. A small molecule that directly activates procaspase-3 to caspase-3 leading to induction of apoptosis⁴⁵.

2. Results and discussion

2.1.1. Synthesis of (3-allyl-2-hydroxybenzaldehyde) (18)

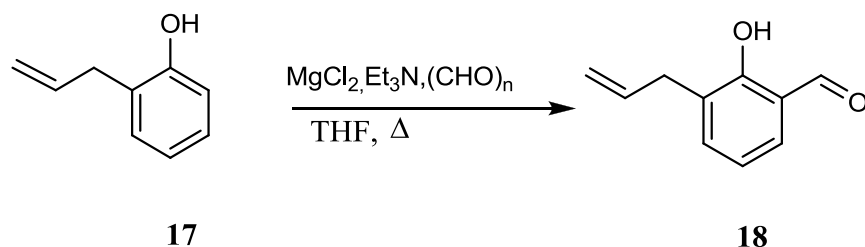
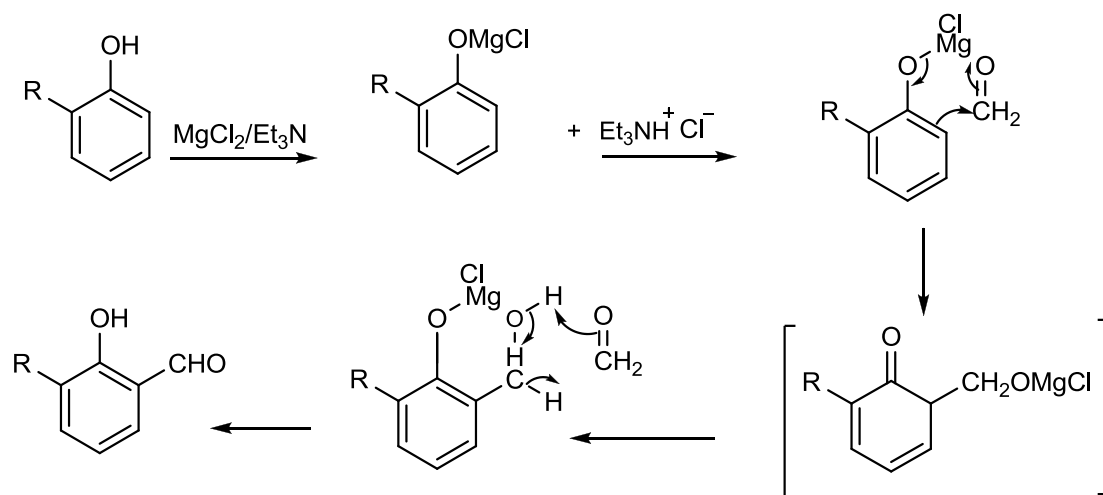


Figure 17. Depiction of the *ortho*-formylation reaction.

The reaction depicted above in figure 17 is an *ortho*-formylation. The reaction was carried out under dry conditions and resulted easily in the formation of the preferred compound (18). A plausible mechanism for the reaction depicted in Scheme 1 starts with the formation of a salt in an acid-base reaction; this salt reacts with the paraformaldehyde and forms an alcohol, which also reacts with the paraformaldehyde in a redox reaction leading to the product formation⁵⁵. The reaction mixture was purified by chromatography and resulted in 3-allyl-2-hydroxybenzaldehyde (18) with 69 % yield.



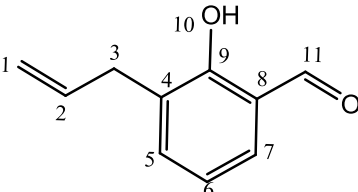
Scheme 1

A plausible reaction mechanism for the *ortho* formylation. R= allyl.

Structural elucidation of (3-allyl-2 hydroxybenzaldehyde) (18)

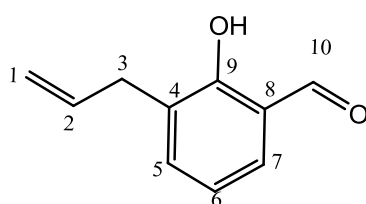
A summary of the $^1\text{H-NMR}$ obtained for **18** is given table 1. The singlet at 11.28 ppm is for (H-11), this is the least shielded proton due to the inductive effect of the oxygen. (H-10) proton is also experiencing the same effect and is seen at 9.87 ppm as a singlet. The next protons are the aromatic protons which are chemically equivalent (H-5 and 7) seen as a multiplet at 7.41 ppm. In between them comes (H-6) as a triplet at 6.95 ppm with $J = 11.34$ Hz. The aromatic protons are all observed downfield because of deshielding which results from the delocalized π - electrons. All three protons from the alkene moiety are seen as multiplets, (H-2) is assigned 5.98 ppm since the other two according to integration values come at 5.00 - 5.08 ppm. At 4.10 ppm a quartet is seen which belongs to ethyl acetate since it was used as an eluting solvent⁴⁶. Lastly (H-3) is seen as a doublet at 3.42 ppm with $J = 9.84$ Hz. A summary of the spectrum is given below, while the whole spectrum is given in Appendix 1 in page 85.

Table 1. Summary of $^1\text{H NMR}$ for 3-allyl-2 hydroxybenzaldehyde (**18**).

	δ ^1H (ppm)	Integral (H)	Multiplicity	Proton (nr)
	11.28	1	s	11
	9.87	1	s	10
	7.41	2	m	5,7
	6.95	1	t	6
	5.98	1	m	2
	5.08	2	m	1
	3.42	2	d	3

The carbon spectrum displays all the 10 carbons since there is no equivalency or symmetry. The methylene carbon (C-3) resonates at the highest upfield at 33.18 ppm. The nearest neighbour it has is the alkene carbon (C-1) at 116.64 ppm. The aromatic carbons are lead by (C-6 and C-8) showing their signals at 119.72 and 120.43 ppm respectively. The carbons (C-7 and C-4) come at 128.94 and 132.04 ppm respectively. To complete the aromatic carbons the last one (C-5) comes at 137.27 ppm. The second carbon from the alkene moiety (C-2) is detected at 136.72 ppm. The last two carbons come at downfield because of the deshielding from the electronegative oxygen the carbons are bearing. They are (C-10) for the aldehyde carbon and (C-9) for the alcohol seen at 196.86 and 159.67 ppm respectively. A summary of carbon spectre is shown in next page, while the whole spectrum is given in Appendix 2 in page 85.

Table 2. Summary of ^{13}C NMR for for 3-allyl-2 hydroxybenzaldehyde (**18**).

	δ ^{13}C (ppm)	Atom (nr)
	196.86	10
	159.67	9
	120.35	8
	128.94	7
	119.72	6
	137.27	5
	131.94	4
	33.18	3
	135.93	2
	116.40	1

Synthesis of ethyl 2-(4-benzylpiperazin-1-yl) acetate (**21**)

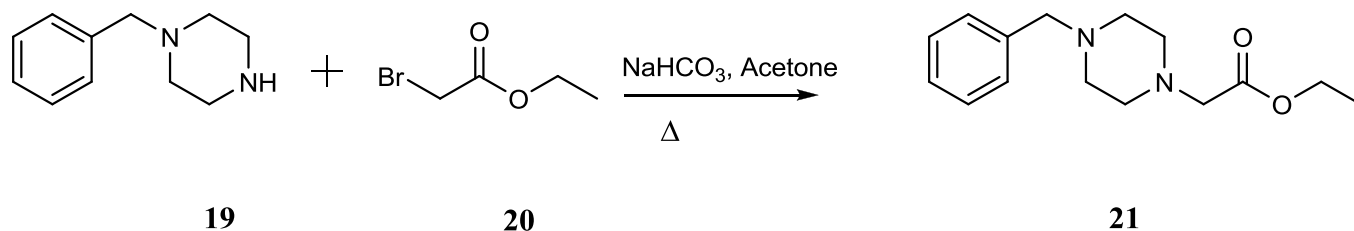


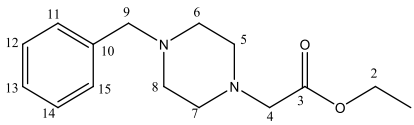
Figure 18. Depiction of the ester (**21**) formation.

In this is bimolecular nucleophilic substitution (S_N2) reaction, see figure 18 above, the piperazine (**19**) and the ester (**20**) are the nucleophile and electrophile respectively, the base is used to deprotonate the nucleophile in order to make it stronger. In the literature this reaction was carried out using chloride ester, this resulted in a longer reaction time than when bromide ester was used. This could be attributed to bond length since the bromide has longer bond length and weaker bond strength than the chloride⁴⁷. The reaction was carried out several times with isolated yields ranging from 54-67 %. The low yield could be due to lack of experience considering that it was the start of the project.

Structural elucidation of ethyl 2-(4-benzylpiperazin-1-yl) acetate (**21**)

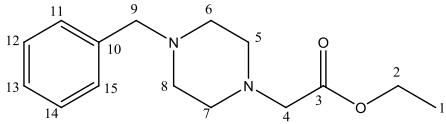
The methyl protons (H-1) are shown by the triplet signal at 1.24 ppm ($J = 7.1\text{Hz}$), since they are shielded, they give NMR resonance far upfield. They are neighbored by the broad signal from the piperazine protons (H-4, 5, 6, 7) at 2.59 and 2.52 ppm. The methylene protons attached to the piperazine (H-3, H-8) are shown as singlets at 3.51 and 3.18ppm, but it is difficult to decide which is which. Ethyl or methyl protons are usually known to appear at an upfield region between 1-3 ppm, but these an exception because they are attached to electronegative bearing carbons, this leads to deshielding and a signal further downfield. Therefore the ethyl attached to the ester (H-2) comes as a quartet at 4.16 ppm ($J= 7.1 \text{ Hz}$). Lastly, we can see the benzene protons as a multiplet at 7.30 ppm and 7.28 ppm. A summary of the spectrum is given in the next page, while the whole spectrum is presented in Appendix 3 in page 86.

Table 3. Summary of ^1H NMR for ethyl 2-(4-benzylpiperazin-1-yl) acetate (**21**)

	δ ^1H (ppm)	Integral (H)	Multiplicity	J (Hz)	Proton (nr)
	7.28	2	m		11, 15
	7.30	2	m		12, 14
	7.22	1	m		13
	3.18/3.51	4	s		4, 9
	2.52/2.59	2	brs		8
	2.52/2.59	2	brs		7
	2.52/2.59	2	brs		6
	2.52/2.59	2	brs		5
	4.16	2	q	7.1	2
	1.24	3	t	7.1	1

The ^{13}C - NMR spectrum of this compound has fewer signals than the number of carbons in the compound, due to several carbons being in the assigned identical chemical shift values, giving fewer signals. To start with the aromatic ring and carbons like (C-12, C-14) are good examples to demonstrate such symmetry both appearing at 128.38 ppm. They are followed by their neighbors (C-11, C-15) appearing at 129.38 ppm. The only aromatic carbon that is neither shown as symmetrical nor as a quartet is (C-13) appearing at 127.22 ppm while the only quartet carbon atom (C-10) is shown at 138.21 ppm. The nearest signal to the aromatic ring in the upfield region is the methylene carbon (C-9) which is seen at 63.14 ppm, while the piperazine carbon atoms are seen at 53.25 and 52.95 ppm for (C-5, C-7) and (C-6, C-8) respectively. The next carbon signal is for (C-4) the methylene between the ester and the piperazine ring coming at 59.73 ppm, while the ester carbon (C-3) is seen at 170.47 ppm. The ethylene carbon (C-2) is seen at 60.74 ppm, while the methyl carbon (C-1) is shown at 14.42 ppm. A summary of the spectrum is given in the next page, while the whole spectrum is presented in Appendix 4 in page 86.

Table 4. Summary of ^{13}C NMR for 2-(4-benzylpiperazin-1-yl) acetate (**21**)

	δ ^{13}C (ppm)	Atom (nr)
	129.38	11,15
	128.38	12,14
	127.22	13
	138.21	10
	63.14	9
	52.95	6,8
	53.25	5,7
	59.73	4
	170.48	3
	60.74	2
	14.42	1

Synthesis 2-(4-benzylpiperazin-1-yl) acetohydrazide (23)

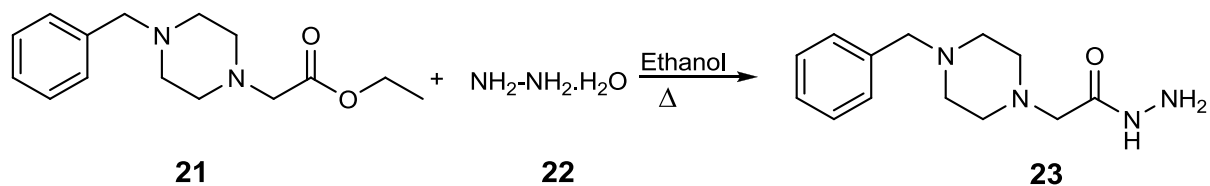


Figure 19: depiction of the hydrazine formation.

In this synthesis ethyl 2-(4-benzylpiperazin-1-yl) acetate **21** reacted with hydrazine **22** producing 2-(4-benzylpiperazin-1-yl) acetohydrazide **23**, in a classical nucleophilic addition-elimination reaction. See figure 19. According to the literature⁴⁸, the crude product is oil, which is then crystallized and further recrystallized to form the pure solid. In this particular synthesis the solid product formed upon using rotatory evaporation to remove the solvent. The product had some traces of impurities, as evidenced by ¹H-NMR in appendix 5 on page 89. This was attributed to rest of ethanol⁴⁶, but it was still used for further reaction. This experiment was also carried out in several batches resulting in isolated yields from 76-92 %.

Structural elucidation: 2-(4-benzylpiperazin-1-yl) acetohydrazide (23).

The summary of the ¹H-NMR data for this molecule is given in the next page. Starting with (H-1), the proton from the primary amine is not visible, due to the probability of exchanging with the water in chloroform. The amide proton (H-2) is seen furthest downfield at 8.10 ppm as a singlet⁴⁹. The (H-3) protons are difficult to distinguish these from (H-8), but since (H-3) are neighbouring the electronegative amide, they will most probably be deshielded corresponding to the 3.49 ppm singlet, while (H-8) will be seen at further upfield at 3.06 ppm as a singlet. The piperazine protons are also difficult to distinguish, but they are chemically equivalent as (H-5 and H-6) and (H-7 and H-8) respectively. They are seen as broad signals with two peaks at 2.52 and 2.45 ppm. The remaining 5 aromatic protons are seen at 7.31 ppm as a multiplet, here too there is chemical equivalency following (H-9 and H-13) and (H-10 and H-12), while (H-11) is supposed to be seen as a singlet. A summary of the spectrum is given in the next page, while the whole spectrum is presented in Appendix 5 in page 87.

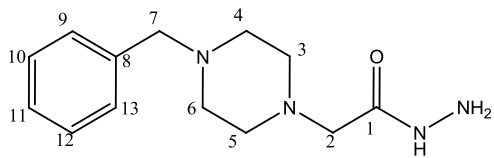
Table 5. Summary of ^1H NMR for 2-(4-benzylpiperazin-1-yl) acetohydrazide (**23**)

	δ ^1H (ppm)	Integral (H)	Multiplicity	Proton (nr)
	7.29	2	m	9,13
	7.31	2	m	10,12
	7.28	1	m	11
	3.49/3.05	2	s	8
	2.52/2.45	4	br	5,7
	2.52/2.45	4	br	4,6
	3.49/3.05	2	s	3
	8.10	1	s	2
				1

The ^{13}C - NMR has shown only 9 signals despite the molecule having 13 carbon atoms, due to the chemical shift equivalency. (C-9 and C-13) exhibit such equivalency and come at 129.32 ppm, while the other equivalent carbons from the aromatic ring are (C-10 and C-12) seen at 128.45 ppm. The other carbons with identical environments are the piperazine carbons and they are seen as (C-3 and C-5) at 53.90 ppm, and (C-4 and C-6) are seen at 53.25 ppm. The rest of carbons are single signals due to the lack of identical environments. The methylene carbons both from the benzene and the piperazine are difficult to distinguish they are (C-7 and C-2) coming at 63.08 and 60.81 ppm. The remaining carbon of the aromatic ring (C-11) is seen at 127.34 ppm, while the only quartet carbon atom (C-8) is seen at 138.07 ppm. The aldehyde carbon being much deshielded is seen farthest downfield at 170.74 ppm. A summary of the spectrum is given in the next page, while the whole spectrum is presented in Appendix 6 in page 87.

Table 6. Summary of ^{13}C NMR for 2-(4-benzylpiperazin-1-yl) acetohydrazide (**23**)

	δ ^{13}C (ppm)	Atom (nr)
	129.32	9, 13
	128.45	10, 12
	127.34	11
	138.07	8
	63.08	2/7
	60.81	2/7
	53.25	4, 6
	53.90	3, 5
	170.74	1



2.1.2. Synthesis of new PAC-1 derivatives

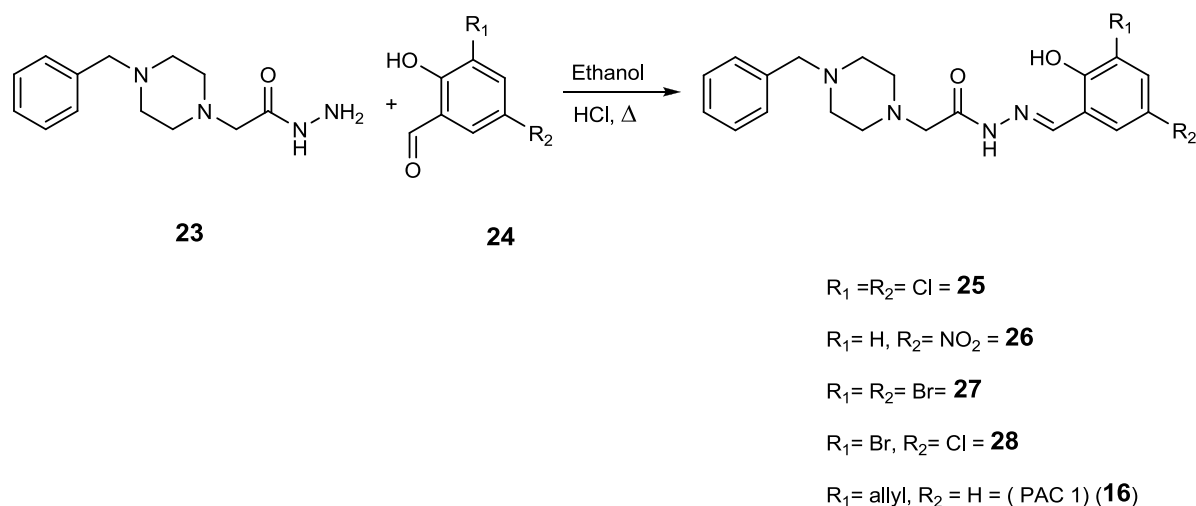


Figure 20: depiction of imine formation

In this synthesis 4-benzyl piperazino acetic acid (**23**) reacted with substituted salicylic aldehydes (**24**) resulting in an imine. See figure 20. The reaction time varied between 3- 48 hrs depending on the aldehyde. After refluxing, $^1\text{H-NMR}$ was taken to both verify the product and see if recrystallization was needed. In all the cases the product had to be purified by recrystallization due to compound decomposition in silica. The isolated yields were found to be between 89-99 %.

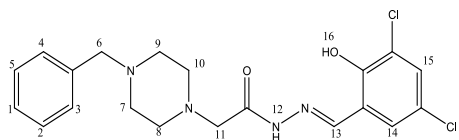
Structural elucidation:

(E)-2-(4-benzylpiperazin-1-yl)-N'-(3,5-dichloro-2-hydroxybenzylidene) acetohydrazide (25).

The product compounds all have similar ^1H and ^{13}C NMR signals with only small variations. For compound (**25**), two singlets are seen far downfield at 11.58 and 10.13 ppm, these are believed to belong to (H-12) and (H-16) respectively, due to the deshielding from the electronegative oxygen. The imine proton (H-13) appears at 8.55 ppm as a singlet. The aromatic protons appear according to the aromatic ring they belong. While those belonging to the benzene ring are shown as a multiplet at 7.30 ppm, the other two belonging to the phenol ring are shown as singlets at 7.37 and 7.11 ppm. The methylene protons (H-6, H-11) are shown as singlets at 3.54 and 3.18 ppm though it is difficult to exactly assign which is which. The same case applies to the piperazine ring appearing as a broad signal having two peaks at 2.62 and 2.53 ppm. A summary of the spectrum is given in the next page, while the whole spectrum is presented in Appendix 7 in page 88

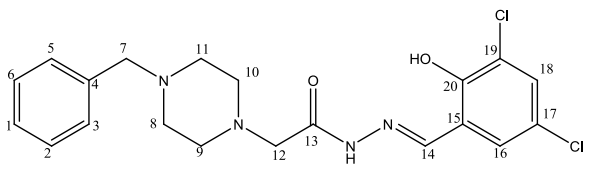
Table 7. Summary of ^1H NMR for (*E*)-2-(4-benzylpiperazin-1-yl)-*N*'-(3,5-dichloro-2-hydroxybenzylidene) acetohydrazide (**25**)

	δ ^1H (ppm)	Integral (H)	Multiplicity	Proton (nr)
	11.58	1	s	16
	7.37	1	s	15
	7.11	1	s	14
	8.54	1	s	13
	10.13	1	s	12
	3.54	2	s	6, 11
	3.18	2	s	6, 11
	2.62	4	br	(7, 9/8,10)
	2.53	4	br	(7,9/8, 10)
	7.30	2	m	2, 5
	7.30	2	m	3, 4



The carbon spectrum does not display 20 signals for the 20 carbons signals due to symmetry. All the aromatic carbons have their signals between 127.83-131.83 ppm with the exception of (C-15, C-18 and C-20) that has their peaks at 119.62, 123.10 and 153.32 ppm respectively. The rest of atoms are easily assigned, with the piperazine ring giving its peaks at 53.21 and 53.89 for (C-8, 10) and (C-9, 11) respectively. These are neighbored by the upfield methylene carbons of (C-7, 12) coming at 63.12 and 61.25 respectively. The imine carbon (C-14) is downfield at 149.52 ppm, while the amide carbon (C-13) is seen at 166.62 ppm. A summary of the spectrum is given in the next page, while the whole spectrum is presented in Appendix 8 in page 88.

Table 8. Summary of ^{13}C NMR for (*E*)-2-(4-benzylpiperazin-1-yl)-*N'*-(3,5-dichloro-2-hydroxybenzylidene) acetohydrazide (**25**)

	δ ^{13}C (ppm)	Atom (nr)
	153.32	20
	131.83	18
	119.62	15
	149.51	14
	166.61	13
	61.25	12
	53.21	8, 11
	53.89	9, 10
	63.12	7

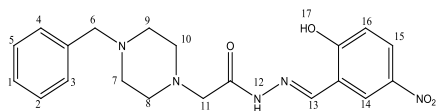
Structural elucidation:

(*E*)-2-(4-benzylpiperazin-1-yl)-*N'*-(2-hydroxy-5-nitrobenzylidene) acetohydrazide (**26**)

For this compound, the ^1H NMR spectrum is similar to compound **25**, but with a few variations. The two most downfield signals are almost similar coming at 11.87 and 10.20 ppm and belong to the amide and alcohol proton respectively. The next signals are singlets at 8.58, 8.17, 8.16 and 7.06 ppm for (H-13, H-16, H-15, and H-14) respectively. Next to these is the benzene ring whose signals occur in the aromatic region of as a multiplet at 7.30 ppm and integrate for 5 protons. In addition to that, the piperazine ring has its signals far upfield and appears as a broad peak containing all the 8 protons with chemical shifts at 2.63 and 2.53 ppm. This means that they occur as two sets of four protons showing equivalency and environmental likeliness. Lastly, one can see the methylene protons at 3.54 and 3.20 ppm are (H-6 and H-11), though it is difficult to ascertain which signal belongs to which proton. A summary of the spectrum is given in the next page, while the whole spectrum is presented in Appendix 9 in page 89.

Table 9. Summary of ^1H NMR for (*E*)-2-(4-benzylpiperazin-1-yl)-*N'*-(2-hydroxy-5-nitrobenzylidene) acetohydrazide (**26**)

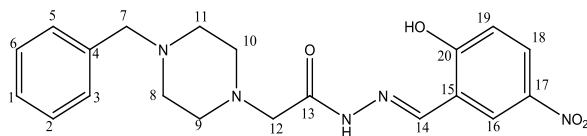
	δ ^1H (ppm)	Integral (H)	Multiplicity	Proton (nr)
	10.20	1	s	17
	8.17	1	m	16
	8.16	1	m	15
	7.06	1	s	14
	8.58	1	s	13
	11.87	1	s	12
	3.20	2	s	6, 11
	3.54	2	s	6, 11
	2.53/2.63	4	br	(7,9/8,10)
	2.53/2.63	4	br	(7,9/8,10)
	7.30	5	m	1-5



Concerning the ^{13}C NMR spectrum the compound has 20 carbons but due to symmetry only 16 signals were seen. The carbon resonating at farthest downfield is the aldehyde (C-13) with its signal at 166.47 ppm, while its nearest neighbor is no doubt from the hydroxyl carbon (C-20) coming at 163.97 ppm. Following these is the imine carbon (C-14) at 148.91 ppm. With the exception of (C- 4) seen at 140.56 ppm, the rest of carbons from the benzene ring are seen between 126.99 -129.41 ppm, together with some of the carbons from the phenol ring. Those from the phenol ring not seen in that interval are (C-15 and C-19) seen at 118.26 and 117.44 ppm respectively. Remaining then are the methylene and the piperazine carbons. They are seen further upfield neighboring signals. The methylene are the first, appearing at 62.97 and 61.05 ppm for (C-7 and C-12) respectively, while the piperazine signals are symmetrical for (C-8, 11) and (C-9, 10) at 53.07 and 53.81 ppm respectively. A summary of the spectrum is given in the next page, while the whole spectrum is presented in Appendix 10 in page 89.

Table 10. Summary of ^{13}C NMR for (*E*)-2-(4-benzylpiperazin-1-yl)-*N'*-(2-hydroxy-5-nitrobenzylidene) acetohydrazide (**26**)

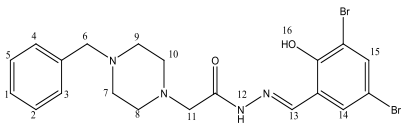
	δ ^{13}C (ppm)	Atom (nr)
	163.97	20
	117.44	19
	118.26	15
	148.91	14
	166.47	13
	61.05	12
	53.81	8,11
	53.07	9,10
	62.97	7



Structural elucidation for (*E*)-2-(4-benzylpiperazin-1-yl)-*N'*-(3,5-dibromo-2-hydroxybenzylidene) acetohydrazide (27**).**

The ^1H -NMR spectrum of this compound has similar features with the other compounds. One can see the fast pattern that is seen for all the other compounds. To start with, the far most downfield signal belongs to the amide hydrogen (H-12) at 11.73 ppm. To its right side one can see the phenol proton (H-16) with its shift value of 10.13 ppm as a singlet. Following these is the imine proton (H-13) as a singlet at 8.50 ppm. The benzene ring and the phenol ring have their protons between 7.28-7.66 ppm both as a doublet and as a multiplet. Upfield one can figure the singlets at 3.54 and 3.18 ppm for the methylene protons (H-6 and H-11) even though we cannot be certain which one belongs where. Lastly the piperazine protons are seen as two peaks at 2.62 and 2.52 ppm for (H-8, 10) and (H-7, 9). A summary of the spectrum is given in the next page, while the whole spectrum is presented in Appendix 11 in page 90.

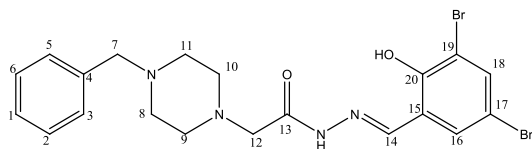
Table 11. Summary of ^1H NMR for (*E*)-2-(4-benzylpiperazin-1-yl)-*N*'-(3,5-dibromo-2-hydroxybenzylidene) acetohydrazide (**27**)

	δ ^1H (ppm)	Integral (H)	Multiplicity	Proton (nr)
	10.13	1	s	16
	7.30	1	s	15
	7.66	1	d	14
	8.50	1	s	13
	11.73	1	s	12
	2.62	4	br	(7, 9/8,10)
	2.52	4	br	(7, 9/8,10)
	3.18	2	s	(6, 11)
	3.54	2	s	(6, 11)
	7.29	2	m	(2, 5)
	7.28	2	m	(3, 4)
	7.28	1	m	1

The ^{13}C NMR spectrum is showing the typical characteristic of symmetry. That implies not all the carbon signals are shown one by one but some signals represent more than one carbon. The signal residing farthest downfield belongs to the aldehyde showing at 166.50 ppm. Close to the aldehyde comes the phenol carbon shown at 154.50 ppm. This is followed by the imine at 149.16 ppm. The carbons for both benzene ring and the phenol ring are seen at the typical benzene ring region between 120-140 ppm. Here the exceptions are (C-17 and C-19) seen at 112.21 and 110.98 ppm, respectively. The only carbons remaining belong to the piperazine and the methylene carbons. The methylene carbons are seen first and are also showing symmetry meaning all of them are not shown. Their signals appear at 63.07 and 61.19 ppm for (C-7 and C-12) respectively. The piperazine carbons have symmetry meaning only two signals are detected for the four carbons; (C-8 and C-11) have peaks at 53.17 ppm, while (C-9 and C-10) are appearing at 53.95 ppm. A summary of the spectrum is given in the next page, while the whole spectrum is presented in Appendix 12 in page 90.

Table 12. Summary of ^{13}C NMR for (*E*)-2-(4-benzylpiperazin-1-yl)-*N'*-(3,5-dibromo-2-hydroxybenzylidene) acetohydrazide (**27**)

	δ ^{13}C (ppm)	Atom (nr)
	154.50	20
	110.98	19
	112.21	17
	149.16	14
	166.50	13
	61.19	12
	53.17	8,11
	53.95	9,10
	63.07	7

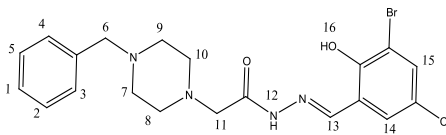


Structural elucidation:

(*E*)-2-(4-benzylpiperazin-1-yl)-*N'*-(3-bromo,5-chloro-2-hydroxybenzylidene) acetohydrazide (**28**)

The ^1H NMR spectrum of **28** is also similar to the other compounds. One can see the same pattern as the others. To start with the far downfield signals at 11.71 and 10.15 ppm belong to the amide and phenolic protons of (H-12 and H-16) respectively. The imine proton of (H-13) is seen not far from the two at 8.52 ppm. The seven aromatic protons are shown in the aromatic region between 7-8 ppm. Farther upfield one can see the methylene protons of (H-6 and H-11) as singlets at 3.54 and 3.18 ppm. Lastly we can see the piperazine protons as a broad signal containing the symmetrical protons of (H-7, 9 and H-8, 10) at 2.62 and 2.53 ppm. A summary of the spectrum is given in the next page, while the whole spectrum is presented in Appendix 13 in page 91.

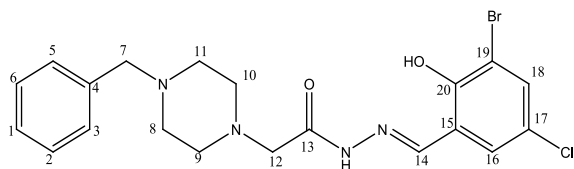
Table 13. Summary of ^1H NMR for (*E*)-2-(4-benzylpiperazin-1-yl)-*N'*-(3-bromo,5-chloro-2-hydroxybenzylidene) acetohydrazide (**28**)

	δ ^1H (ppm)	Integral (H)	Multiplicity	Proton (nr)
	10.15	1	s	16
	7.53	1	s	15
	7.52	1	s	14
	8.52	1	s	13
	11.71	1	s	12
	3.54	2	s	6, 11
	3.18	2	s	6, 11
	2.62	4	br	(7, 9/8, 10)
	2.53	4	br	(7,9/8, 10)
	7.30	2	m	(2, 5)
	7.30	2	m	(3, 4)
	7.16	1	m	1

The ^{13}C NMR spectrum is also not very different from the other compounds. Farthest downfield we can see the aldehyde carbon (C-13) at 166.37 ppm. Close to the aldehyde comes the phenol carbon shown at 154.02 ppm. This is followed by the imine at 149.21 ppm. The carbons for both benzene and the phenol ring are seen at the typical benzene ring region between 120-140 ppm, here the exception is (C-19) seen at 111.80. The only carbons remaining now belong to the piperazine and the methylene carbons. The methylene carbons are farther upfield are also showing symmetry meaning all of them are not shown. The methylene carbons are (C-7) at 62.89 ppm and (C-12) at 61.01 ppm. The piperazine are (C-8, 11) having peaks at 52.99 ppm, while (C-9, 10) are shown at 53.61 ppm. A summary of the spectrum is given in the next page, while the whole spectrum is presented in Appendix 14 in page 91.

Table 14. Summary of ^{13}C NMR for (*E*)-2-(4-benzylpiperazin-1-yl)-*N'*-(3-bromo,5-chloro-2-hydroxybenzylidene) acetohydrazide (**28**)

	δ ^{13}C (ppm)	Atom (nr)
	154.02	20
	111.80	19
	149.21	14
	166.37	13
	61.01	12
	52.99	8,11
	53.61	9,10
	62.89	7



Structural elucidation:

(*E*)-*N'*-(3-allyl-2-hydroxybenzylidene)-2-(4-benzylpiperazin-1-yl) acetohydrazide PAC-1(16).

This structure was elucidated before by Hergenrother *et al.* in late 2006. It starts as usual with the aldehyde and the phenol as singlets at 11.17 and 9.95 ppm respectively. The characteristic feature of the other compounds continues until the imine proton is visible at 8.35 ppm as a singlet. From there this molecule has shown distinct pattern with the following signals. The aromatic protons are shown as complicated multiplets and it is difficult to assign which is which. The alkene moiety has a clear signal with two of its protons coming close to one another at 4.96 ppm and 5.05 ppm, while the third one is seen at 5.96 ppm as a doublet of a doublet since it couples with the methylene and the other alkene protons. The methylene protons are also seen clearly with the downfield signal belonging to the methylene between the piperazine and the benzene, while the one next to it is for the other methylene of the piperazine. The last of those signals belongs to the methylene of the phenol. The signal at the highest upfield belongs to the eight piperazine protons. A summary of the spectrum is given in the next page, while the whole spectrum is presented in Appendix 15 in page 92.

Table 15. Summary of ^1H NMR for (*E*)-*N'*-(3 allyl-2 hydroxybenzylidene)-2-(4-benzylpiperazin-1-yl) acetohydrazide (**16**)

	δ ^1H (ppm)	Integral (H)	Multiplicity	Proton (nr)
	9.95	1	S	20
	5.00	2	m	19
	5.96	1	dd	18
	3.11	2	s	17
	6.99	1	m	16
	6.81	1	m	15
	7.02	1	m	14
	8.35	1	s	13
	11.17	1	s	12
	3.39	2	s	11
	2.54	4	d	(7, 10/8, 9)
	2.46	4	d	(7, 10/8, 9)
	3.48	2	s	6
	7.12	2	m	(2, 5)
	7.08	2	m	(3, 4)

The carbon spectrum shows expected signals for the compounds synthesized; at the same time it also shows the signals typical for this compound. There is no doubt that the two signals at farthest downfield belong to the aldehyde and the phenol respectively. They are followed by the imine carbon at 151.33 ppm. What follows these are the aromatic carbons stretching between 115.80 and 137.87 ppm. On the other side of the chloroform signal we first figure the signals belonging to the methylene carbons, which are followed by the signals of the piperidine ring. The last signal belongs to the methylene of the phenol, while the alkene signals come in the alkene region between 120-140 ppm. A summary of the spectrum is given in the next page, while the whole spectrum is presented in Appendix 16 in page 92.

Table 16. Summary of ^{13}C NMR for (*E*)-*N*'-(3-allyl-2-hydroxybenzylidene)-2-(4-benzylpiperazin-1-yl)acetohydrazide (**16**)

	δ ^{13}C (ppm)	Atom (nr)
	115.80	23
	136.64	22
	33.99	21
	156.51	20
	117.02	15
	151.33	14
	165.99	13
	61.10	12
	52.80	8, 11
	53.82	9, 10
	63.00	7

2.1.3. Efforts to synthesize other PAC-1 derivatives

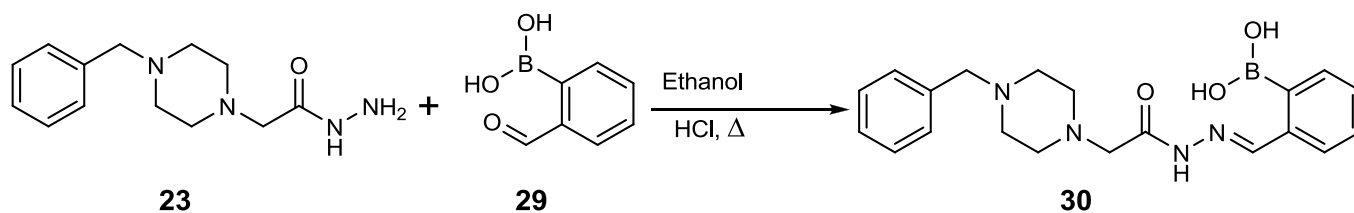


Figure 21: depiction of the imine with boronic acid derivate

The reaction depicted in figure 21 was also attempted. Generally it is similar to the reactions that resulted in compounds **16**, **25-28**. The idea behind the reaction was if the phenol moiety is important and part of the pharmacophore then creating a boronic acid moiety would fulfil that function. Under the same conditions for the previous reactions, the product was formed after 4 hours. As was the case for the other products this one too had to be recrystallized, after trying several solvents both in one solvent and two solvent methods, the product was still not pure and the process was therefore stopped.

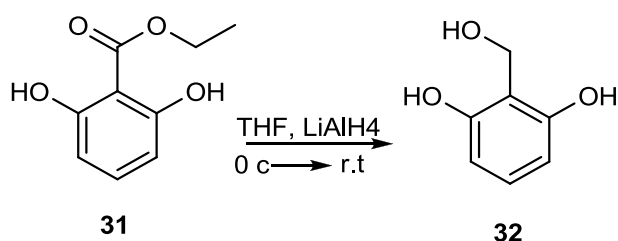


Figure 22: depiction of the ester reduction

The reaction shown in figure 22 was also attempted. In the literature a similar ester was reduced using the same conditions⁵⁰. It is a standard reduction reaction with lithium aluminium hydride reducing an ester to an alcohol. This was to be followed by oxidizing the alcohol to the desired aldehyde. The first step of the reaction was unsuccessful, leading to discarding the idea.

2.1.4. Biological testing

A total of 5 new compounds were synthesised including PAC-1 as positive control. An overview of the compounds is shown in Figure 23. With the biological results from in-vitro testing, the potency of these compounds compared to PAC-1 can be ascertained/ evaluated. The biological testing further elucidates the structural activity relationship of the compounds.

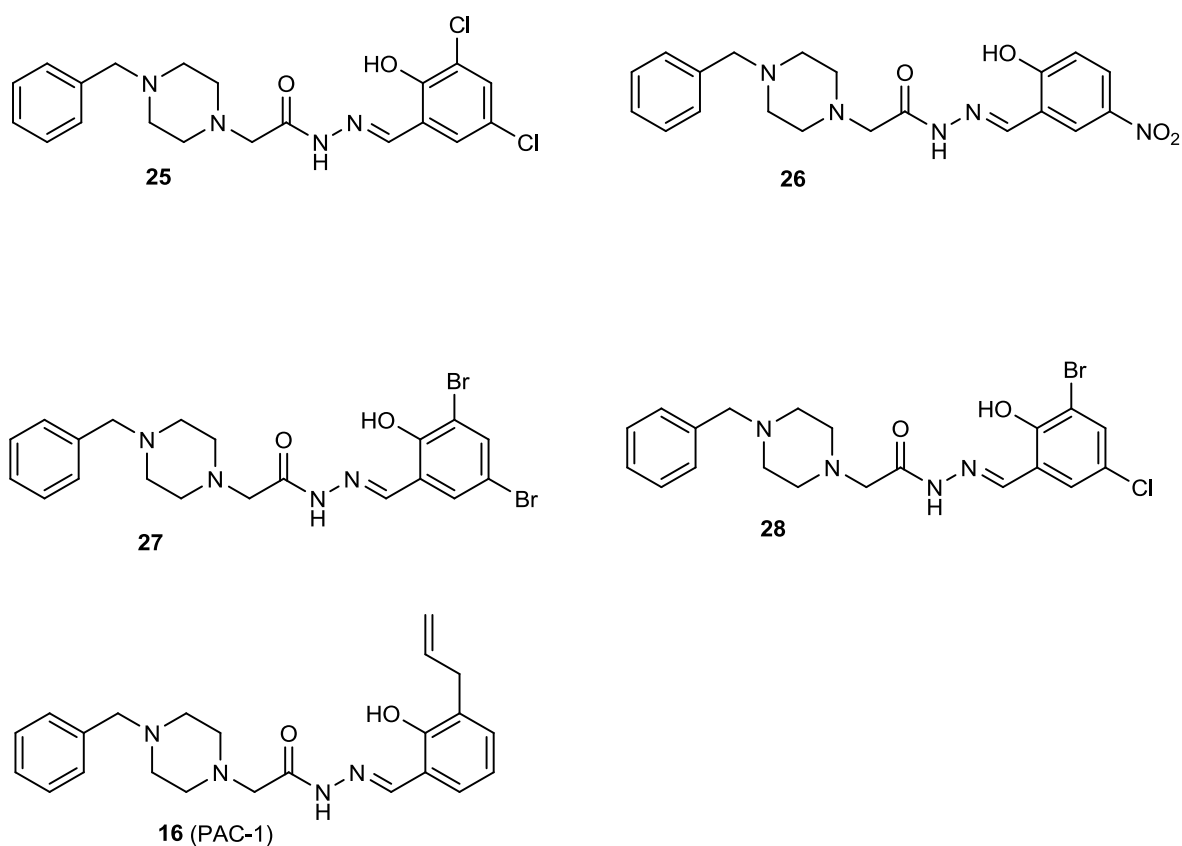
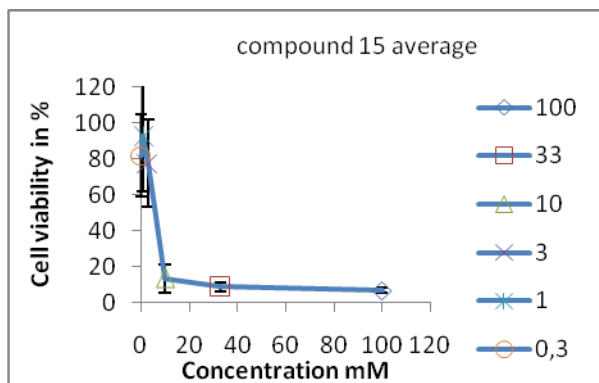


Figure 23: structures of the synthesized compounds that were subjected to biological testing.

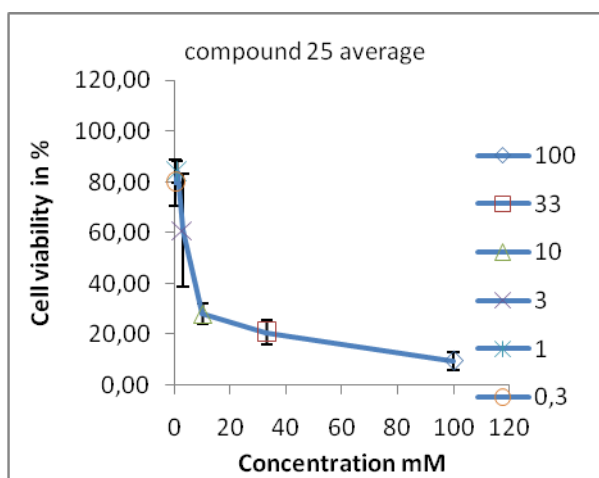
The compounds have two variations. The first group has halogen substituents on the phenol, see figure 23 for the structures of **25**, **27**, and **28** representing the halogens. While the other variation with a nitro group on the phenol is shown in figure 23 as compound **26**. PAC-1 shown as compound **16** in figure 23 was used as control. A 96 wells plate with PC-12 cells was used for the detection of cell viability. Here the cell viability was determined for the concentration interval 0.3-100 mM. For a detailed description of method see the experimental part of the thesis on page 79.

The biological test done on these molecules is an in-vitro test with the aim of determining cell viability meaning how many cells survived after subjected to the treatment of the compounds. The in-vitro testing was done in collaboration with Professor Ragnhild Paulsen and her group. From these biological tests, the compounds were all seen to reduce cell viability. The average result from three experiments will be reported and discussed below. The result is showing is how each molecule is able to reduce cell viability. On the other hand these results do not explain the exact pharmacological process that has taken place. In order words the result can point to something that is to be subjected to further studies.

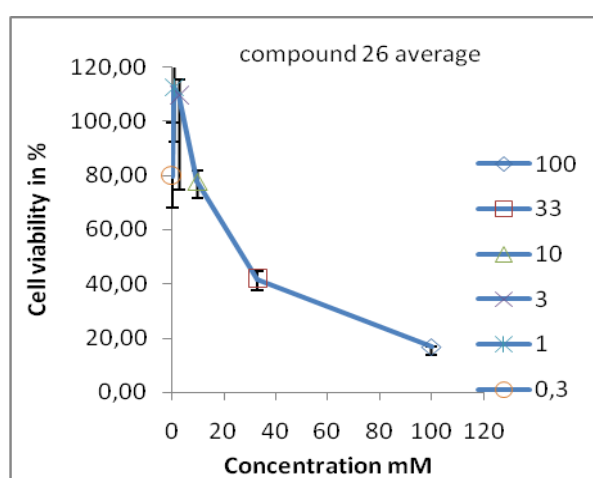
The following graphs in figure 24 are the percent effect in cell viability in Y axis and concentration in X-axis. The graphs were made from mean of the three experiments, and concentration interval of 0.3, 1, 3, 10, 30 and 100 mM was used to determine the percentage of cell viability shown in the graphs. Each graph represents a compound, and the overview of the compound concerned is shown in the figure 23.



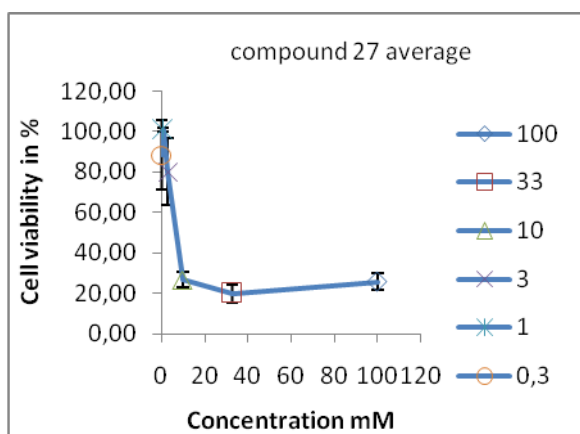
a)



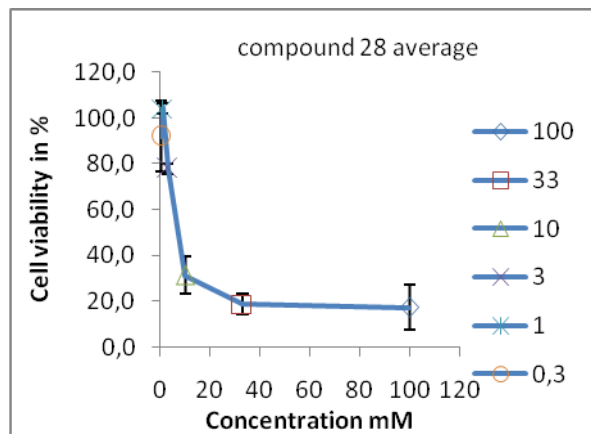
b)



c)



d)



e)

Figure 24: the graphs a, b, c, d and e which are for the test compounds are showing the percentage cell viability the cells have when subjected to compounds 16, 25, 26, 27 and 28 respectively. DMSO (0, 1%) was used as negative control. The compounds were subjected to the cells for 48 hours, before an MTT assay was run. The data represent the average \pm Standard deviation ($n=3$).

Figure 24 a, b, c, d and e shows the percentage cell viability for compounds **16**, **25-28** in different concentrations. The effect is measured as the number of cells viable after a certain time of treatment with the compounds. Such an effect is measured in percentage. Concentration interval of 0, 3 - 100 mM of every compound was used in the experiment, and data from all the measurements will be presented.

The graphs in Figure 25 are meant to highlight how each compound reduces cell viability in comparison with PAC-1. Graphically one can see that the halogen compounds are almost overlapping with PAC-1, while the graph representing the nitro compound is slightly higher than PAC-1 in cell viability tests. This indicates that the percentages of cells viable when treated with the nitro compound are higher than both those treated with PAC-1 and any of the compounds with the halogens.

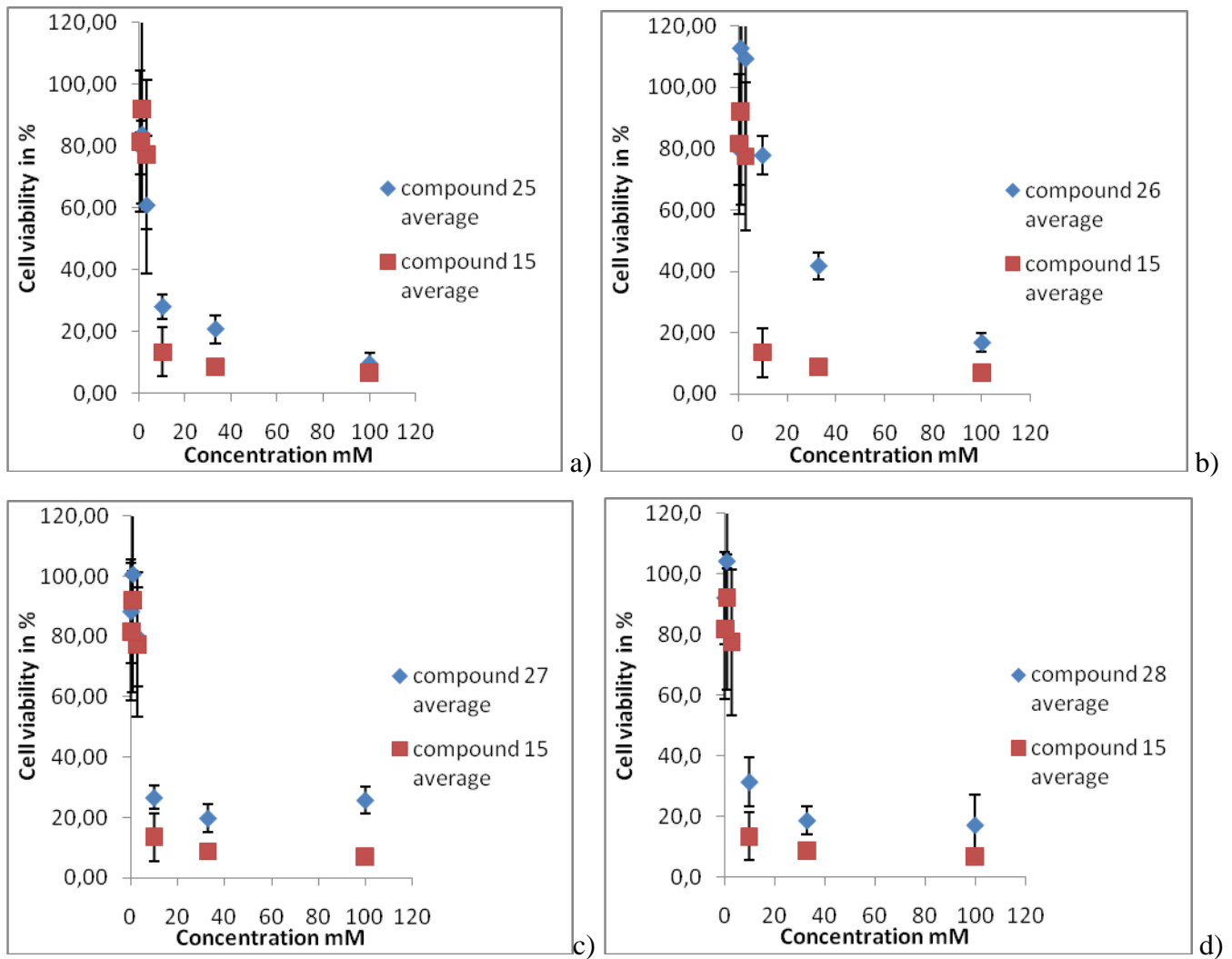


Figure 25: the graphs a, b, c and d represent compounds 25, 26, 27 and 28 respectively. The graphs are plotted using the same data as the graphs in figure 24. The axis have even the same denominator, but the difference here is that each and every compound is plotted and shown in the same figure with the positive control compound here named as compound 16. The data represent the average \pm Standard deviation ($n=3$).

2.1.5. PAC-1 and its derivatives reduce cell viability.

Taking the graphs in Figure 24 and 25 into consideration one can clearly see that all the compounds are leading to cell death. The compounds are all having IC₅₀ values equal or similar to PAC-1, with the exception of the compound with the nitro group.

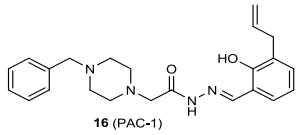
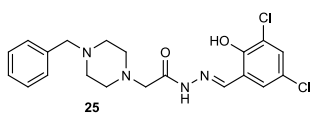
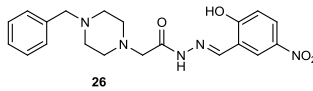
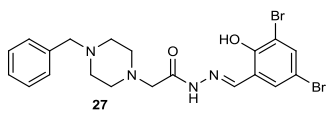
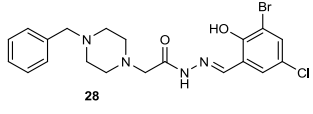
Compound structure	IC ₅₀ value
 16 (PAC-1)	3-10 mM
 25	3-10 mM
 26	20-30 mM
 27	3-10 mM
 28	3-10 mM

Table 17: overview of the compounds with their respective IC₅₀ values.

2.1.6. Discussion

Taking the graphs shown in figure 24 and 25 into account, we can conclude that all the compounds are effective in reducing cell viability. The nitro group shows lower potency compared to the other compounds. The results show that the phenol moiety is important for the activity of the compounds. Comparison of all the compounds clearly indicates that the substituent on the phenol moiety is a good indicator of the activity and/ or potency of the compound.

There several ways of increasing the potency a lead compound. One can do homologation, meaning increasing the number hydrophobic groups. Others ways include chain branching, ring transformation and even adding bioisosteric groups⁵¹. The last measure was applied here. Use of bioisosteric group can lead to changes in many features within the molecule. The pharmacological and even pharmacokinetic properties can be altered. In this case the aim was to change the pharmacological aspects in order to get more potent products.

There are three hypotheses about the mechanism of action of these compounds; the first one suggested by Hergenrother *et.al.* is one that the cleavage of procaspase-3 to caspase-3 takes places when its released from it is safety catch. Releasing from the safety catch occurs only when there are acidic conditions. The piperazine ring is believed to be acidified at normal pH. Such acidification is dependent on the substituents. This implies that when there are strongly electrons withdrawing groups like nitro, the inductive effect is reduced; hence the piperazine ring would not take up a proton, in contrast to when there are weakly electron withdrawing groups like the halogens.

The second hypothesis concerning the mechanism of action is that the phenol ring is important either by a hydrogen binding with the imine or of acidification of the safety catch and hence conversion of procaspase-3 to caspase-3. We think the latter is what happens due to the analysis of the other substituent's of the phenol ring; one can see the stronger electron withdrawing the substituent is, the less potent the compound and vice versa.

In 2001, a review article by Tran *et al.* discusses the role of zinc in caspase activation and apoptotic cell death. Substantial evidence has linked Zn deficiency with increased susceptibility of cells and tissues to die by apoptosis. The pool of Zinc with such effects on apoptosis is the more exchangeable (labile) Zn, which are also readily depleted in Zn deficiency and augmented following Zn supplementation⁵¹. Caspase-3 was found to be insensitive to exogenous Zn when a metal chelator and thiol reducing agent were used. This was attributed to the fact that Zn can bind to the chelator and hence lower concentration of Zn to inhibit the caspase. However using a cell-free system with PARP and caspase-3, Zinc was found to inhibit PARP proteolysis by caspase-3 in μM range⁵¹.

Recently Hergenrother *et al.* reported a third hypothesis that zinc is important since zinc an inhibitor of procaspase-3. When PAC-1 enters the cells it competes for the labile zinc pool, reducing the level of zinc available to inhibit procaspase-3. This results in auto activation of procaspase-3 to caspase-3 when it is liberated. With the generation of caspase-3 more substrates are cleaved and apoptosis occurs⁵².

According to SAR studies by Hergenrother and his group, PAC-1 was effective in inducing both procaspase-3 activation and cell death in cancer cell cultures with IC₅₀ and EC₅₀ of 0.22 and 0.92 μ M respectively. Of all the other compounds they tested, the derivative lacking the allyl was also able to induce activation of procaspase-3 and cell death at levels similar to those induced by PAC-1. What these two compounds have in common that is lacking in the other derivatives is the phenolic hydroxyl and the benzyl moiety.

In our group SAR was done for PAC-1 derivatives with electron withdrawing groups. By substituting the allyl, which is electron donating, with an electron withdrawing group like halides; one makes the phenolic hydroxyl more acidic, leading auto catalysation of procaspase-3 to caspase-3 and eventually cell death. The compounds with a single halogen substitution show cytotoxicity effects, increasing the number of halogens to increase the potency of the compounds was thought to materialise.

While the halogen substituted derivatives show the same activity as PAC-1, the nitro derivative is four times lower. This can be attributed to resonance stabilization of the nitro group, which makes it hard for the hydrogen bond to be broken, in order to increase the acidity of the safety catchment. Thus there is not as much procaspase-3 conversion to caspase-3. Another reason why this compound is less active than all the rest is because it is more hydrophilic, with estimated log P of 0.62 this would lead to problems penetrating the cell membrane. The compound is localized in aqueous instead of the active site, rendering it inactive.

In this master thesis, the compounds were not tested for the cleavage of procaspase-3 to caspase-3. The only tests done on these compounds were cell viability test by using MTT. If cell death tests because of caspase activating molecules were to be carried out, the experiment had to have a caspase inhibitor in order to exactly decide that the compounds with caspase activating properties lead to cell death. The MTT test is done to measure the mitochondrial activity in viable cells. By using spectrophotometry the assay provides rapid and reproducible results. The disadvantage with assay is it provides no morphological information, and its lack of ability to distinguish reversible mitochondrial impairment and injury from cell death⁵⁶.

In that connection it is natural that one considers other types of assays. There are few other examples like lactate dehydrogenase (LDG). It is based on the principal that cell death processes eventually lead to an increase in membrane permeability, allowing the release of cytoplasmic enzymes. Both tryptan blue and propidium iodide assays are based on the same principal of membrane permeability. However the tryptan blue and propidium iodide quantify the extent to which cells are unable to exclude these two dyes from their cytoplasm. Tryptan blue although not automated and time consuming is gold standard for assaying viability. Propidium has an advantage over tryptan blue that its calometric change can be automated⁵⁶.

3. Conclusion and further studies

The preparations of the compounds in figure 16 were achieved with high overall yields. Due to decomposition on silica, all of them were purified by recrystallization. In testing the compounds for biological activity, PC-12 cells were used. However all the compounds have shown activity in reducing cell viability. What was not elaborated in this thesis is how the mechanism behind the compounds reducing cell viability.

The biological tests done on the compounds have shown that the compounds all lead to reduction of cell viability. There is however, a variation of potency among the compounds with the compounds with halogen substituent's giving a reduction in cell viability almost the same as PAC-1, while the one with the nitro substituent was almost inactive.

Concerning the mechanism of activation, there are currently three suggested ways these compounds can lead to cell death. Whether it is only one mechanism or a synergy of all three is what needs to be studied further. Further studies should also focus on a way of increasing the potency of the compounds and should subject them to further biological studies that will tell us values like EC_{50} .

4. Experimental

4.1.1. General synthesis

All the chemicals used were commercially available with analytical quality of (p.a, puriss or purum) and were delivered from Sigma-Aldrich. With the exception of one experiment carried out under dry conditions all reactions were refluxed, some were purified by chromatography while those decomposing in silica were recrystallized. Nitrogen for working in inert atmosphere was used as delivered from AGA.

4.1.2. Apparatus

The compounds were analyzed with the aid of TLC, $^1\text{H-NMR}$, $^{13}\text{C-NMR}$ and melting point. LC-MS analysis was out carried for the final products

NMR

$^1\text{H-NMR}$ and $^{13}\text{C-NMR}$ spectra were recorded on a Bruker Avance DPX 300 instrument at 300 MHz for $^1\text{H-NMR}$ and 75 MHz for $^{13}\text{C-NMR}$ at 25°C. The spectres were processed in MestreNova and CDCl_3 was used as reference. Chemical shift (δ) is given in ppm relative to the solvent CDCl_3 (7.24 ppm for $^1\text{H-NMR}$, 77.0 ppm for $^{13}\text{C-NMR}$).

LC-MS

LC-MS experiments were done using Agilent technologies liquid chromatograph 1200 series connected to an Agilent technologies ion trap mass spectrometer 3610 series. The instrument was further devised with an Agilent technologies auto sampler. In order to process the data Agilent LC-MS trap software 5.3 was used. Gradient mobile phase was used.

The sample was injected by using the auto sampler. The column was Eclipse CDB, C-18 packed with particles at 5 μm and was 4.6 x 150 mm. The compounds were detected in the MS with TIC (total ion currence) and EIC (extracted ion currence). The amount injected was 1-2 μL , the flow rate was 0.8 ml/min with varying total chromatography time between 10-20 minutes. The maximum pressure was set to be 400 bar, while the temperature was 25°C. The UV absorption had a wave length of 254 nm.

Melting point

The melting point was measured for the final products. The instrument used was Barnstead Electrothermal 9200 with capillary size of 100 x 2 mm from Electrothermal. A minimum of 2 parallels were taken for each compound. The melting points are all uncorrected.

4.1.3. Synthesis of intermediates 18, 21 and 23

Synthesis of 3-allyl- salicylic aldehyde (18)

A 250 mL round bottom flask was charged with 4.6 g (48 mmol) magnesium chloride. To this was added 2.2 g (72 mmol) paraformaldehyde and 150 mL tetrahydrofuran through a syringe. To the mixture 6.7 mL triethylamine was also added with the aid of a syringe. After stirring for 10 minutes, a color change from white to purple was observed. To all these, 3.2 g (24 mmol) allyl phenol was added. The mixture was then immersed in an oil bath with a temperature of 75 °C. The heating was maintained for 3.5 hours and TLC analysis indicated the aldehyde formation was complete. The reaction mixture was cooled to room temperature before 60 mL of ether was added. The mixture was washed with 1 N HCl (3x 60 mL) and later with the same amount of water. The organic phase was dried over MgSO₄, filtered and solvent evaporated. The crude product was purified by flash chromatography (H. 50 cm, diameter 0.5 mm) with ethyl acetate and hexane as eluting solvents in the ratio 1:9. The vials containing traces of product after TLC analysis were pooled together in a round bottomed flask and the solvent evaporated. The yield was found to be 69 % of 3 allyl salicylic aldehyde.

¹H-NMR (CDCl₃, 300 MHz): δ 11.28 (s, 1H), 9.87 (s, 1H), 7.41 (m, 2H), 6.95 (t, 1H), 5.98 (m, 1H), 5.08 (m, 2H), 3.42 (d, 2H) ppm.

¹³C- NMR (CDCl₃, 75 MHz): δ 196.86, 159.67, 137.27, 135.93, 131.94, 128.94, 120.35, 119.72, 116.40, 33.18 ppm.

Synthesis of ethyl (4-benzylpiperazino) acetate (21)

A 250 ml round bottomed flask was charged with 5 g (28.5 mmol) 1-benzylpiperazine, 3.0 g (35.7 mmol) NaHCO₃, and 57 mL of acetone. To the stirring solution 5.3 g (31.6 mmol) of ethyl bromoacetate was added dropwise for a period of 2 minutes. The reaction was refluxed for 22 hours before TLC analysis was performed with the following system hexane:ethyl acetate 1: 4 and showed that the reaction was complete. The solution was filtered and the insoluble salts washed with acetone. Another TLC was taken to determine the ΔR_f as 0.49. The solvent in the reaction mixture was evaporated and an oily remnant was applied to a silica column, flashed a gradient eluting system consisting of hexane: ethyl acetate 1: 1 and hexane: ethyl acetate 1: 4. The product was concentrated after the flash to afford 4.45 g (60 %) of ethyl (4-benzylpiperazino) acetate 20 as a yellow liquid. The same experiment was done for two other batches and yields were between 54% and 58.%.

¹H-NMR (CDCl₃, 300 MHz): δ 7.30 (m, 2H), 7.28 (m, 2H), 7.22 (m, 1H), 4.16 (q, 2H), 3.51 (s, 2H), 3.18 (s, 2H), 2.59 (br, 4H), 2.52 (br, 4H), 1.24 (t, 3H).

¹³C- NMR (CDCl₃, 75 MHz): δ 170.48, 138.21, 129.38, 128.38, 127.22, 63.14, 60.74, 59.73, 53.25, 52.95, 14.42 ppm

Synthesis of 2-(4- benzylpiperazino-1-yl) acetatohydrazide (23)

A 250 mL round-bottom flask was charged with 4.75 g (18.1 mmol) of ethyl (4- benzylpiperazino) acetate (20) and 25 mL of ethanol. After adding 2.76 mL (50 mmol) hydrazine dropwise over a period of 2 minutes, the reaction was refluxed for 16 hrs. The mixture was concentrated via rotatory evaporation after TLC assessment showed the reaction as complete. The yellow liquid formed after distillation was transferred to a separatory funnel containing 20 mL of 1:1 brine: H₂O made basic with NaOH (pH > 12). The aqueous layer was extracted with three 15 mL portions of CH₂Cl₂ and one 15 mL portion of EtOAc. The organic layers were pooled together, concentrated to yellow oil and combined with 5 mL hot ethanol, then slowly mixed with anhydrous diethyl ether. The formation of only a few crystals brings the idea of evaporating the solvent in order to retrieve the product. After washing the crystals with cold hexane, the result was 4.106 g (91.3 %) of (4- benzylpiperazino) acetic acid hydrazide (22). This reaction was also carried out in several other batches since a substantial amount of these intermediate was required further in the project. The yield in those other synthesis was 76 % as isolated yields.

¹H-NMR (CDCl₃, 300 MHz): δ 8.10 (s, 1H), 7.31 (m, 2H), 7.29 (m, 2H), 7.28 (m, 1H), 3.49 (s, 2H), 3.05 (s, 2H), 2.52 (br, 4H), 2.45 (br, 4H).

¹³C- NMR (CDCl₃, 75 MHz): δ 170.74, 138.07, 129.32, 128.45, 127.34, 63.08, 60.81, 53.90, 53.25.

4.1.4. Synthesis of the products 16, 25, 26, 27 and 28

Synthesis of (*E*)-*N*-(3-allyl-2-hydroxybenzylidene)-2-(4-benzylpiperazin-1-yl) acetohydrazide.(16)

A 100 mL round bottomed flask was charged with 0.26 g (1.63 mmol) of 3-allyl salicylaldehyde and 2 mL of ethanol. To the stirring solution, 0.49 g (1.98 mmol) of (4-benzylpiperazino) acetic acid hydrazide, 8 mL of ethanol and 10 μ L of 12M HCl as catalytic amount were added. The reaction was heated at reflux for 46 hrs. The reaction mixture was concentrated to form a solid that was recrystallized with 1:15 ethanol: hexane to afford 0.64 g (94 %) PAC-1 as white solid.

¹H-NMR (CDCl₃, 300 MHz): δ 11.17 (s, 1H), 9.95 (s, 1H), 8.35 (s, 1H) 7.12 (m, 8H), 6.81 (t, 1H), 6.02 (dd, 1H), 5.05 (dd, 2H), 3.48 (s, 2H), 3.39 (d, 2H), 3.11 (s, 2H), 2.54 (br, 8H).

¹³C NMR (CDCl₃ 75 MHz): δ 165.99, 156.60, 137.84, 136.70, 132.47, 128.52, 127.45, 119.23, 117.066, 115.83, 63.04, 61.12, 53.86, 53.17, 34.04

Melting point: 135.6°C-136.4°C.

LC-MS: 9.44 min. MS: m/z 393 ([M+1]) = 100 %

Synthesis of (*E*)-2-(4-benzylpiperazin-1-yl)-*N*'-(3,5-dichloro-2-hydroxybenzylidene)

acetohydrazide.(25)

A 100 mL round bottom flask was charged with 0.38 g (1.97 mmol) of 3,5-dichlorosalicylaldehyde and 10 mL of ethanol. To the stirring solution, 0.54 g (2.17 mmol) of 4-benzylpiperazino acetic acid hydrazide was added with a catalytic amount (10 μ l) of 1M HCl. The reaction was heated at reflux for 3 and ½ hrs. The reaction mixture was concentrated via rotatory evaporation and the yellow solid powder was recrystallized with methanol to afford 0.82 g (99 %) of (*E*)-2-(4-benzylpiperazin-1-yl)-*N*'-(3, 5-dichloro-2-hydroxybenzylidene) acetohydrazide (25) as crystals. The crystals were filtered and washed with cold hexane and dried in vacuum.

¹H-NMR (CDCl₃, 300 MHz): δ 11.58 (s, 1H), 10.13 (s, 1H), 8.55 (s, 1H), 7.37 (s, 1H), 7.30 (m, 4H), 7.11 (s, 1H), 3.54 (s, 2H), 3.18 (s, 2H), 2.63 (br, 4H), 2.53 (br, 4H).

¹³C NMR (CDCl₃ 75 MHz): δ 166.61, 153.32, 149.52, 131.83, 128.87, 127.83, 123.11, 119.62, 63.12, 61.25, 53.88, 53.21.

Melting point: 189.7°C-191.4°C.

LC-MS: 11.35 min. MS: m/z 421 ([M+1]) = 100 %

Synthesis of (E)-2-(4-benzylpiperazin-1-yl)-N^o-(2-hydroxy-5-nitrobenzylidene)

acetohydrazide.(26)

A 100 mL round bottom flask was charged with 0.165 g (0.99 mmol) of 2 hydroxy, 5 nitrobenzaldehyde and 5 mL of ethanol. To the stirring solution, 0.27 g (1.087 mmol) of 4-benzylpiperazino acetic acid hydrazide was added with a catalytic amount (10 μ l) of 1M HCl. The reaction was heated at reflux for 3.5 hrs. The reaction mixture was concentrated via rotatory evaporation and the yellow solid powder was recrystallized with ethanol to afford 0.393 g (94 %) of (E)-2-(4-benzylpiperazin-1-yl)-N^o-(5 nitro, hydroxybenzylidene) acetohydrazide (26) as crystals. The crystals were filtered and washed with cold hexane and dried in vacuum.

¹H-NMR (CDCl₃, 300 MHz): δ 11.87 (s, 1H), 10.20 (s, 1H), 8.58 (s, 1H), 8.17 (m, 2H), 7.30 (m, 5H), 7.06 (d, 1H), 3.54 (s, 2H), 3.20 (s, 2H), 2.62 (br, 4H), 2.53 (br, 4H).

¹³C NMR (CDCl₃; 75 MHz): δ 166.47, 163.97, 148.91, 140.56, 129.41, 128.57, 127.59, 127.32, 126.99, 118.26, 117.44, 62.97, 61.05, 53.81, 53.07.

LC-MS: 10.01 min. MS: m/z 399 ([M+1]) = 100 %

Synthesis of (E)-2-(4-benzylpiperazin-1-yl)-N-(3,5-dibromo-2-hydroxybenzylidene)

acetohydrazide.(27)

A 100 mL round bottom flask was charged 0.55 g (1.97mmol) of 3,5- dibromosalicylaldehyde and 10 mL of ethanol. To the stirring solution, 0.54 g (2.17 mmol) of 4-benzylpiperazino acetic acid hydrazide was added and a catalytic amount (10 μ l) of 1M HCl. The reaction was heated at reflux for 3 hrs. The reaction mixture was concentrated via rotatory evaporation and the yellow solid powder was recrystallized with dichloromethane and hexane to afford 0.997 g (99 %) of (E)-2-(4-benzylpiperazin-1-yl)-N-(3, 5-dibromo-2-hydroxybenzylidene) acetohydrazide (27) as white crystals. The crystals were filtered and washed with cold hexane and dried in before an NMR was taken.

¹H-NMR (CDCl₃, 300 MHz): δ 11.73 (s, 1H), 10.13 (s, 1H), 8.50 (s, 1H), 7.66 (d, 1H), 7.30 (s,1H), 7.29 (m, 2H), 7.28 (m, 3H), 3.54 (s, 2H), 3.18 (s, 2H), 2.62 (br, 4H), 2.52 (br, 4H).

¹³C NMR (CDCl₃75 MHz): δ 166.50, 154.50, 149.16, 137.10, 132.36 129.34, 128.54, 127.48, 119.88, 112.21, 110.98, 63.07, 61.19, 53.95, 53.17.

Melting point: 200.8 - 202.5°C

LC-MS: 11.18 min. MS: m/z 511 ([M+1]) = 100 %

Synthesis of (*E*)-2-(4-benzylpiperazin-1-yl)-*N*'-(3-bromo,5-chloro-2-hydroxybenzylidene) acetohydrazide.(28)

A 100 mL round bottom flask was charged with 0.46g (1.97 mmol) of 3-bromo-5-chlorosalicylaldehyde and 10 mL of ethanol. To the stirring solution, 0.54 g (2.17 mmol) of 4-benzylpiperazino acetic acid hydrazide was added and a catalytic amount (10 μ l) of 1M HCl. The reaction was heated at reflux for 4 hrs. The reaction mixture was concentrated via rotatory evaporation and the yellow solid powder was recrystallized with ethanol to afford 0.820 g (89 %) of (*E*)-2-(4-benzylpiperazin-1-yl)-*N*'-(3-bromo-5-chloro-2-hydroxybenzylidene) acetohydrazide (28) as white crystals. The crystals were filtered and washed with cold hexane and dried in vacuum.

¹H-NMR (CDCl₃, 300 MHz): δ 11.71 (s, 1H), 10.15 (s, 1H), 8.52 (s, 1H), 7.53 (s, 1H), 7.52 (s, 1H), 7.30 (m, 4H), 7.16 (d, 1H J= 2.4 Hz), 3.54 (s, 2H), 3.18 (s, 2H), 2.62 (br, 4H), 2.53 (br, 4H).

¹³C NMR (CDCl₃75 MHz): δ 166.37, 154.02, 149.20, 134.47, 129.51, 128.62, 127.72, 124.43, 119.24, 111.80, 62.89, 61.00, 53.61, 53.00.

Melting point: 197.6 - 199.1°C

LC-MS: 10.98 min. MS: m/z 467 ([M+1]) = 100 %

4.1.5. Methods

4.1.6. Measuring cell viability using 96 well methods

It was by the use of this method that the effects of the synthesized compounds were quantified in PC-12 cells. The PC-12 cells were harvested in 96 well cell plates and incubated with the substances after a day of division. The substances and the cells were then left undisturbed for 48 hours, before the substances were removed and MTT was added for an hour, after an hour, MTT was removed and DMSO added to aid the wavelength measurement

The five different compounds, **16, 25-28** were tested for their cell viability activities. For all of them a concentration interval of 0.3-100 mM in DMSO was used. Some of the wells were used as control and treated with only (0.1 %) DMSO while others were left untreated meaning. All the wells were otherwise subjected to the same treatment. For each substance 12 wells were used and 3 separate trials were done. The cells were incubated for two days when they were subjected/ treated with 100 μ L of their respective substance. When the substances were removed after two days the cells were treated with 50 μ L of MTT for an hour. When the MTT was removed the cells were treated with 100 μ L of DMSO.

4.1.7. PC-12 cells

PC-12 cells from rat pheochromocytoma were used. They were grown in 5 % horse serum and 10 % fetal bovine serum. The old media was aspirated. The flask was hit to dislodge remaining cells. Serum was added to 10 ml of media and pipetted 5-10 times to dispense the cells. To a flask of 150 cm containing 20 ml of media was added 2 ml of media cells. This was incubated at 37 °C with 12 % CO₂. A 96 well plate was used and the cell density was found to be 4000 cells per well. After 24 hours incubation the cells were treated with the compounds.

4.1.8. Cell viability studies by using MTT

The aim of this study was to see the effect of the five compounds and to compare them. Principal is based on the breakdown of tetrazolium salt (MTT) by mitochondrial de-hydrogenases of the living cells. The tetrazolium ring of MTT is cleaved and it is reduced to a blue formazan, see figure 26 below. The result is colour change, the intensity of which reflects the enzymatic activity of the living cells⁵⁴.

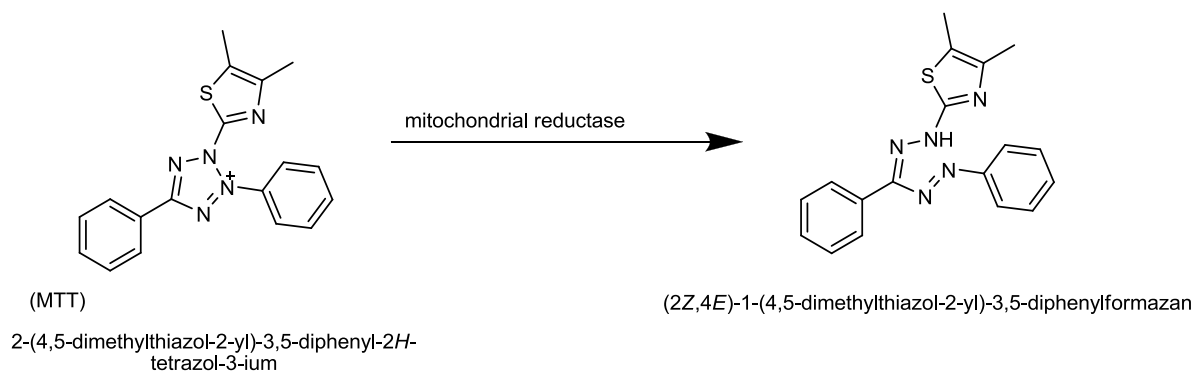


Figure 26: depiction of how MTT is reduced to a blue formazan.

PC-12 cells which were newly seeded into 96 wells plate were used for the cell viability study. The compounds were weighed so that the final concentration was to be 100 mM. DMSO was used as solvent. The starting concentration was diluted from 100 to 33, 10, 3, 1, and 0.3 mM. After 24 hours incubation, the cells were treated with 100 μ l of compounds **16**, **25-28**. The wells had 8 columns and each compound was assigned a column for it is duplicate test, while DMSO as positive control was assigned a column. The remaining two columns were untreated. The cells with the compounds were then incubated at 37 °C for two days, before the media and the compounds were removed and 50 μ l of MTT added. The MTT had a final concentration of 5 mg/ml. After incubating with MTT for an hour, the MTT was removed and DMSO was added. The cells were illuminated by UV to measure the fluorescence.

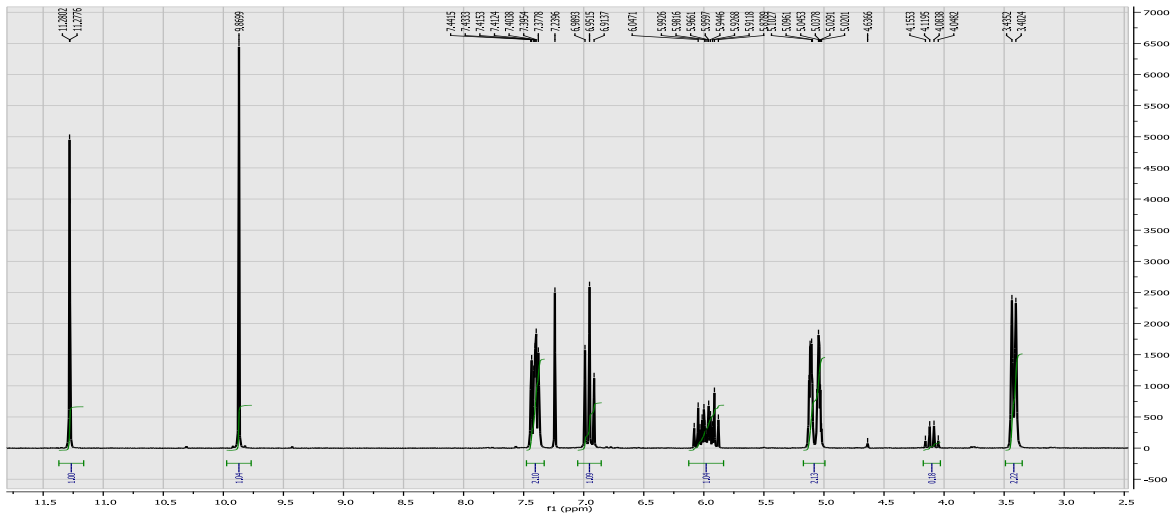
5. References

1. American cancer society. The growing global cancer crisis. http://www.cancer.org/docroot/AA/content/AA_2_5_1x_Case_for_Global_Action.asp?sitearea=AA (8.1.2009)
2. Alberts, B.; Johnson, A.; Lewis, J.; Raff, M.; Roberts, K.; Walter, P. Molecular biology of the cell, Garland science, New York, **2002**, pages 1324-1327
3. Rang, H. P.; Dale, M. M.; Ritter, J. M.; Moore, P. K. Pharmacology, Churchill Livingstone Elsevier. Edinburg, **2003**, pages 693, 698-708
4. Hanahan, D.; Weinberg, R. A. The hallmarks of cancer. *Cell*, **2000**, *100*, 1, 57-70.
5. Peters, J.; Loud, J.; Dimond, E.; Jenkins, J. Cancer genetic fundamentals. *Cancer Nursing*, **2001**, *24*, 6, 446-461.
6. Bryan, R.; Hussain, S.; James, N.; Jankowski, J.; Wallace, M. Molecular pathways in bladder cancer part 1. *BJU international*, **2005**, *95*, 485-490.
7. Solary, E.; Droin, N.; Sordet, O.; Rebe, C.; Filomenko, R.; Wotawa, A.; Plenchette, S.; Ducory, P. Cell death pathways as targets for anticancer drugs in anticancer drug development edited by Baguley, B. C and Kerr, D. J. Academic press, California, **2002**, pages 55-70.
8. Lasorella, A.; Uo, T.; Iavarone, A. Id proteins at the cross-road of development and cancer. *Oncogene*, **2001**, *20*, 8326-8333.
9. Fensterle, J. A trip through the signalling pathways of melanoma. *Journal of the German society of Dermatologist*, **2006**, *3*, 4, 205-216.
10. Marcinkowska, E.; Chrobak, A.; Wiedlocha, A. Evading apoptosis by calcitriol-differentiated human leukemic HL-60 cells is not mediated by changes in CD95 receptor system but by increased sensitivity of these cells to insulin. *Experimental cell research*, **2001**, *270*, 1, 119-127.
11. LaCasse, E. C.; Mahoney, D. J.; Cheung, H. H.; Plenchette, S.; Baird, S.; Korneluk, R. G. IAP-targeted therapies for cancer. *Oncogene*, **2008**, *27*, 6252-6275.
12. Reed, J. C.; Pellecchia, M. Apoptosis-based therapies for hematologic malignancies. *Blood*, **2005**, *106*, 2, 408-418.
13. Maser, R. S.; Depinho, R. A. Connecting chromosomes, crisis and cancer. *Science*, **2002**, *297*, 565-569.

14. Carmeleit, P.; Jain, R. Angiogenesis in cancer and other diseases. *Nature*, **2000**, *407*, 249-257.
15. Pralhad, T.; Madhusudan, S.; Rajendrakumar, K. Concept, mechanism and therapeutics of angiogenesis in cancer and other diseases. *JPP*. **2003**, *55*, 1045-1053.
16. Bouck, N.; Stellmach, V.; Hsu, S. C. How tumours become angiogenic. *Advances in cancer research*, **1996**, *69*, 135-174
17. Mess, C.; Nemunaitis, J.; Senzer, N. Transcription factors: their potential as targets for an individualized therapeutic approach to cancer. *Cancer Gene Therapy*, **2009**, *16*, 103-112.
18. Bogenreider, T.; Herlyn, M. Axis of evil. Molecular mechanism of cancer metastasis. *Oncogene*, **2003**, *22*, 6524-6536.
19. Warwick, G. P. The mechanism of action of alkylating agents. *Cancer research*, **1963**, *23*, 1315-1333.
20. Gmeiner, W. H. Antimetabolites incorporation into DNA. Structural and thermodynamic basis for anticancer activity. *Biopolymers (nucleic acid sciences)*, **2002**, *65*, 180-189.
21. Pettitt, A. R. *British journal of haematology*, **2003**, *121*, 692-702
22. <http://www.legemiddelhandboka.no/xml/> (13.1.2009).
23. Minoti, G.; Menna, P.; Salvatorelli, E.; Cairo, G.; Gianni, L. Anthracyclines. Molecular advances and pharmacologic developments in antitumor activity and cardiotoxicity. *Pharmacol Rev.* **2004**, *56*, 185-229.
24. Korynevskaya, A.; Heffeter, P.; Mastelyukh, B.; Elbing, L.; Micksche, M.; Stoika, R.; Berger, W. Mechanisms underlying the anticancer activities of the angucycline landomycin E. *Biochemical Pharmacology*, **2007**, *74*, 1713-1726.
25. Samuelsson, G. Drugs of natural origin, a text book of pharmacognosy, 5th revised edition, Stockholm, **2004**, Pages 170-171, 350, 548-549.
26. Hait, N. W. Targeted cancer therapeutics. *Cancer Res.* **2009**, *69*, 1263-1267.
27. Laurenzi, V. De. *Cell death and differentiation*, **2009**, *16*, 3-11.
28. Fink, S. L.; Cookson, B. T. Apoptosis, pyroptosis and necrosis. Mechanistic description of dead and dying eukaryotic cells. *Infection and immunity*, **2005**, *73*, 4, 1907-1916.
29. Vandenabeele, P.; Declercq, W.; Berghe, T. V: Necrotic cell death and ``necrostatin``: now we can control cellular explosion. *Trends in biochemical sciences*, **2008**, *33*, 8, 352-355.
30. Zong, W. X.; Thompson, C. B. Necrotic death as a cell fate. *Genes and development*, **2006**, *20*, 1-15.

31. Vermuelen, K.; Van Bockstaele, D. R; Berneman, N. Z. Apoptosis: mechanisms and relevance in cancer. *Ann of Hematol.* **2005**, *84*, 627-639
32. Lawen, A. Apoptosis- an introduction. *BioEssays*, **2003**, *25*, 888-896.
33. May, S. W.; Deng, X. Apoptosis in principles of molecular medicine edited by Runge, M,S and Patterson, C. Humana press, 2nd edition, Totowa, **2006**, 709-719.
34. Hitto, K.; M, Fussenegger, M. Caspase regulation at the molecular level. *Cell engineering*, **2004**, *4*, 1-23.
35. Okun, L.; Balakin, K. V.; Tkachenko, S. E; Ivachtchenko, A. V. Caspase activity modulators as anticancer agents. *Anticancer Agents in Medicinal Chemistry*, **2008**, *8*, 322-341.
36. Fischer, U.; Osthoff-schulze, K. Pharmacological Modulation of Caspase Activation. *Curr. Med. Chem. - Anti –inflammatory and Anti- Allergy Agents*, **2005**, *4*, 407-419
37. Piana, S.; Rothlisberger, U. Molecular dynamics simulation of structural changes during procaspase-3 activation. *Proteins: Structure, function and Bioinformatics*, **2004**, *55*, 932-941.
38. Feeney, B.; Clark, C. A. Reassembly of active caspase-3 is facilitated by the propeptide. *The journal of biological chemistry*, **2005**, *280*, 48, 39772-39785.
39. Kim, Y. H.; Chang, K. A.; Park, E. J.; Park; IL-S, Yoon.; M. S, Lee. S, J. Procaspase-3 activation by a metalloprotease secreted from vibrio vulnificus. *International journal of molecular medicine*, **2007**, *20*,591-595.
40. Sakai, J.; Yoshimori, A.; Nose, Y.; Mizoroki, A.; Okita, N.; Takasawa, R. Tanuma, S. Structure-based discovery of novel non-peptidic small molecular inhibitor of caspase-3. *Bioorg. Med. Chem.* **2008**, *16*, 4854-4859.
41. Scott, C. W.; Sobotka-B. C.; Wilkins, D. E.; Jacobs, R. T.; Folmer, J. J.; Frazee, W. J.; Bhat, R. V.; Ghanekar, S. V.; Aharony. D. Novel small molecule inhibitors of caspase-3 block cellular and biochemical features of apoptosis. *The journal of pharmacology and experimental therapeutics*, **2003**, *304*, 433-440.
42. Lavrik, I. N.; Golks, A; Krammer, P. H. Caspases. Pharmacological manipulation of cell death. *The journal of clinical investigation*, **2005**, *115*, 2665-2672.
43. Nguyen, J. T.; Wells, J. A. Direct activation of the apoptosis machinery as a mechanism to target cancer cells. *Pro Natl Acad Sci USA*, **2003**, *100*, 7533-7538.
44. Jiang, X.; Kim, H.; Shu, H.; Zhao, Y.; Zhang, H.; Kofron, J.; Donnelly, J.; Burns, D.; Ng, S.; Rosenberg, S.; Wang, X. Distinctive roles of PHAP proteins and Prothymosin- α in a death regulatory pathway. *Science*, 2003, *299*, 223-226.

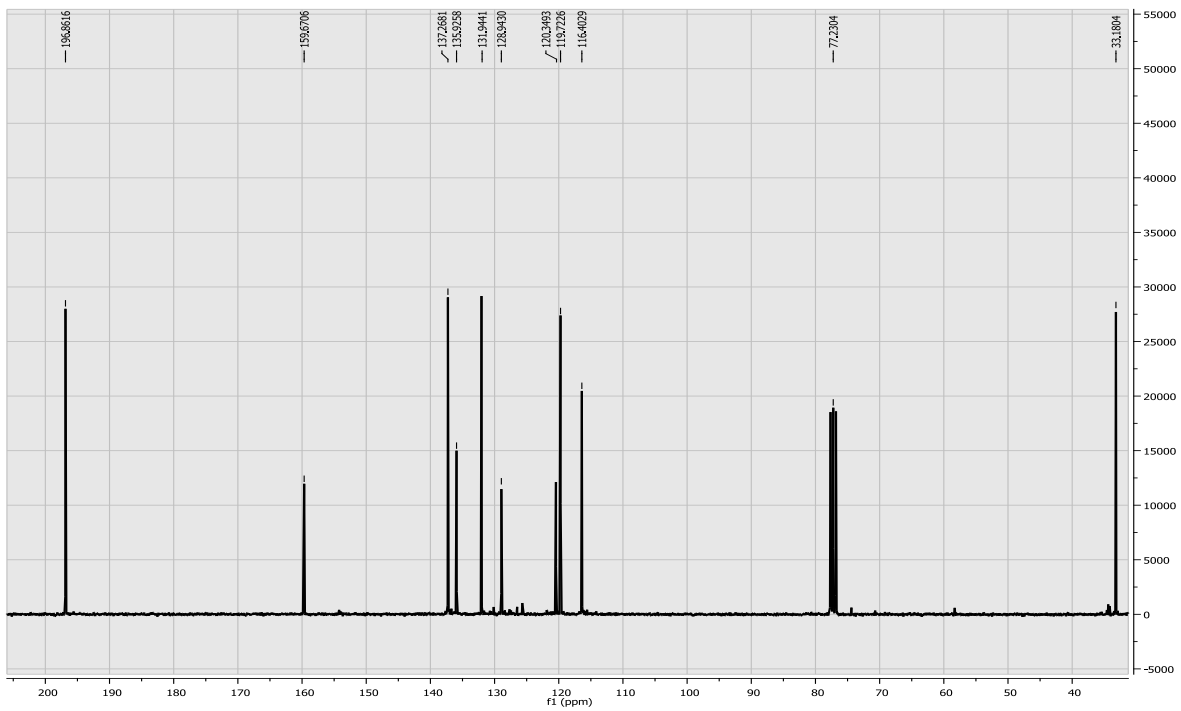
45. Putt, S. K.; Chen, W. G.; Pearson, M. J.; Sandhorst, S. J.; Hoagland, S. M.; Kwon, T. J.; Hwang, K. S.; Jin, H.; Churchwell, I. M.; Cho, H. M.; Doerge, R. D.; Helferich, G. W.; Hergenrother, J. P. Small-molecule activation of procaspase-3 to caspase-3 as a personalized anticancer strategy. *Nature Chemical Biology*, **2006**, 2, 10, 543-550.
46. Gottlieb, H. E.; Kotlyar, V.; Nudelman, A. NMR chemical shifts of common laboratory solvents as trace impurities. *Journal of organic chemistry*, **1997**, 62, 7512-7515.
47. Solomons, T. W, G.; Fryhle, C. B. Organic Chemistry. 8th edition. Wiley. New York, **2002**, Page 239.
48. Putt, S. K.; Chen, W. G.; Pearson, M. J.; Sandhorst, S. J.; Hoagland, S. M.; Kwon, T. J.; Hwang, K. S.; Jin, H.; Churchwell, I. M.; Cho, H. M.; Doerge, R. D.; Helferich, G. W.; Hergenrother, J. P. Supporting information.
49. Breitmaier, E. Structure elucidation by NMR in organic Chemistry: A practical guide. Third revised edition. Wiley. Chichester, **2002**, p XII, pages 258.
50. Naganawa, A.; Saito, T.; Nagao, Y.; Egashira, H.; Iwahashi, M.; Kambe, T.; Koketsu, M.; Yamamoto, H.; Kobayashi, M.; Maruyama, T.; Ohuchida, S.; Nakai, H.; Kodo, K.; Tooda, M. Discovery of new chemical leads for selective EP1 receptor antagonist. *Bioorg. Med. Chem.* **2006**, 14, 5562-5577.
51. Silverman, R. B. The organic chemistry of drug design and drug action. Elsevier. California, **2004**, Pages 29-34.
52. Tran, T. A.; Carter, J.; Ruffin, R. E; Zalewski, P. D. The role of zinc in caspase activation and apoptotic cell death. *Biometals*, **2001**, 14, 315-330.
53. Peterson, Q. P.; Goode, D. R.; West, D. C.; Ramsey, K. N.; Lee, J.; Hergenrother, P. J. PAC-1 activates procaspase-3 in vitro through relief of zinc mediated inhibition. Uncorrected proof. *Journal of molecular biology*, 2009.
54. Hussain, R. F.; Nouri, A. M, E.; Oliver, R. T. D. *Journal of immunological methods*, **1993**, 160, 89-96.
55. a) Hofsløkken, N. U.; Skattebøl, L. Convenient method for the *ortho*-formylation of phenols. *Acta chemica Scandinavia*, **1999**, 53, 258-262; b) Hansen, T. V.; Skattebøl, L. Ortho-formylation of phenols: preparation of 3- bromosalicylaldehyde. *Organic synthesis*, 82.
56. Aras, M. A.; Harnett, K. A.; Aizenman, E. Assesment of cell viability in primary neuronal cultures. *Current protocols in neuroscience*, **2008**, 44, 7, 7.18.1-7.18.15.



Appendix 1

¹H-NMR spectrum for compound **18**.

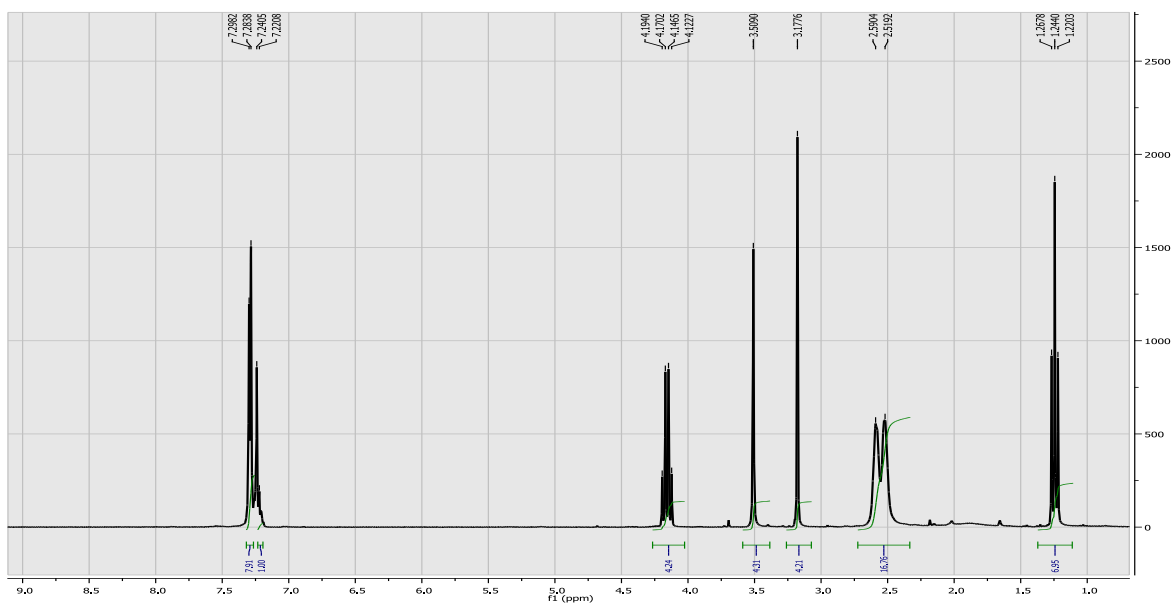
(3-Allyl-2-hydroxybenzaldehyde).



Appendix 2

¹³C NMR spectrum for compound **18**.

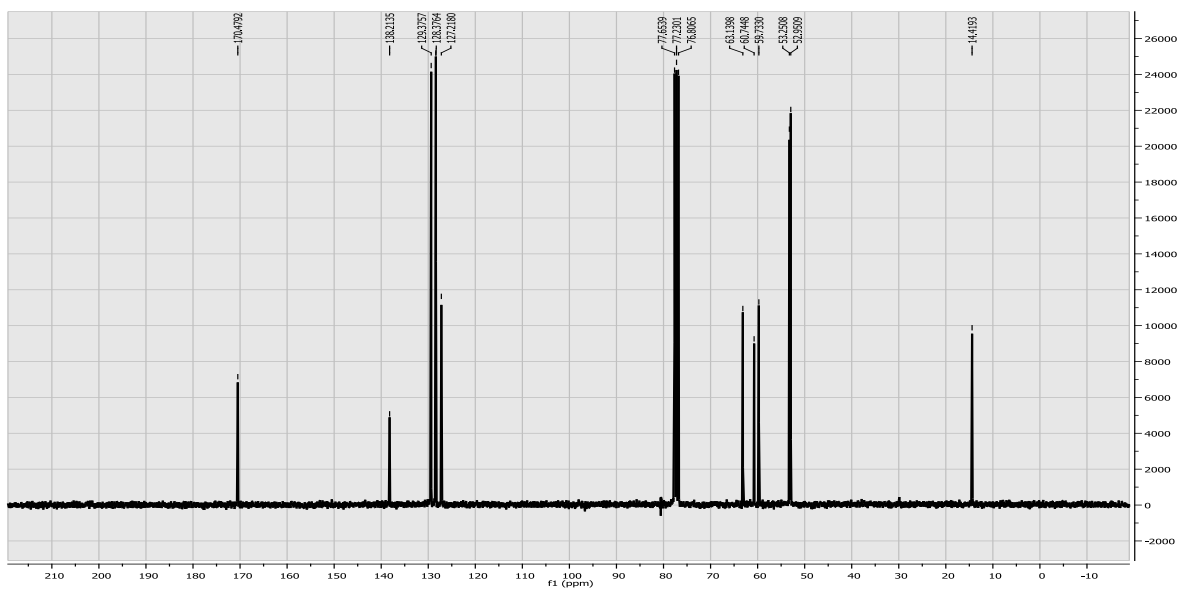
(3-Allyl-2-hydroxybenzaldehyde).



Appendix 3

^1H -NMR spectrum for compound **21**.

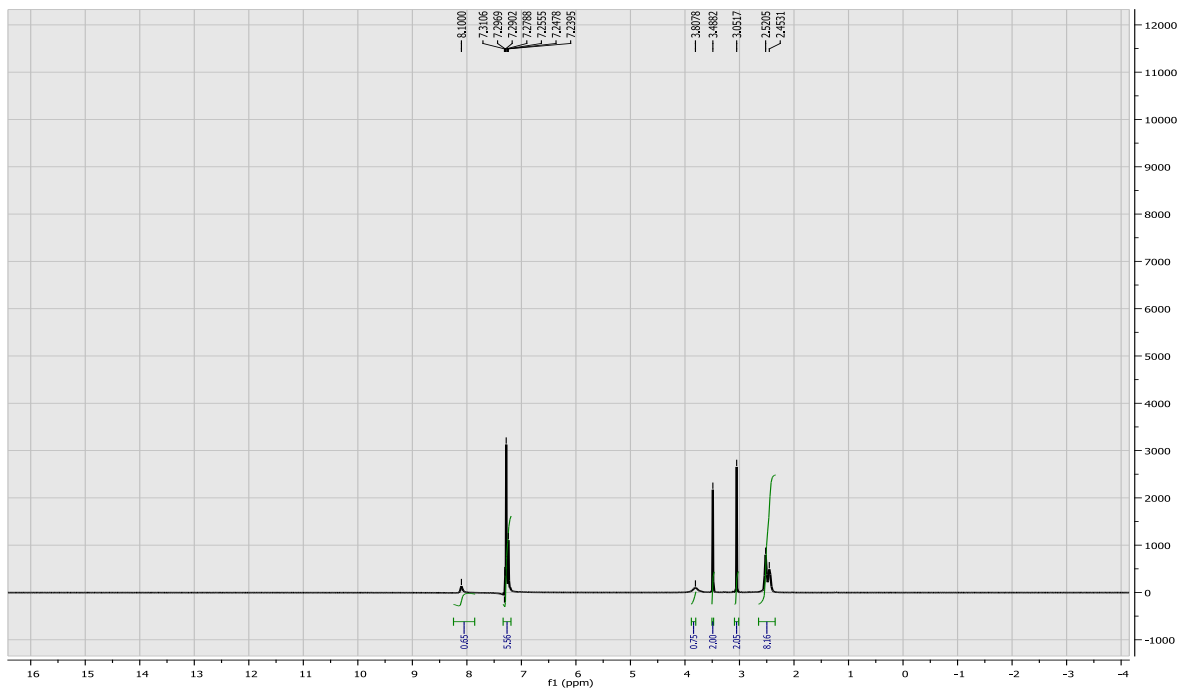
(Ethyl 2-(4-benzylpiperazin-1-yl) acetate)



Appendix 4

^{13}C NMR spectrum for compound **21**.

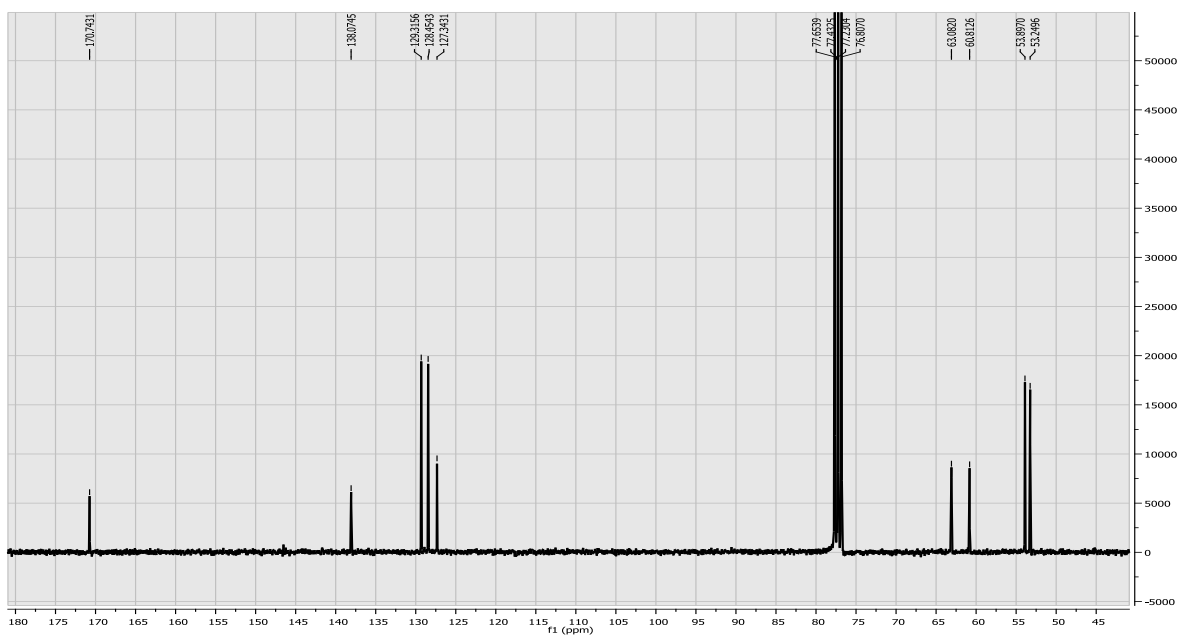
(Ethyl 2-(4-benzylpiperazin-1-yl) acetate)



Appendix 5

^1H -NMR spectrum for compound **23**.

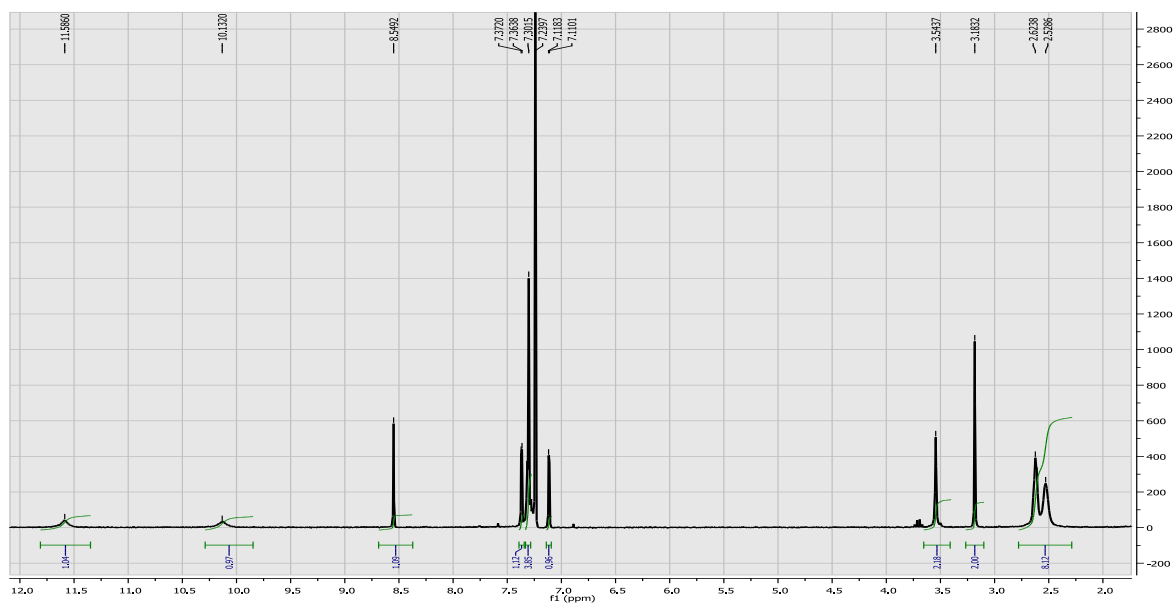
((4- Benzylpiperazino) acetic acid hydrazide))



Appendix 6

^{13}C NMR spectrum for compound **23**.

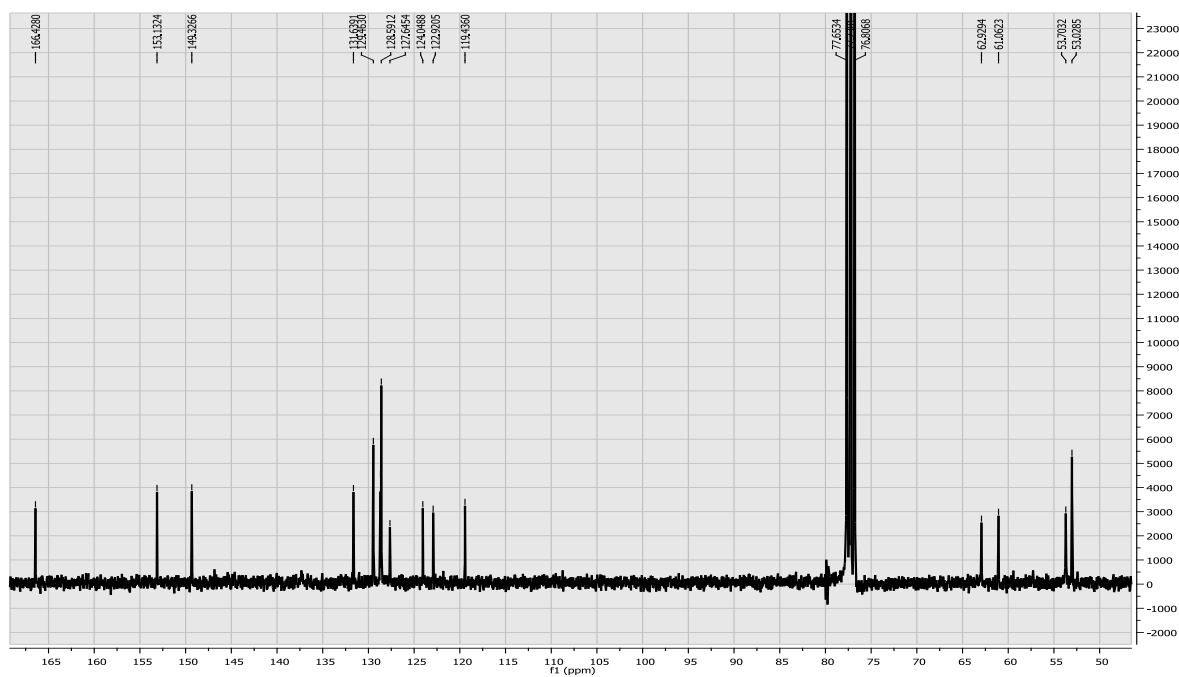
((4- Benzylpiperazino) acetic acid hydrazide).



Appendix 7

$^1\text{H-NMR}$ spectrum for compound **25**.

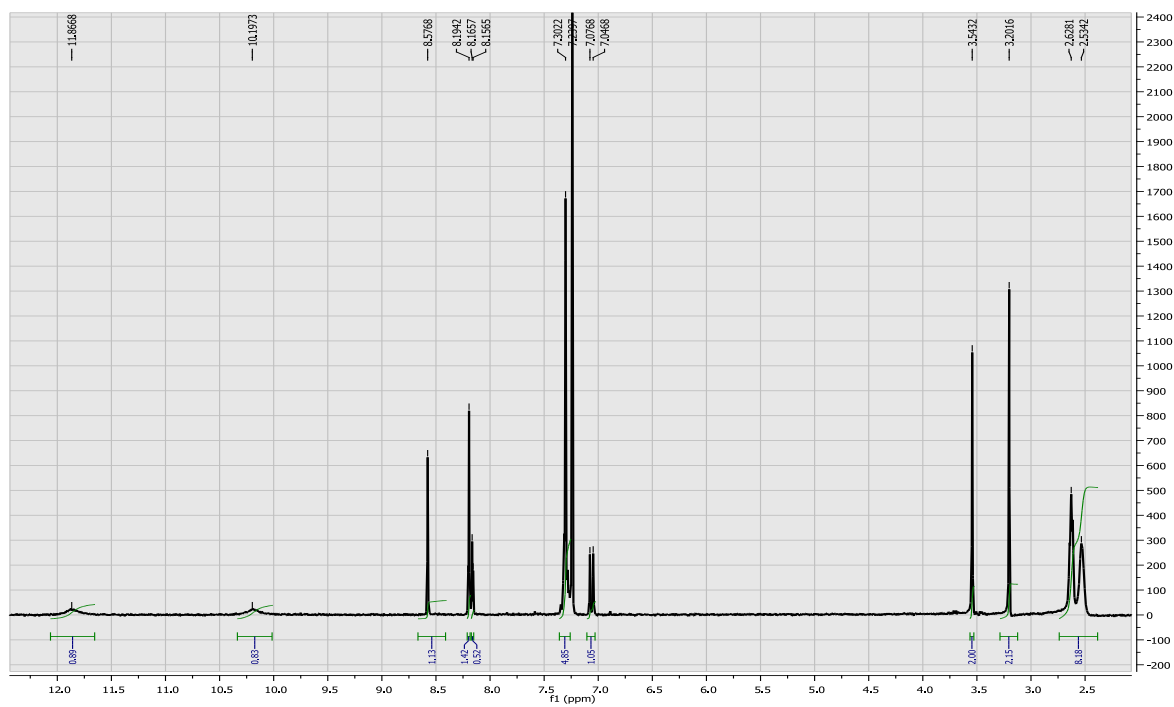
((*E*)-2-(4-benzylpiperazin-1-yl)-*N'*-(3,5-dichloro-2-hydroxybenzylidene) acetohydrazide).



Appendix 8

$^{13}\text{C-NMR}$ spectrum for compound **25**.

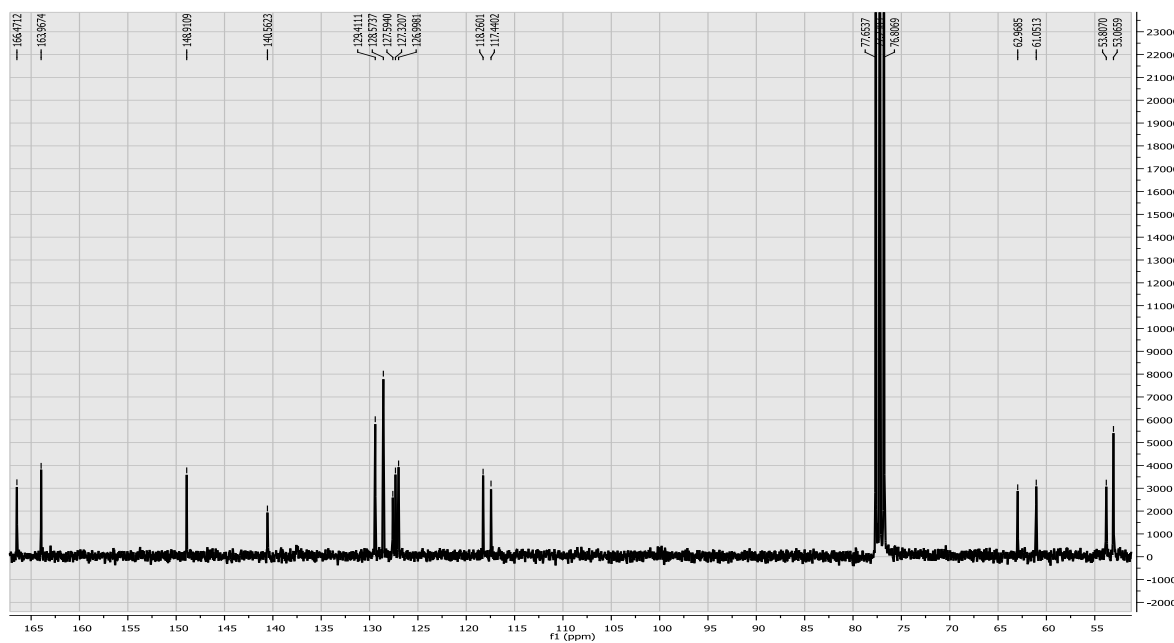
((*E*)-2-(4-benzylpiperazin-1-yl)-*N'*-(3,5-dichloro-2-hydroxybenzylidene) acetohydrazide).



Appendix 9

^1H NMR spectrum for compound **26**.

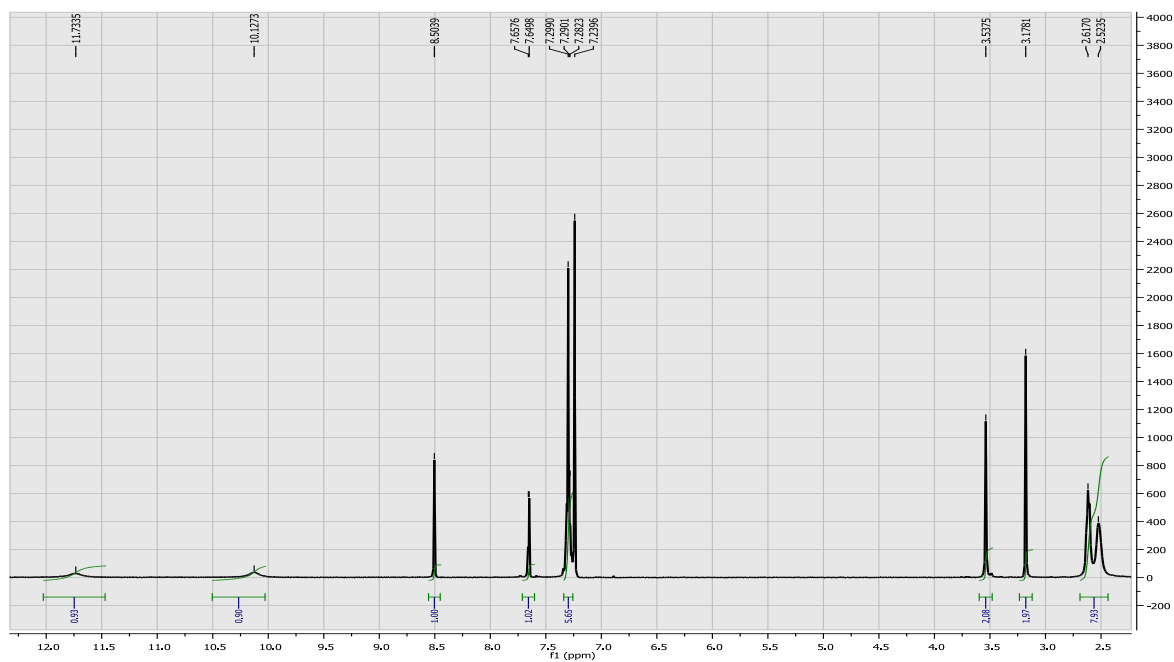
((*E*)-2-(4-benzylpiperazin-1-yl)-*N*'-(2-hydroxy-5-nitrobenzylidene) acetohydrazide).



Appendix 10

^{13}C NMR spectrum for compound **26**.

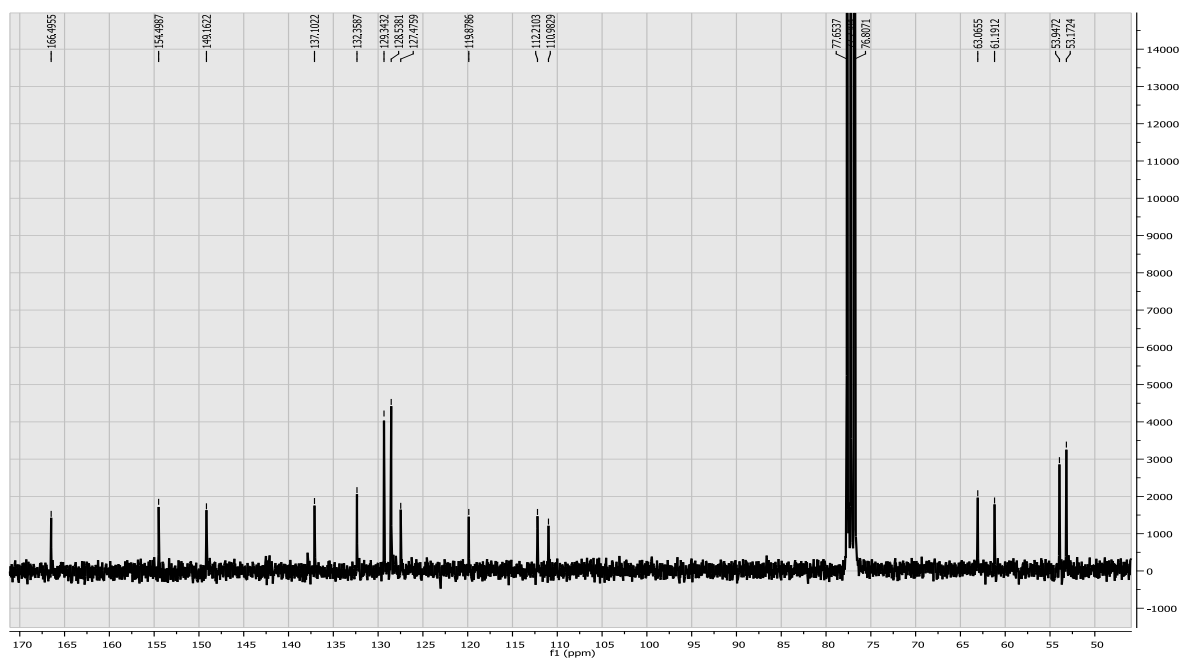
((*E*)-2-(4-benzylpiperazin-1-yl)-*N*'-(2-hydroxy-5-nitrobenzylidene) acetohydrazide).



Appendix 11

$^1\text{H-NMR}$ spectrum for compound **27**

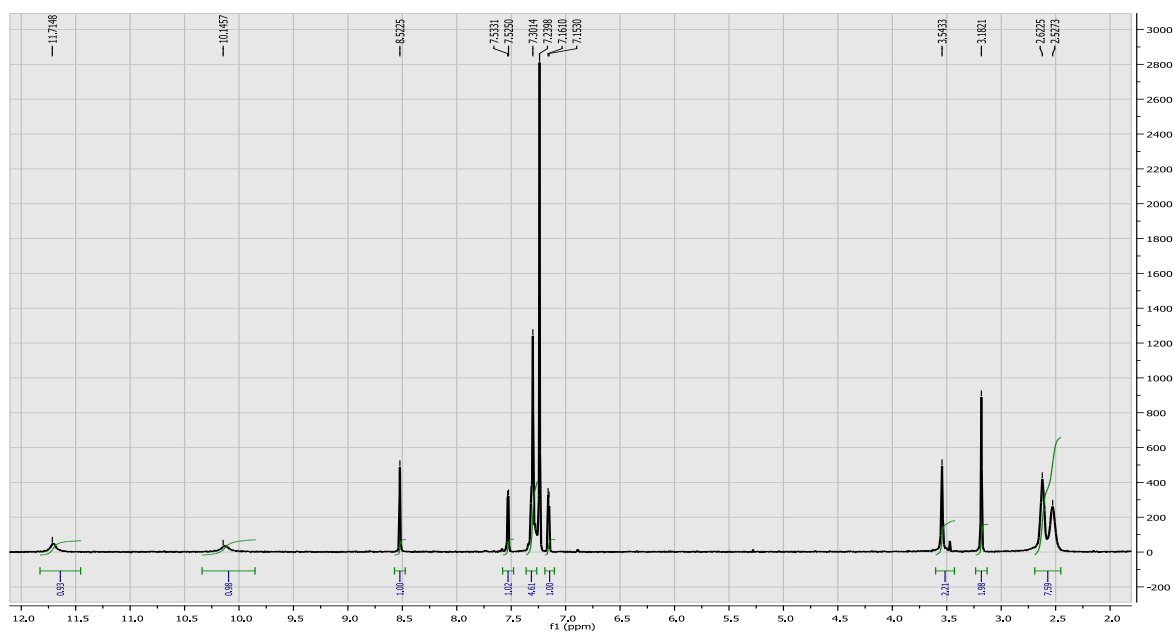
((E)-2-(4-benzylpiperazin-1-yl)-N²-(3,5-dibromo-2-hydroxybenzylidene) acetohydrazide).



Appendix 12

$^{13}\text{C NMR}$ spectrum for compound **27**.

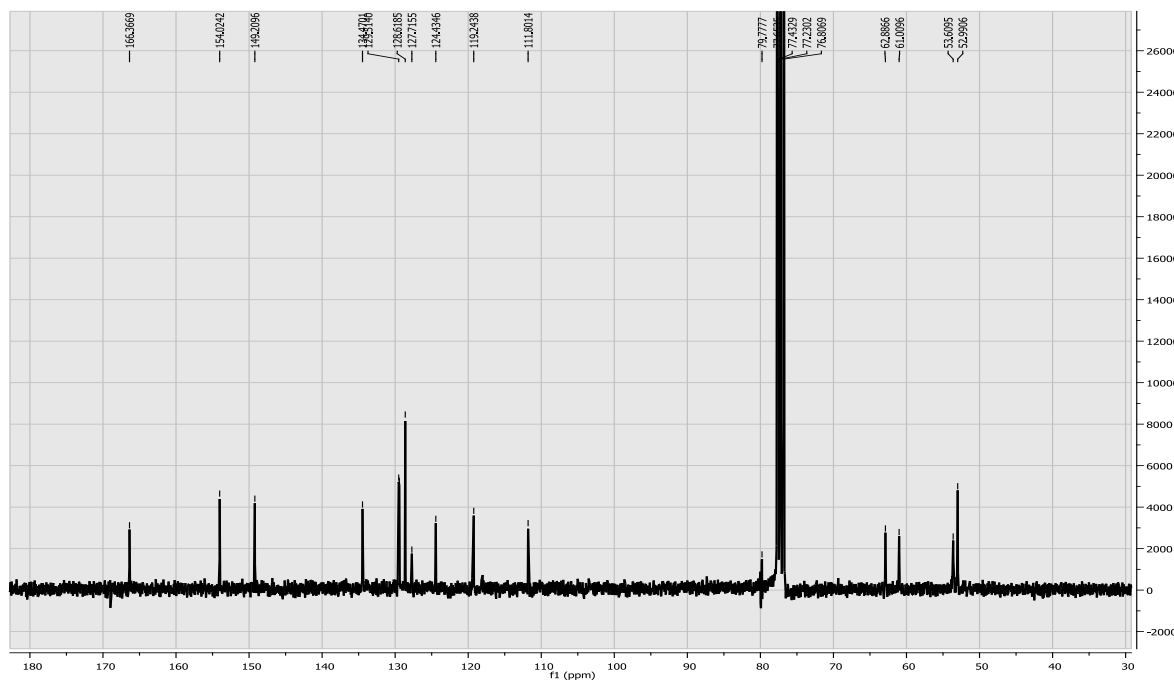
((E)-2-(4-benzylpiperazin-1-yl)-N²-(3,5-dibromo-2-hydroxybenzylidene) acetohydrazide).



Appendix 13

$^1\text{H-NMR}$ spectrum for compound **28**.

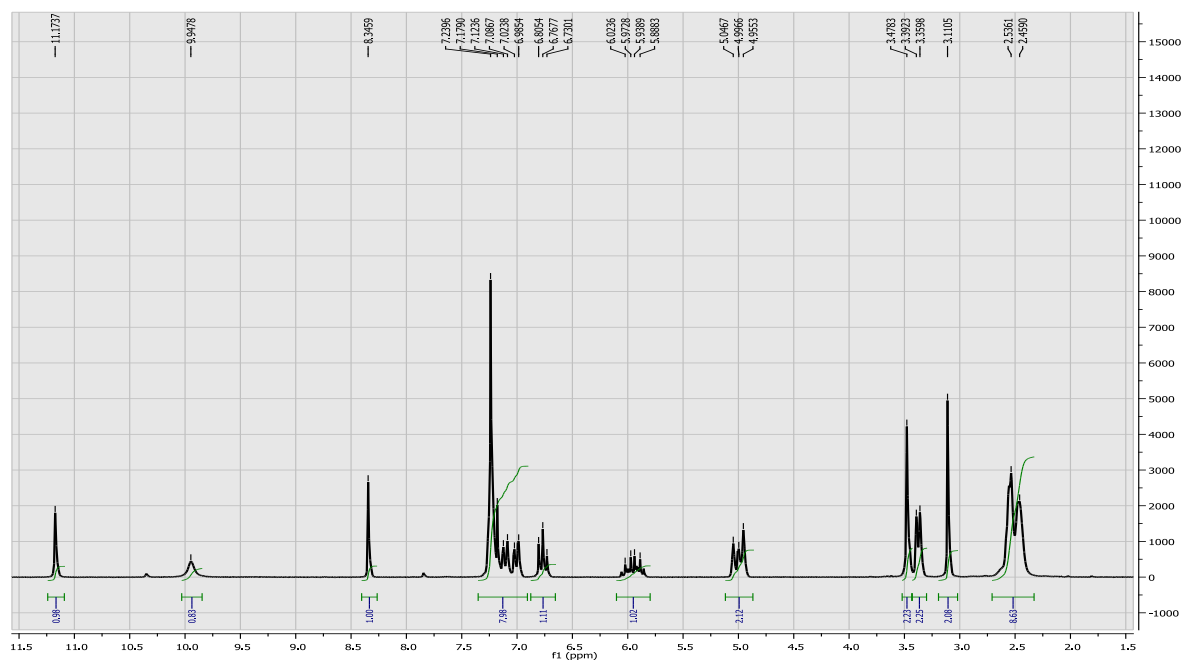
((*E*)-2-(4-benzylpiperazin-1-yl)-*N'*-(3-bromo,5-chloro-2-hydroxybenzylidene) acetohydrazide).



Appendix 14

$^{13}\text{C-NMR}$ spectrum for compound **28**.

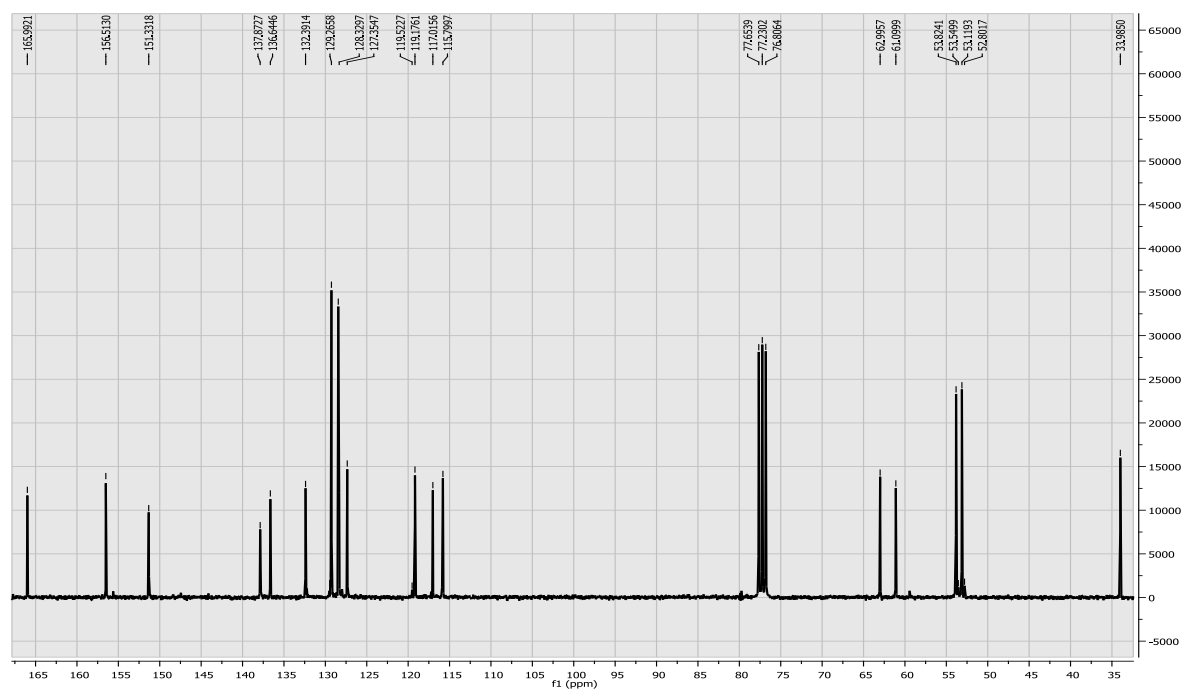
((*E*)-2-(4-benzylpiperazin-1-yl)-*N'*-(3-bromo,5-chloro-2-hydroxybenzylidene) acetohydrazide).



Appendix 15

$^1\text{H-NMR}$ spectrum for compound **16**.

((E)-N-(3-allyl-2-hydroxybenzylidene)-2-(4-benzylpiperazin-1-yl) acetohydrazide).



Appendix 16

$^{13}\text{C-NMR}$ spectrum for compound **16**.

((E)-N-(3-allyl-2-hydroxybenzylidene)-2-(4-benzylpiperazin-1-yl) acetohydrazide).

	Raw data from first biological testing						
CONC.	COMP 25	COMP 26	COMP 27	COMP 28	COMP 16	DMSO	
100	0,1	0,2533	0,1244	0,1175	0,085	2,1134	
33	0,2444	0,9357	0,2432	0,265	0,1131	0,9098	
10	0,6063	1,4176	0,534	0,5429	0,1307	2,1538	
3	1,6974	1,771	1,3385	1,3514	1,3406	1,7727	
1	1,7646	1,5179	1,8171	1,9687	1,7032	1,9914	
0,3	1,5359	0,9253	1,659	1,7864	1,4172	1,712	
100	0,2447	0,2311	0,0701	0,124	0,0981	2,0547	
33	0,706	0,7756	0,2897	0,3017	0,1083	1,8358	
10	0,5392	1,5296	0,2824	0,3604	0,1128	1,9599	
3	1,1316	2,0668	1,4327	1,4186	1,4618	1,824	
1	1,4867	1,898	1,9028	1,7828	1,5867	1,7812	
0,3	1,338	1,5089	1,921	1,9065	1,8675	2,6437	

	Raw data from second biological testing.					
CONC.	COMP 25	COMP 26	COMP 27	COMP 28	COMP 16	DMSO
100	0,1414	0,3156	0,1324	0,4379	0,1169	1,9478
33	0,2108	0,6171	0,3663	0,3446	0,2039	0,7435
10	0,5188	0,9962	0,5112	0,7103	0,4566	1,7542
3	0,9884	1,0829	1,0319	1,0122	1,7429	1,5941
1	1,4291	2,1908	1,6584	1,8261	1,813	1,6078
0,3	1,4949	1,5838	1,4705	1,7289	1,4455	1,7638
100	0,1471	0,3035	0,205	0,4077	0,1184	1,8755
33	0,4199	0,6547	0,4123	0,4357	0,1353	1,8722
10	0,2477	1,2994	0,3948	0,6095	0,2645	1,5843
3	0,1716	1,4338	1,1202	1,5078	1,5743	1,668
1	1,2672	2,1441	1,5788	1,6453	2,2171	2,008
0,3	1,4216	1,2567	1,7504	1,5551	1,7794	1,4253

	Raw data from third biological testing					
CONC.	COMP 25	COMP 26	COMP 27	COMP 28	COMP 16	DMSO
100	0,1996	0,2871	0,1992	0,3655	0,1381	1,6357
33	0,2805	0,6743	0,3699	0,2803	0,1520	1,6485
10	0,5559	1,6483	0,4998	0,5645	0,1953	2,4906
3	1,1870	2,8969	1,9694	1,4813	1,2266	1,5936
1	1,4262	2,1855	1,7735	2,0229	1,4617	2,2620
0,3	1,4710	1,3065	1,0747	1,1786	1,0990	1,6607
100	0,2364	0,2937	0,2597	0,2551	0,1291	1,6358
33	0,2781	0,6135	0,3117	0,2637	0,1651	1,6383
10	0,4013	1,0357	0,4724	0,3823	0,1830	1,6738
3	1,1031	1,8624	1,2410	1,1498	0,5297	1,5635
1	1,1933	1,4519	1,5319	1,3481	0,5928	1,1338
0,3	0,8682	1,4830	1,1611	1,2544	0,7269	0,6814